NASA Technical Memorandum 81296

NASA-TM-81296 19810017538

TAIR - a Transonic Airfoil Analysis Computer Code

F. Carroll Dougherty, Terry L. Holst, Karen L. Gundy and Scott D. Thomas

May 1981

National Aeronautics and
Space Administration

NASA Technical Memorandum 81296

TAIR - a Transonic Airfoil Analysis Computer Code

F. Carroll Dougherty
Terry L. Holst, Ames Research Center, Moffett Field, California
Karen L. Gundy
Scott D. Thomas, Informatics Inc., Palo Alto, California

National Aeronautics and
Space Administration

Ames Research Center
Moffett Field, California 94035

TAIR — A TRANSONIC AIRFOIL ANALYSIS COMPUTER CODE

F. Carroll Dougherty, Terry L. Holst, Karen L. Gundy, and Scott D. Thomas

Ames Research Center

SUMMARY

The operation of the TAIR (Transonic AIRfoil) computer code, which uses a fast, fully implicit algorithm to solve the conservative full-potential equation for transonic flow fields about arbitrary airfoils, is described. The code description is given in two levels of sophistication: simplified operation and detailed operation. In addition, detailed descriptions of the program organization and theory are provided to simplify modification of TAIR for new applications. Examples with input and output are given for a wide range of cases, including incompressible, subcritical compressible, and transonic calculations.

1. INTRODUCTION

This report describes the operation of TAIR, a transonic airfoil analysis computer program written in FORTRAN. TAIR solves the conservative full-potential equation for the steady transonic flow field about an arbitrary airfoil immersed in a subsonic free stream. The full-potential formulation is considered exact under the assumptions of irrotational, isentropic, and inviscid flow. These assumptions are valid for a wide range of practical transonic flows typical of modern aircraft cruise conditions.

The primary features of TAIR include: (1) a new fully implicit iteration scheme (AF2) which is typically 4 to 10 times faster than classical successive-line overrelaxation (SLOR) algorithms; (2) a new, reliable artificial density spatial differencing scheme treating the conservative form of the full-potential equation; and (3) a numerical mapping procedure capable of generating curvilinear, body-fitted finite-difference grids about arbitrary airfoil geometries (see refs. 1-3 for theoretical details of these features). The coding in TAIR includes many useful options including: (1) several airfoil-geometry input options, (2) flexible user control over program output, (3) a "built-in" default solution, (4) numerous comments to facilitate program use or modification, and (5) a multiple solution capability.

The most important aspect of TAIR is algorithm reliability. Because this characteristic is generally regarded as the most important quality for a user-oriented CFD computer program, it was emphasized during the development of TAIR. The reliability of TAIR comes from two sources: the algorithm, including the AF2 iteration scheme and the artificial density differencing scheme designed to simulate rotated differencing (ref. 4), and a convergence monitoring section of logic (SUBROUTINE AUTO), which automatically updates solution parameters in an attempt to speed convergence or prevent divergence. Use of

the convergence monitoring logic in TAIR allows the use of "default mode" (ref. 3). In default mode, only three inputs are changed from case to case, free-stream Mach number, angle of attack, and airfoil coordinates. Other parameters, including relaxation factors, acceleration parameters, and temporal-damping coefficients are either held fixed or are automatically adjusted by internal computer code logic. This feature greatly simplifies code operation, especially for inexperienced users. Generally speaking, in the default mode less than 1% of all cases diverge — a considerably better performance than most CFD codes run in any mode of operation.

Besides reliability and simplicity, another important aspect of the TAIR code is speed. The average flow-solver run time for the default mesh (149×30) is about 9 sec. Most subcritical or weak-shock cases require less time and most strong-shock cases (local Mach numbers exceeding 1.3) require more time. The average grid generation time is about 2 sec. Both of these times are on the Ames CDC 7600 computer. The program requires only a modest amount of storage — 153,000 words octal (~55,000 decimal) — and is written to be as transportable as possible.

Instructions for the use of TAIR follow in subsequent chapters. Simplified usage, that is, essentially default mode usage, is described in chapter 2. Chapter 3 describes more detailed operation; it is necessary reading for any major deviation from default mode usage. Chapter 4 discusses program organization, and chapter 5 discusses theory; both of these chapters would be of interest to anyone contemplating a major modification of TAIR. Chapter 6 presents a discussion of results obtained with TAIR for a variety of different cases (CASE HISTORY). Appendix A discusses the appropriate changes required to increase program dimensions, and appendix B provides a table of program variable names with brief descriptions which are cross-referenced with variable names used in the theoretical development.

2. SIMPLIFIED OPERATION

The following sections of this chapter discuss the use of the TAIR computer program for simplified operation: the inputs and outputs, some numerical examples, and the error safeguards built into the program. This level of operation allows the calculation of standard airfoil cases in the transonic regime, using a set of optimized acceleration parameters stored in the code and an automatic updating routine.

Most of the parameter inputs to TAIR are divided between two NAMELISTs. The aerodynamic and flow-field convergence parameters are found in NAMELIST FLOWIN (defined in SUBROUTINE INITL), and the geometric and grid convergence parameters are found in NAMELIST GRIDIN (defined in SUBROUTINE GRGEN). Airfoil coordinates other than those generated in TAIR would be read from cards after the two NAMELISTs. More information regarding these inputs, including formats, individual parameter descriptions, and acceptable parameter ranges, is given in the INPUT/OUTPUT section at the end of the chapter. Default values for the NAMELIST parameters are initialized in INITL and GRGEN. With the NAMELIST format, the user needs to change only the values that differ from the

default values. If no parameters are changed, the predetermined default solution is executed, as discussed in example 1 of the INPUT/OUTPUT examples section.

The following sections define a partial list of input parameters a general user of TAIR might wish to change. For a more complete list of input parameters, or if the values of some of these input parameters vary widely from the default case or if certain options require more changes than are mentioned here, the user is directed to chapter 3.

In this chapter and in the following chapters, all program variable and subroutine names are capitalized. The first section describes the variables in the FLOWIN NAMELIST; the second identifies the parameters in the GRIDIN NAMELIST. The third section discusses three example cases, detailing the proper uses of the input parameters, the correct ordering of the data cards, and the formats required. The fourth section describes briefly the error safeguards built into the program, and the last section contains the actual input data decks and the output generated for the example cases.

Description of FLOWIN NAMELIST Parameters

ALPH — Angle of attack, deg. Acceptable values: real numbers between -10.0 and +10.0. Default value: 1.0.

MESH — Determines which grid generation option is used.

- MESH=0...Grid is generated within the program (see IOPT parameter in NAMELIST GRIDIN for details about airfoil geometry representation). This option also causes the grid coordinates to be written to a scratch file, logical unit 48.
- MESH=1...This option reads the grid from unit 48 and is useful when a series of calculations is to be made with the same mesh (see NCASE parameter discussion later in this section). When using the MESH=1 option, the GRIDIN NAMELIST data card should be omitted.
- MESH=2...This option reads an initial solution grid from unit 48 and adapts it to a new airfoil. The user should read chapter 3 before selecting this option.
- MESH=3...This option reads a mesh created by the program GRAPE (ref. 5). The user should see chapter 3 for further instructions.

Acceptable values: 0,1,2,3. Default value: 0.

MINF — Free-stream Mach number. Acceptable values: real numbers between 0.0 and 1.0, exclusive. Default value: 0.75.

NCASE Number of solutions per job. If multiple cases are run with the same airfoil, computing time can be saved by setting MESH=1 for the second and each succeeding case (see INPUT/OUTPUT example 3). For each new case, all NAMELIST parameters are reset to the default values. Thus, the second, third, etc., cases must each reset the appropriate solution parameters through the NAMELIST READ statements. Acceptable values: any positive integer. Default value: 1.

NI The number of mesh points in the ξ direction, numbered around the airfoil in a clockwise direction (see fig. 1). Note: if input value of NI varies widely from the default value, the user should see chapter 3. Acceptable values: 50 to 151. Default value: 149.

NJ The number of mesh points in the η direction, numbered from the outer boundary inward to the airfoil surface (see fig. 1). Note: if input value of NJ varies widely from the default value, the user should see chapter 3. An NI/NJ ratio of 4 or 5 works best with the flow solver in this code. Acceptable values: 12 to 31. Default value: 30.

NOUT Primary output control parameter. NOUT=0 suppresses all output except for a few error messages. Table 1 shows each NOUT value, the type of output associated with it, and the amount of output generated (in number of pages). The page totals shown do not include error message printouts or update messages, so actual numbers may be slightly larger. For more information about a specific output format, see the INPUT/OUTPUT examples. Acceptable values: integers between 0 and 9. Default value: 5.

NSTEPS Maximum number of iterations of the flow solver. Most cases should converge in less than the default number. Acceptable values: positive integers. Default value: 200.

Description of GRIDIN NAMELIST Parameters

IOPT Determines which geometry option is used.

IOPT=1...This generates a NACA 00XX type airfoil. The input parameter TMAX determines the thickness (see below).

IOPT=2...This IOPT option is a circular-arc airfoil. (See chap. 3 for more detail.)

IOPT=3...A circular cylinder cross section is generated. (Read chap. 3 for more information.)

IOPT=4...This IOPT permits the user to read in an arbitrary airfoil geometry. The first card in the data deck should be the title of the airfoil, with a maximum of 28 characters in a 7A4 format (right justified with left "*" fill; see example at the end of the chapter). The second card contains the number of airfoil coordinate pairs in the data deck (NPTS)

in I5 format. This number is limited to 151 because of program dimensions. The next cards contain the coordinates XB and YB, in a 2F10.5 format. These coordinates should be nondimensionalized by chord, but will automatically be scaled if they are not. They are ordered starting with the lower trailing-edge point at X = 1.0, moving clockwise around the airfoil, and ending with the upper trailing edge point at X = 1.0.

IOPT=5...The Korn airfoil is used for this option (airfoil 75-06-12 in reference 6).

Acceptable values: 1,2,3,4,5. Default value: 1.

TMAX Airfoil thickness parameter, nondimensionalized by chord. This value is necessary for the IOPT=1 and IOPT=2 options. Acceptable values: real numbers between 0.0 and 1.0, exclusive. Default value: 0.12.

Descriptions of INPUT/OUTPUT Examples

This section discusses input/output examples for three cases: (1) the default case, (2) a user-supplied airfoil case (IOPT=4), and (3) a simple multiple-solution case (NCASE=4). Each example is shown with the required input data and the resulting output (at the end of this chapter). The first example shows the input data and output for the default case stored in TAIR. Note that no parameters of any sort need to be modified for this case, which involves a NACA 0012 airfoil at a free-stream Mach number of 0.75 and an angle of attack of 1°. The grid is generated within TAIR (MESH=0) and has dimensions of 149 by 30. The flow solver for this case requires 74 iterations (about 7 sec of CPU time on the CDC 7600 computer) and the grid generation requires 20 iterations (about 2 sec of CPU time).

Output for the default case includes a banner and three pages of input data: the FLOWIN and GRIDIN NAMELIST parameters and the initial airfoil coordinates, nondimensionalized by chord. The next page of output shows the airfoil coordinates, XB and YB, after they have been interpolated and clustered about the airfoil. The ARC LENGTH, normalized by chord, is calculated from the lower trailing-edge point to the upper trailing-edge point. DS is the first difference of the arc length. Note that the NIth point is not printed, since it is identical to the first point because of wrap-around periodicity. Following the interpolated airfoil coordinates are the messages printed by the automatic updating SUBROUTINE AUTO discussed in the next section of this chapter.

The last page of output gives the airfoil surface solution. The first line of output at the top of this page displays the airfoil and flow conditions used for this case. The second line lists the number of iterations needed for convergence; the maximum residual of the last iteration (RMAX); the number of supersonic points (NSP); and the coefficient of lift calculated using the circulation and the Kutta-Joukowski theorem (CL(CIR)). The surface solution is divided into three sets of columns numbered clockwise around the

airfoil starting at the lower surface trailing edge. These columns list the X and Y coordinates normalized by chord, X/C and Y/C; the coefficient of pressure at the airfoil surface; the density; and the surface Mach number. It should be pointed out that the values shown are stored at the halfway points relative to the original mesh, that is, (I+1/2, J+1/2). The last line of output on this page gives the lift, wave-drag, and quarter-chord moment coefficients determined from the final surface solution by numerical integration (trapezoid rule).

The second INPUT/OUTPUT example employs the IOPT=4 option with the theoretical CAST 7 airfoil coordinates (ref. 7) and shows the order and format of the airfoil coordinates as well as the appropriate changes for the parameters in the FLOWIN and GRIDIN NAMELISTs. The chosen case runs the CAST 7 airfoil with a Mach number of 0.7 and an angle of attack of 1.5°. The output control parameter NOUT has been set to 3, limiting the total solution output to the one page airfoil surface solution. Note that the title of the airfoil on the first data card is right justified in the 28 space field and the remaining spaces are filled with asterisks. The solution converged in 85 iterations (about 9 sec of CPU time) and produced 191 supersonic points, a lift coefficient of 1.0008, and a wave-drag coefficient of 0.0042.

The third INPUT/OUTPUT example is a simple multiple-solution run (NCASE=4) in which four solutions for the Korn airfoil (IOPT=5) are obtained. The Mach number in each case is held fixed at 0.7 while the angle of attack varies from 0° to 2°. Since this example could be used for a lift versus alpha curve, NOUT=2 is used to reduce the output. Note that the MESH=1 option is used, so the GRIDIN card is omitted for the last three solutions. Also, parameter values that differ from the default values must be reset on each FLOWIN card. This is because all parameters are reset to default values at the beginning of each solution. The NCASE change, however, need only be made on the first data card. The NOUT=2 specification considerably reduces the amount of output. Only the number of iterations, the maximum residual, the number of supersonic points, the lift coefficient calculated from the circulation, and the lift, drag, and moment coefficients computed from the pressure integration are printed for each of the four cases.

Error Safeguards

TAIR includes in its programming many checks and safeguards to ensure that the code runs smoothly. Throughout the program, parameters and arrays are checked for incorrect or out-of-range values. Two subroutines carry the bulk of this safeguarding, SUBROUTINEs CHECK and AUTO. If any value is corrected, or if the program is stopped, there is always an error message generated explaining the problem and the steps taken to resolve it. If NOUT is less than 4, however, the messages printed by the AUTO updating procedure will be suppressed. The remaining safeguards are contained in various subroutines and are discussed in the individual subroutine descriptions in chapter 4.

INPUT/OUTPUT example 1- The following data cards were used for INPUT/OUTPUT example 1 — the default case. The output for this case is on the next six pages.

```
$FLOWIN   $
$GRIDIN   $
```

APPLIED COMPUTATIONAL AERODYNAMICS BRANCH

NASA - AMES RESEARCH CENTER

MOFFETT FIELD, CA 94035

```
TTTTTT    AA    II  RRRR
  TT     A  A   II  RR  RR
  TT    AAAAAA  II  RRRR
  TT    AA  AA  II  RR RR
  TT    AA  AA  II  RR  RR
```

THIS COMPUTER PROGRAM SOLVES THE CONSERVATIVE FULL POTENTIAL EQUATION FOR THE TRANSONIC FLOW AROUND AN ARBITRARY AIRFOIL, USING A FULLY IMPLICIT APPROXIMATE FACTORIZATION SCHEME (AF2).

WRITTEN BY

DR. TERRY L. HOLST

AND

F. CARROLL DOUGHERTY

```
SFLOWIN
MINF    = .75E+ØØ,
NI      = 149,
NJ      = 3Ø,
ALPH    = .1E+Ø1,
NSTEPS  = 2ØØ,
NOUT    = 5,
NOUT1   = 2Ø1,
NOUT2   = 8,
IINCR   = 3,
JINCR   = 2,
NCASE   = 1,
ERR     = -.1E-Ø1,
OMEGA   = .18E+Ø1,
BETA    = .45E+Ø1,
ALOW    = .7E-Ø1,
AHIGH   = .15E+Ø1,
K       = Ø,
M       = 8,
RGAM    = .1E+Ø1,
MESH    = Ø,
CON     = .2E+Ø1,
NRING   = 3,
AFAC    = .14E+Ø2,
G       = .14E+Ø1,
NDIF    = Ø,
IAUTO   = 1,
ICHECK  = 1,
SEND
```

```
$GRIDIN
BINN    = -.1E+01,
RADMAX  = .6E+01,
IOPT    = 1,
TMAX    = .12E+00,
IOPEN   = 0,
XC      = .2E+00,
IOUT    = 1,
HTMAX   = .4E+01,
WDTHMX  = .6E+01,
MAXIT   = 50,
OMEG    = .2E+01,
KGRID   = 0,
MGRID   = 8,
AHGRID  = .2E-01,
ALGRID  = .1E-04,
ERGRID  = .1E-01,
XCN     = .5E+00,
YCN     = 0.0,
$END
```

*** INITIAL AIRFOIL COORDINATES FROM INPUT ***

********** NACA ØØ12 AIRFOIL **********

I	XB	YB	I	XB	YB	I	XB	YB
1	1.ØØØØØ	-.ØØØØØ	51	.23785	-.Ø5861	1Ø1	.2749Ø	.Ø5937
2	.99955	-.ØØØØ6	52	.22ØØ1	-.Ø5795	1Ø2	.294Ø5	.Ø5948
3	.9982Ø	-.ØØØ26	53	.2Ø268	-.Ø5712	1Ø3	.31357	.Ø5943
4	.99595	-.ØØØ57	54	.18589	-.Ø561Ø	1Ø4	.33343	.Ø592Ø
5	.99281	-.ØØ1Ø2	55	.16966	-.Ø5489	1Ø5	.35359	.Ø5881
6	.98878	-.ØØ158	56	.154Ø3	-.Ø5351	1Ø6	.374Ø1	.Ø5827
7	.98387	-.ØØ227	57	.139Ø2	-.Ø5195	1Ø7	.39466	.Ø5758
8	.978Ø8	-.ØØ3Ø7	58	.12466	-.Ø5Ø21	1Ø8	.4155Ø	.Ø5675
9	.97144	-.ØØ398	59	.11Ø98	-.Ø483Ø	1Ø9	.43649	.Ø5579
1Ø	.96394	-.ØØ5ØØ	6Ø	.Ø98ØØ	-.Ø4622	11Ø	.4576Ø	.Ø547Ø
11	.95561	-.ØØ613	61	.Ø8575	-.Ø4399	111	.47878	.Ø535Ø
12	.94646	-.ØØ735	62	.Ø7424	-.Ø4161	112	.5ØØØØ	.Ø5219
13	.93651	-.ØØ866	63	.Ø6349	-.Ø39Ø7	113	.52122	.Ø5Ø78
14	.92576	-.Ø1ØØ6	64	.Ø5354	-.Ø364Ø	114	.5424Ø	.Ø4929
15	.91425	-.Ø1155	65	.Ø4439	-.Ø336Ø	115	.56351	.Ø4771
16	.9Ø2ØØ	-.Ø131Ø	66	.Ø36Ø6	-.Ø3Ø68	116	.5845Ø	.Ø46Ø6
17	.889Ø2	-.Ø1472	67	.Ø2856	-.Ø2764	117	.6Ø534	.Ø4435
18	.87534	-.Ø1641	68	.Ø2192	-.Ø245Ø	118	.62599	.Ø4258
19	.86Ø98	-.Ø1815	69	.Ø1613	-.Ø2125	119	.64641	.Ø4Ø76
2Ø	.84597	-.Ø1993	7Ø	.Ø1122	-.Ø1791	12Ø	.66657	.Ø3891
21	.83Ø34	-.Ø2176	71	.ØØ719	-.Ø1449	121	.68643	.Ø37Ø3
22	.81411	-.Ø2362	72	.ØØ4Ø5	-.Ø1Ø98	122	.7Ø595	.Ø3512
23	.79732	-.Ø2551	73	.ØØ18Ø	-.ØØ739	123	.7251Ø	.Ø332Ø
24	.77999	-.Ø2742	74	.ØØØ45	-.ØØ373	124	.74385	.Ø3127
25	.76215	-.Ø2934	75	Ø.ØØØØØ	Ø.ØØØØØ	125	.76215	.Ø2934
26	.74385	-.Ø3127	76	.ØØØ45	.ØØ373	126	.77999	.Ø2742
27	.7251Ø	-.Ø332Ø	77	.ØØ18Ø	.ØØ739	127	.79732	.Ø2551
28	.7Ø595	-.Ø3512	78	.ØØ4Ø5	.Ø1Ø98	128	.81411	.Ø2362
29	.68643	-.Ø37Ø3	79	.ØØ719	.Ø1449	129	.83Ø34	.Ø2176
3Ø	.66657	-.Ø3891	8Ø	.Ø1122	.Ø1791	13Ø	.84597	.Ø1993
31	.64641	-.Ø4Ø76	81	.Ø1613	.Ø2125	131	.86Ø98	.Ø1815
32	.62599	-.Ø4258	82	.Ø2192	.Ø245Ø	132	.87534	.Ø1641
33	.6Ø534	-.Ø4435	83	.Ø2856	.Ø2764	133	.889Ø2	.Ø1472
34	.5845Ø	-.Ø46Ø6	84	.Ø36Ø6	.Ø3Ø68	134	.9Ø2ØØ	.Ø131Ø
35	.56351	-.Ø4771	85	.Ø4439	.Ø336Ø	135	.91425	.Ø1155
36	.5424Ø	-.Ø4929	86	.Ø5354	.Ø364Ø	136	.92576	.Ø1ØØ6
37	.52122	-.Ø5Ø78	87	.Ø6349	.Ø39Ø7	137	.93651	.ØØ866
38	.5ØØØØ	-.Ø5219	88	.Ø7424	.Ø4161	138	.94646	.ØØ735
39	.47878	-.Ø535Ø	89	.Ø8575	.Ø4399	139	.95561	.ØØ613
4Ø	.4576Ø	-.Ø547Ø	9Ø	.Ø98ØØ	.Ø4622	14Ø	.96394	.ØØ5ØØ
41	.43649	-.Ø5579	91	.11Ø98	.Ø483Ø	141	.97144	.ØØ398
42	.4155Ø	-.Ø5675	92	.12466	.Ø5Ø21	142	.978Ø8	.ØØ3Ø7
43	.39466	-.Ø5758	93	.139Ø2	.Ø5195	143	.98387	.ØØ227
44	.374Ø1	-.Ø5827	94	.154Ø3	.Ø5351	144	.98878	.ØØ158
45	.35359	-.Ø5881	95	.16966	.Ø5489	145	.99281	.ØØ1Ø2
46	.33343	-.Ø592Ø	96	.18589	.Ø561Ø	146	.99595	.ØØØ57
47	.31357	-.Ø5943	97	.2Ø268	.Ø5712	147	.9982Ø	.ØØØ26
48	.294Ø5	-.Ø5948	98	.22ØØ1	.Ø5795	148	.99955	.ØØØØ6
49	.2749Ø	-.Ø5937	99	.23785	.Ø5861	149	1.ØØØØØ	.ØØØØØ
5Ø	.25615	-.Ø59Ø8	1ØØ	.25615	.Ø59Ø8			

*** FINAL AIRFOIL COORDINATES AFTER CUBIC SPLINE INTERPOLATION ***

I	XB	YB	ARC LENGTH	DS	I	XB	YB	ARC LENGTH	DS	I	XB	YB	ARC LENGTH	DS
1	1.00000	-.00000	0.00000	.00053	51	.21801	-.05787	.78501	.01697	101	.25289	.05901	1.28891	.01791
2	.99896	-.00015	.00105	.00142	52	.22131	-.05704	.80173	.01646	102	.27102	.05932	1.30704	.01835
3	.99719	-.00040	.00284	.00225	53	.18514	-.05605	.81793	.01593	103	.28958	.05947	1.32566	.01875
4	.99450	-.00078	.00555	.00319	54	.16952	-.05488	.83359	.01538	104	.30853	.05946	1.34455	.01914
5	.99086	-.00129	.00923	.00417	55	.15448	-.05355	.84869	.01481	105	.32785	.05928	1.36387	.01949
6	.98625	-.00193	.01388	.00514	56	.14003	-.05206	.86322	.01423	106	.34750	.05895	1.38353	.01981
7	.98068	-.00271	.01951	.00611	57	.12620	-.05040	.87716	.01363	107	.36747	.05846	1.40350	.02011
8	.97415	-.00361	.02610	.00707	58	.11300	-.04860	.89047	.01301	108	.38770	.05783	1.42374	.02037
9	.96667	-.00463	.03365	.00801	59	.10045	-.04664	.90317	.01238	109	.40818	.05706	1.44424	.02060
10	.95827	-.00577	.04212	.00893	60	.08858	-.04453	.91522	.01173	110	.42887	.05615	1.46494	.02079
11	.94897	-.00702	.05151	.00984	61	.07739	-.04229	.92663	.01108	111	.44972	.05512	1.48583	.02096
12	.93877	-.00837	.06180	.01072	62	.06691	-.03991	.93739	.01042	112	.47072	.05397	1.50685	.02108
13	.92772	-.00981	.07295	.01157	63	.05714	-.03741	.94747	.00975	113	.49182	.05271	1.52799	.02117
14	.91583	-.01134	.08493	.01239	64	.04809	-.03478	.95689	.00908	114	.51298	.05134	1.54920	.02123
15	.90313	-.01296	.09773	.01319	65	.03980	-.03204	.96563	.00840	115	.53417	.04988	1.57044	.02124
16	.88966	-.01464	.11131	.01395	66	.03225	-.02920	.97369	.00773	116	.55536	.04833	1.59168	.02122
17	.87543	-.01640	.12564	.01469	67	.02547	-.02624	.98108	.00706	117	.57649	.04670	1.61288	.02116
18	.86050	-.01820	.14068	.01538	68	.01947	-.02320	.98781	.00641	118	.59754	.04500	1.63399	.02105
19	.84489	-.02006	.15641	.01604	69	.01426	-.02006	.99390	.00578	119	.61846	.04323	1.65498	.02091
20	.82864	-.02196	.17277	.01667	70	.00984	-.01683	.99936	.00517	120	.63921	.04141	1.67582	.02073
21	.81178	-.02389	.18974	.01726	71	.00626	-.01353	1.00426	.00462	121	.65975	.03954	1.69645	.02051
22	.79435	-.02584	.20728	.01780	72	.00347	-.01018	1.00806	.00413	122	.68005	.03764	1.71683	.02024
23	.77639	-.02781	.22534	.01831	73	.00152	-.00679	1.01251	.00375	123	.70006	.03570	1.73693	.01994
24	.75794	-.02979	.24390	.01878	74	.00037	-.00339	1.01610	.00350	124	.71974	.03376	1.75671	.01959
25	.73904	-.03177	.26290	.01921	75	.00000	-.00000	1.01951	.00341	125	.73904	.03177	1.77612	.01921
26	.71974	-.03376	.28231	.01959	76	.00037	.00339	1.02292	.00350	126	.75794	.02979	1.79512	.01878
27	.70006	-.03570	.30208	.01994	77	.00152	.00679	1.02660	.00375	127	.77639	.02781	1.81367	.01831
28	.68005	-.03764	.32218	.02024	78	.00347	.01018	1.03041	.00413	128	.79435	.02584	1.83174	.01780
29	.65976	-.03954	.34257	.02051	79	.00626	.01353	1.03477	.00462	129	.81178	.02389	1.84928	.01726
30	.63921	-.04141	.36320	.02073	80	.00984	.01683	1.03965	.00517	130	.82864	.02196	1.86625	.01667
31	.61846	-.04323	.38403	.02091	81	.01426	.02006	1.04512	.00578	131	.84489	.02006	1.88261	.01604
32	.59754	-.04500	.40502	.02105	82	.01947	.02320	1.05120	.00641	132	.86050	.01820	1.89833	.01538
33	.57649	-.04670	.42614	.02116	83	.02547	.02624	1.05793	.00706	133	.87543	.01640	1.91337	.01469
34	.55536	-.04833	.44734	.02122	84	.03225	.02920	1.06533	.00773	134	.88966	.01464	1.92770	.01395
35	.53417	-.04988	.46857	.02124	85	.03980	.03204	1.07339	.00840	135	.90313	.01296	1.94128	.01319
36	.51298	-.05134	.48982	.02123	86	.04809	.03478	1.08213	.00908	136	.91583	.01134	1.95408	.01239
37	.49182	-.05271	.51103	.02117	87	.05714	.03741	1.09154	.00975	137	.92772	.00981	1.96607	.01157
38	.47072	-.05397	.53216	.02108	88	.06691	.03991	1.10163	.01042	138	.93877	.00837	1.97722	.01072
39	.44972	-.05512	.55319	.02096	89	.07739	.04229	1.11238	.01108	139	.94897	.00702	1.98750	.00984
40	.42887	-.05615	.57407	.02079	90	.08858	.04453	1.12379	.01173	140	.95827	.00577	1.99689	.00893
41	.40818	-.05706	.59478	.02060	91	.10045	.04664	1.13585	.01238	141	.96667	.00463	2.00537	.00801
42	.38770	-.05783	.61527	.02037	92	.11300	.04860	1.14856	.01301	142	.97415	.00361	2.01291	.00707
43	.36747	-.05846	.63552	.02011	93	.12620	.05040	1.16187	.01363	143	.98068	.00271	2.01950	.00611
44	.34750	-.05895	.65549	.01981	94	.14003	.05206	1.17580	.01423	144	.98625	.00193	2.02513	.00514
45	.32785	-.05928	.67514	.01949	95	.15448	.05355	1.19033	.01481	145	.99086	.00129	2.02979	.00417
46	.30853	-.05946	.69446	.01914	96	.16952	.05488	1.20543	.01538	146	.99450	.00078	2.03346	.00319
47	.28958	-.05947	.71342	.01875	97	.18514	.05605	1.22109	.01593	147	.99719	.00040	2.03618	.00225
48	.27102	-.05932	.73197	.01835	98	.20131	.05704	1.23729	.01646	148	.99896	.00015	2.03796	.00089
49	.25289	-.05901	.75011	.01791	99	.21801	.05787	1.25401	.01697					
50	.23521	-.05852	.76779	.01745	100	.23521	.05852	1.27122	.01745					

*** PARAMETER UPDATE BY SUBROUTINE AUTO... BETA = 3.0 ***
*** PARAMETER UPDATE BY SUBROUTINE AUTO... CON =1.20 ***

********** NACA 0012 AIRFOIL SURFACE SOLUTION.....MINF = .750, ALPH = 1.000 DEG **********

***** SOLUTION AFTER 74 ITERATIONS, RMAX = .3456E-04, NSP = 110, CL(CIR) = .2441 *****

I	X/C	Y/C	CP	RHO	M	I	X/C	Y/C	CP	RHO	M	I	X/C	Y/C	CP	RHO	M
1	.9995	-.0001	.5082	.8726	.5292	51	.2097	-.0575	-.5086	.6530	.9640	101	.2620	.0592	-1.0831	.6150	1.2329
2	.9981	-.0003	.4640	.8636	.5497	52	.1932	-.0566	-.5083	.6531	.9638	102	.2803	.0594	-1.0809	.6135	1.2359
3	.9958	-.0006	.4199	.8545	.5697	53	.1773	-.0555	-.5037	.6542	.9618	103	.2991	.0595	-1.0918	.6128	1.2374
4	.9927	-.0010	.3760	.8454	.5894	54	.1620	-.0542	-.4947	.6562	.9580	104	.3182	.0594	-1.0988	.6130	1.2369
5	.9886	-.0016	.3323	.8364	.6087	55	.1473	-.0528	-.4813	.6593	.9522	105	.3377	.0591	-1.0841	.6147	1.2334
6	.9835	-.0023	.2993	.8295	.6231	56	.1331	-.0513	-.4635	.6633	.9445	106	.3576	.0587	-1.0672	.6190	1.2247
7	.9774	-.0032	.2702	.8234	.6357	57	.1196	-.0495	-.4413	.6684	.9350	107	.3776	.0582	-1.0287	.6286	1.2051
8	.9704	-.0041	.2430	.8177	.6474	58	.1067	-.0476	-.4147	.6744	.9237	108	.3979	.0575	-.9235	.6547	1.1530
9	.9625	-.0052	.2172	.8123	.6585	59	.0945	-.0456	-.3835	.6815	.9104	109	.4185	.0566	-.4870	.6580	.9546
10	.9536	-.0064	.1927	.8071	.6689	60	.0830	-.0434	-.3474	.6896	.8951	110	.4393	.0557	-.2283	.7162	.8451
11	.9439	-.0077	.1694	.8022	.6788	61	.0721	-.0411	-.3059	.6989	.8776	111	.4602	.0546	-.2789	.7067	.8630
12	.9332	-.0091	.1471	.7975	.6883	62	.0620	-.0387	-.2583	.7095	.8577	112	.4813	.0534	-.2892	.7027	.8706
13	.9218	-.0106	.1258	.7929	.6973	63	.0526	-.0361	-.2037	.7216	.8348	113	.5024	.0520	-.2931	.7018	.8723
14	.9095	-.0122	.1053	.7886	.7059	64	.0439	-.0335	-.1405	.7365	.8085	114	.5236	.0506	-.2883	.7029	.8703
15	.8964	-.0138	.0856	.7844	.7142	65	.0360	-.0307	-.0670	.7516	.7779	115	.5448	.0491	-.2784	.7051	.8661
16	.8825	-.0155	.0666	.7803	.7222	66	.0288	-.0278	.0197	.7703	.7418	116	.5659	.0475	-.2653	.7088	.8606
17	.8680	-.0173	.0482	.7764	.7299	67	.0224	-.0248	.1231	.7924	.6984	117	.5870	.0459	-.2501	.7114	.8542
18	.8527	-.0191	.0302	.7725	.7374	68	.0168	-.0217	.2476	.8187	.6455	118	.6080	.0441	-.2337	.7150	.8474
19	.8368	-.0210	.0127	.7688	.7447	69	.0120	-.0185	.3975	.8499	.5798	119	.6288	.0423	-.2165	.7188	.8402
20	.8202	-.0229	-.0044	.7651	.7518	70	.0080	-.0152	.5744	.8861	.4977	120	.6496	.0405	-.1989	.7227	.8328
21	.8031	-.0249	-.0213	.7615	.7589	71	.0048	-.0119	.7709	.9257	.3959	121	.6699	.0386	-.1809	.7267	.8253
22	.7854	-.0268	-.0379	.7579	.7658	72	.0024	-.0085	.9627	.9637	.2729	122	.6901	.0367	-.1628	.7306	.8178
23	.7672	-.0288	-.0543	.7543	.7726	73	.0009	-.0051	1.1048	.9915	.1308	123	.7099	.0347	-.1446	.7346	.8102
24	.7485	-.0308	-.0707	.7508	.7794	74	.0001	-.0017	1.1472	.9997	.0240	124	.7294	.0328	-.1263	.7386	.8026
25	.7294	-.0328	-.0870	.7472	.7862	75	.0001	.0017	1.0626	.9833	.1839	125	.7486	.0308	-.1079	.7427	.7949
26	.7099	-.0347	-.1033	.7437	.7930	76	.0009	.0051	.8617	.9438	.3421	126	.7672	.0288	-.0894	.7467	.7872
27	.6901	-.0367	-.1196	.7401	.7998	77	.0024	.0085	.5912	.8895	.4895	127	.7854	.0268	-.0708	.7507	.7795
28	.6699	-.0386	-.1361	.7365	.8067	78	.0048	.0119	.3110	.8319	.6180	128	.8031	.0249	-.0520	.7548	.7717
29	.6495	-.0405	-.1527	.7328	.8136	79	.0080	.0152	.0630	.7796	.7237	129	.8202	.0229	-.0331	.7589	.7638
30	.6288	-.0423	-.1696	.7291	.8206	80	.0120	.0185	-.1380	.7361	.8075	130	.8368	.0210	-.0138	.7631	.7558
31	.6080	-.0441	-.1866	.7254	.8277	81	.0168	.0217	-.2945	.7015	.8729	131	.8527	.0191	.0057	.7673	.7476
32	.5870	-.0459	-.2040	.7216	.8350	82	.0224	.0248	-.4162	.6741	.9243	132	.8680	.0173	.0257	.7716	.7393
33	.5659	-.0475	-.2216	.7177	.8423	83	.0288	.0278	-.5136	.6519	.9661	133	.8825	.0155	.0460	.7759	.7308
34	.5448	-.0491	-.2394	.7137	.8498	84	.0360	.0307	-.5998	.6319	1.0038	134	.8964	.0138	.0670	.7804	.7220
35	.5236	-.0506	-.2576	.7097	.8574	85	.0439	.0335	-.6630	.6172	1.0318	135	.9095	.0122	.0885	.7850	.7130
36	.5024	-.0520	-.2761	.7056	.8651	86	.0526	.0361	-.7132	.6053	1.0544	136	.9218	.0106	.1107	.7897	.7036
37	.4813	-.0534	-.2948	.7014	.8730	87	.0620	.0387	-.7591	.5944	1.0754	137	.9332	.0091	.1338	.7946	.6939
38	.4602	-.0546	-.3137	.6972	.8809	88	.0721	.0411	-.8007	.5845	1.0946	138	.9439	.0077	.1577	.7997	.6838
39	.4393	-.0557	-.3328	.6929	.8890	89	.0830	.0434	-.8390	.5752	1.1126	139	.9536	.0064	.1826	.8050	.6732
40	.4185	-.0566	-.3520	.6886	.8971	90	.0945	.0456	-.8740	.5668	1.1291	140	.9625	.0052	.2086	.8105	.6622
41	.3979	-.0575	-.3711	.6843	.9052	91	.1067	.0476	-.9053	.5591	1.1441	141	.9704	.0041	.2357	.8162	.6506
42	.3776	-.0582	-.3901	.6800	.9132	92	.1196	.0495	-.9335	.5522	1.1578	142	.9774	.0032	.2642	.8222	.6383
43	.3575	-.0587	-.4088	.6758	.9211	93	.1331	.0513	-.9589	.5460	1.1702	143	.9835	.0023	.2946	.8286	.6251
44	.3377	-.0591	-.4269	.6717	.9289	94	.1473	.0528	-.9819	.5403	1.1816	144	.9886	.0016	.3288	.8356	.6102
45	.3182	-.0594	-.4442	.6677	.9363	95	.1620	.0542	-1.0026	.5352	1.1919	145	.9927	.0010	.3737	.8450	.5904
46	.2991	-.0595	-.4604	.6641	.9432	96	.1773	.0555	-1.0211	.5305	1.2012	146	.9958	.0006	.4188	.8543	.5702
47	.2803	-.0594	-.4750	.6607	.9495	97	.1932	.0566	-1.0376	.5264	1.2095	147	.9981	.0003	.4641	.8636	.5496
48	.2620	-.0592	-.4877	.6578	.9549	98	.2097	.0575	-1.0520	.5228	1.2169	148	.9995	.0001	.5096	.8729	.5285
49	.2440	-.0588	-.4979	.6555	.9593	99	.2266	.0582	-1.0645	.5197	1.2233	149	.9995	-.0001	.5082	.8726	.5292
50	.2266	-.0582	-.5050	.6538	.9624	100	.2440	.0588	-1.0749	.5170	1.2287						

*** LIFT, WAVE DRAG, AND QUARTER-CHORD MOMENT COEFFICIENTS.....CL = .2426, CD = .0014, CM = .0003 ***

INPUT/OUTPUT example 2- These data cards are the input for INPUT/OUTPUT example 2 — an IOPT=4 case using the CAST 7 airfoil. Please note the format of the airfoil coordinates. The output for this case is shown on the next page.

```
 $FLOWIN  MINF=Ø.7,ALPH=1.5,NOUT=3,    $
 $GRIDIN  IOPT=4,    $
********** CAST 7 AIRFOIL
   61
   1.ØØØØØ   -.ØØ215
    .9775Ø   -.ØØ123
    .95ØØØ   -.ØØØ4Ø
    .92ØØØ    .ØØØ79
    .875ØØ    .ØØ1Ø4
    .815ØØ   -.ØØ2Ø9
    .755ØØ   -.ØØ81Ø
    .695ØØ   -.Ø1566
    .635ØØ   -.Ø2372
    .575ØØ   -.Ø3153
    .515ØØ   -.Ø3854
    .455ØØ   -.Ø443Ø
    .395ØØ   -.Ø4836
    .335ØØ   -.Ø5Ø27
    .275ØØ   -.Ø4965
    .215ØØ   -.Ø4632
    .155ØØ   -.Ø4Ø4Ø
    .115ØØ   -.Ø3518
    .Ø875Ø   -.Ø31Ø2
    .Ø65ØØ   -.Ø2713
    .Ø475Ø   -.Ø2363
    .Ø35ØØ   -.Ø2Ø85
    .Ø25ØØ   -.Ø1853
    .Ø175Ø   -.Ø1663
    .Ø125Ø   -.Ø15Ø5
    .ØØ75Ø   -.Ø127Ø
    .ØØ5ØØ   -.Ø1Ø82
    .ØØ35Ø   -.ØØ927
    .ØØ2ØØ   -.ØØ713
    .ØØ1ØØ   -.ØØ5Ø6
    .ØØØ4Ø   -.ØØ319
   Ø.ØØØØØ   Ø.ØØØØØ
    .ØØØ4Ø    .ØØ337
    .ØØ1ØØ    .ØØ531
    .ØØ2ØØ    .ØØ754
    .ØØ35Ø    .Ø1Ø12
    .ØØ5ØØ    .Ø1229
    .ØØ75Ø    .Ø1534
    .Ø125Ø    .Ø2Ø11
    .Ø35ØØ    .Ø3273
    .Ø475Ø    .Ø377Ø
    .Ø65ØØ    .Ø43Ø8
    .Ø875Ø    .Ø4827
    .115ØØ    .Ø53Ø3
    .155ØØ    .Ø58Ø9
    .215ØØ    .Ø6312
    .275ØØ    .Ø6617
    .335ØØ    .Ø6787
    .395ØØ    .Ø6851
    .455ØØ    .Ø6817
    .515ØØ    .Ø6676
    .575ØØ    .Ø6418
    .635ØØ    .Ø6ØØ8
    .695ØØ    .Ø5423
    .755ØØ    .Ø4639
    .815ØØ    .Ø3662
    .875ØØ    .Ø2541
    .92ØØØ    .Ø1651
    .95ØØØ    .Ø1Ø5Ø
    .9775Ø    .ØØ385
   1.ØØØØØ   -.ØØ215
```

********** CAST 7 AIRFOIL SURFACE SOLUTION.....MINF = .700, ALPH = 1.500 DEG **********

***** SOLUTION AFTER 85 ITERATIONS, RMAX = .4069E-04, NSP = 191, CL(CIR) = 1.0072 *****

I	X/C	Y/C	CP	RHO	M	I	X/C	Y/C	CP	RHO	M	I	X/C	Y/C	CP	RHO	M
1	.9995	-.0021	.4549	.8779	.5169	51	.2098	-.0459	-.8659	.7788	.7253	101	.2651	.0658	-1.4545	.4832	1.2993
2	.9981	-.0021	.4353	.8743	.5253	52	.1934	-.0445	-.8358	.7848	.7134	102	.2834	.0665	-1.4449	.4855	1.2945
3	.9958	-.0020	.4159	.8707	.5337	53	.1776	-.0429	-.0027	.7911	.7010	103	.3022	.0671	-1.4341	.4880	1.2891
4	.9926	-.0018	.3964	.8670	.5419	54	.1623	-.0412	.0304	.7975	.6883	104	.3213	.0676	-1.4226	.4900	1.2833
5	.9885	-.0016	.3770	.8634	.5500	55	.1476	-.0395	.0636	.8039	.6755	105	.3408	.0680	-1.4097	.4938	1.2770
6	.9833	-.0014	.3693	.8620	.5532	56	.1334	-.0377	.0965	.8102	.6627	106	.3606	.0683	-1.3960	.4970	1.2702
7	.9772	-.0012	.3630	.8608	.5558	57	.1199	-.0359	.1284	.8163	.6502	107	.3807	.0684	-1.3807	.5005	1.2628
8	.9702	-.0010	.3536	.8590	.5598	58	.1071	-.0340	.1588	.8221	.6383	108	.4010	.0685	-1.3639	.5045	1.2546
9	.9622	-.0008	.3426	.8570	.5643	59	.0948	-.0322	.1881	.8277	.6267	109	.4216	.0685	-1.3446	.5089	1.2454
10	.9532	-.0005	.3371	.8559	.5666	60	.0833	-.0303	.2174	.8333	.6151	110	.4424	.0683	-1.3214	.5143	1.2343
11	.9434	-.0001	.3463	.8577	.5628	61	.0723	-.0285	.2486	.8392	.6026	111	.4634	.0680	-1.2903	.5214	1.2197
12	.9327	.0003	.3691	.8619	.5533	62	.0621	-.0266	.2847	.8461	.5880	112	.4844	.0676	-1.2433	.5322	1.1979
13	.9211	.0008	.3933	.8665	.5432	63	.0525	-.0247	.3274	.8541	.5706	113	.5056	.0671	-1.1592	.5511	1.1600
14	.9088	.0011	.4098	.8696	.5362	64	.0437	-.0228	.3762	.8633	.5504	114	.5268	.0664	-.9223	.6033	1.0584
15	.8956	.0012	.4184	.8712	.5326	65	.0356	-.0210	.4227	.8720	.5307	115	.5480	.0655	-.4728	.6976	.8802
16	.8816	.0012	.4217	.8718	.5312	66	.0279	-.0192	.4550	.8780	.5169	116	.5692	.0645	-.4390	.7045	.8672
17	.8669	.0008	.4203	.8715	.5317	67	.0211	-.0176	.4678	.8804	.5113	117	.5903	.0633	-.5095	.6901	.8943
18	.8516	.0002	.4147	.8705	.5341	68	.0149	-.0159	.4735	.8814	.5089	118	.6113	.0619	-.5536	.6810	.9113
19	.8356	-.0006	.4053	.8687	.5381	69	.0095	-.0138	.5383	.8934	.4802	119	.6322	.0603	-.5789	.6750	.9211
20	.8189	-.0018	.3923	.8663	.5436	70	.0052	-.0110	.7661	.9351	.3687	120	.6528	.0585	-.5906	.6734	.9256
21	.8017	-.0032	.3761	.8632	.5584	71	.0022	-.0075	1.0311	.9827	.1878	121	.6732	.0566	-.5906	.6734	.9256
22	.7840	-.0049	.3566	.8596	.5586	72	.0005	-.0037	1.1283	1.0000	.0998	122	.6934	.0544	-.5783	.6769	.9209
23	.7658	-.0069	.3345	.8554	.5677	73	.0000	.0000	1.0203	.9808	.1973	123	.7132	.0521	-.5545	.6808	.9116
24	.7472	-.0090	.3103	.8509	.5776	74	.0004	.0035	.7784	.9373	.3621	124	.7326	.0496	-.5224	.6875	.8992
25	.7281	-.0114	.2845	.8460	.5881	75	.0016	.0067	.5165	.8894	.4899	125	.7516	.0469	-.4840	.6953	.8845
26	.7087	-.0139	.2571	.8408	.5992	76	.0033	.0098	.2820	.8455	.5891	126	.7702	.0441	-.4401	.7043	.8676
27	.6889	-.0165	.2288	.8355	.6106	77	.0054	.0128	.0417	.7996	.6839	127	.7882	.0412	-.3939	.7136	.8500
28	.6689	-.0192	.1997	.8299	.6221	78	.0081	.0160	-.2281	.7468	.7869	128	.8058	.0382	-.3485	.7228	.8327
29	.6486	-.0219	.1700	.8243	.6339	79	.0114	.0192	-.5307	.6858	.9024	129	.8228	.0352	-.3053	.7314	.8163
30	.6280	-.0247	.1400	.8186	.6457	80	.0155	.0224	-.8498	.6189	1.0286	130	.8392	.0323	-.2642	.7397	.8006
31	.6073	-.0274	.1100	.8128	.6574	81	.0203	.0255	-.9967	.5871	1.0895	131	.8549	.0293	-.2242	.7476	.7855
32	.5864	-.0301	.0801	.8071	.6690	82	.0260	.0286	-1.0493	.5766	1.1119	132	.8700	.0264	-.1840	.7556	.7702
33	.5654	-.0327	.0506	.8014	.6805	83	.0324	.0316	-1.0483	.5768	1.1116	133	.8844	.0235	-.1424	.7638	.7544
34	.5444	-.0352	.0216	.7958	.6917	84	.0395	.0346	-1.0268	.5895	1.1238	134	.8981	.0208	-.1033	.7714	.7396
35	.5233	-.0376	-.0068	.7903	.7026	85	.0474	.0377	-1.1697	.5488	1.1646	135	.9110	.0183	-.0739	.7772	.7283
36	.5022	-.0399	-.0345	.7849	.7132	86	.0560	.0405	-1.2621	.5279	1.2066	136	.9232	.0159	-.0637	.7792	.7244
37	.4811	-.0420	-.0612	.7797	.7234	87	.0654	.0432	-1.3314	.5120	1.2391	137	.9346	.0137	-.0692	.7781	.7266
38	.4601	-.0439	-.0864	.7747	.7331	88	.0755	.0457	-1.3848	.4998	1.2644	138	.9451	.0116	-.0682	.7783	.7261
39	.4392	-.0456	-.1098	.7702	.7420	89	.0863	.0480	-1.4237	.4905	1.2839	139	.9547	.0095	-.0600	.7836	.7157
40	.4185	-.0470	-.1307	.7661	.7499	90	.0978	.0502	-1.4518	.4839	1.2979	140	.9634	.0074	.0094	.7934	.6964
41	.3979	-.0482	-.1486	.7626	.7567	91	.1100	.0523	-1.4697	.4796	1.3070	141	.9711	.0055	.0665	.8044	.6743
42	.3776	-.0492	-.1626	.7598	.7621	92	.1229	.0542	-1.4801	.4772	1.3123	142	.9780	.0037	.1234	.8154	.6522
43	.3575	-.0498	-.1724	.7579	.7658	93	.1364	.0560	-1.4855	.4759	1.3150	143	.9839	.0022	.1705	.8259	.6306
44	.3377	-.0502	-.1772	.7569	.7676	94	.1505	.0576	-1.4873	.4754	1.3160	144	.9888	.0009	.2331	.8363	.6088
45	.3182	-.0504	-.1765	.7570	.7674	95	.1653	.0591	-1.4868	.4756	1.3157	145	.9929	-.0002	.2945	.8479	.5840
46	.2991	-.0502	-.1702	.7583	.7650	96	.1806	.0605	-1.4848	.4760	1.3147	146	.9960	-.0011	.3563	.8595	.5587
47	.2803	-.0498	-.1586	.7606	.7606	97	.1965	.0618	-1.4815	.4768	1.3130	147	.9981	-.0016	.4184	.8711	.5326
48	.2620	-.0492	-.1415	.7639	.7541	98	.2129	.0630	-1.4766	.4788	1.3105	148	.9995	-.0020	.4808	.8828	.5057
49	.2441	-.0483	-.1198	.7682	.7458	99	.2298	.0640	-1.4704	.4795	1.3073	149	.9995	-.0021	.4549	.8779	.5169
50	.2267	-.0472	-.0944	.7732	.7361	100	.2472	.0650	-1.4631	.4812	1.3036						

*** LIFT, WAVE DRAG, AND QUARTER-CHORD MOMENT COEFFICIENTS.....CL = 1.0008, CD = .0042, CM =-.1470 ***

INPUT/OUTPUT example 3- The cards below form the data deck for the multiple case run for INPUT/OUTPUT example 3. Note that due to the use of the MESH=1 option, no GRIDIN card is necessary for the last three solutions. The output for this example is shown on the next page.

```
$FLOWIN  MINF=Ø.7,ALPH=Ø.Ø,NOUT=2,NCASE=4,    $
$GRIDIN  IOPT=5,    $
$FLOWIN  MINF=Ø.7,ALPH=Ø.5,NOUT=2,MESH=1,    $
$FLOWIN  MINF=Ø.7,NOUT=2,MESH=1,    $
$FLOWIN  MINF=Ø.7,ALPH=2.Ø,NOUT=2,MESH=1,    $
```

```
     ***** SOLUTION AFTER   29 ITERATIONS,   RMAX = .2784E-04,   NSP =  13,   CL(CIR) =  .5293 *****
*** LIFT, WAVE DRAG, AND QUARTER-CHORD MOMENT COEFFICIENTS......CL =  .5263,   CD =-.0005,   CM =-.1324  ***

     ***** SOLUTION AFTER   53 ITERATIONS,   RMAX = .3347E-04,   NSP =  37,   CL(CIR) =  .6286 *****
*** LIFT, WAVE DRAG, AND QUARTER-CHORD MOMENT COEFFICIENTS......CL =  .6250,   CD =-.0004,   CM =-.1320  ***

     ***** SOLUTION AFTER   67 ITERATIONS,   RMAX = .4122E-04,   NSP =  73,   CL(CIR) =  .7331 *****
*** LIFT, WAVE DRAG, AND QUARTER-CHORD MOMENT COEFFICIENTS......CL =  .7287,   CD =  .0001,   CM =-.1301  ***

     ***** SOLUTION AFTER  102 ITERATIONS,   RMAX = .3877E-04,   NSP = 187,   CL(CIR) =  .9834 *****
*** LIFT, WAVE DRAG, AND QUARTER-CHORD MOMENT COEFFICIENTS......CL =  .9768,   CD =  .0041,   CM =-.1294  ***
```

3. DETAILED OPERATION

This chapter discusses additional input/output options available in TAIR and provides more information about parameters defined in chapter 2. Additional INPUT/OUTPUT examples are included to embellish this more detailed discussion. The default values of the acceleration parameters listed in this section have been optimized for the standard transonic case. The use of some options requires that these acceleration parameters be changed to aid convergence or to prevent divergence. Some of the necessary changes are written into SUBROUTINE CHECK discussed in chapter 4 and, therefore, are implemented automatically. Other changes can be made by the user; they are discussed in this chapter. The examples show some of the different ways in which TAIR can be used, with appropriate changes in various parameters.

The input parameters discussed in this chapter include not only new variables, but also more complete information for some of the parameters described in chapter 2. If a particular parameter must be changed for a certain option, a note will be made in the description of that option to that effect. All program variable and subroutine names are capitalized. In addition, any program variable mentioned but not defined below is defined in appendix B.

Description of FLOWIN NAMELIST Parameters

AFAC ALPHA multiplier parameter. The value of ALPHA (see definition in appendix B and more detailed discussion in chapter 5) near the airfoil boundary, that is, within NRING ξ lines of the airfoil boundary, is restricted to never fall below AFAC*ALOW. This allows ALOW to be made smaller, that is, larger effective pseudotime steps over most of the flow field, and, therefore, it provides for much faster convergence. NRING and ALOW are inputs and are defined later in this section. Acceptable values: real numbers between 1.0 and 20.0. Default value: 14.0.

AHIGH Largest element in the ALPHA acceleration parameter sequence. This element represents the inverse of the minimum pseudotime step in a sequence of M elements. The larger values of ALPHA damp out the high-frequency errors in the solution. The combination of the two default ALOW and AHIGH parameters leads to the fastest convergence for the most cases. Acceptable values: real numbers greater than 0.5. Default value: 1.5.

ALOW Smallest element in the ALPHA acceleration parameter sequence. This element represents the inverse of the maximum pseudotime step in a sequence of M elements. The smaller values in this sequence damp out the low-frequency errors. The default ALOW value (0.07) is very close to the stability bound — for instance ALOW=0.06 is usually unstable. It is insensitive to small changes to the grid (changing airfoils, etc.), but very sensitive to major changes to the number of points in the grid or to the spacing. The running of TAIR with a GRAPE grid is

one of these changes; ALOW=0.07 is unstable and must be increased to 0.08. This change will be made within CHECK if that subroutine is called. A large change in RADMAX or BINN in the GRIDIN NAMELIST might also necessitate a change in ALOW. Acceptable values: real numbers between 0.05 and 1.0. Default value: 0.07.

BETA $\Phi_{\xi t}$ coefficient. Proper specification of this parameter is very important for maintaining algorithm stability. SUBROUTINE AUTO contains a fairly complex modification or updating procedure for BETA, based on the changes in the average and maximum residuals and the NSP and circulation (GNP) buildups. If the user were to switch off SUBROUTINE AUTO, the default BETA would probably be too high for optimal convergence, but would maintain stability for most cases. Generally, small values of BETA (~1.0) are required for small regions of supersonic flow, moderate values of BETA (~3.0 to 4.0) are required for moderate regions of supersonic flow, etc. (See chap. 5 for a detailed description of the BETA update logic.) Acceptable values: positive real numbers. Default value: 4.5.

CON Parameter controlling amount of upwind bias on the density. The default value is set for strong-shock cases and should be lowered by the user for easier cases if AUTO (which decreases CON automatically in these cases) has been turned off. The higher the CON value, the more the shock profile is smeared. Acceptable values: real numbers between 0.5 and 4.0. Default value: 2.0.

ERR Convergence criteria. There are two different convergence tests available in TAIR. The sign of ERR designates which test is used, and the magnitude specifies the convergence tolerance.

ERR<0.0...The solution is declared converged after N iterations if the following three conditions are met:

$$(1)\ \frac{RMAX^N}{RMAX^1} \le |ERR|$$

$$(2)\ \frac{|NSP^N - NSP^{N-M}|}{NSP^N} \le \frac{|ERR|}{2}$$

$$(3)\ \frac{|\Gamma^N - \Gamma^{N-M}|}{\Gamma^N} \le \frac{|ERR|}{2}$$

where NSP is the number of supersonic points, Γ is the circulation (GNP), and M is the number of elements in the ALPHA acceleration parameter sequence (see subsequent discussion of M). Suggested value: -0.01.

ERR>0.0...The solution is declared converged after N iterations if:

$$\frac{RMAX^N}{RMAX^1} \leq ERR$$

Suggested value: 0.001.

If $RMAX^N$ ever exceeds 10 times $RMAX^1$ then the iteration process is terminated and a message is printed indicating solution divergence. Acceptable values: $|ERR| \leq 0.05$. Default value: -0.01.

G Ratio of specific heats. TAIR can be used for computations involving different fluids by changing G. Acceptable values: real numbers between 1.0 and 2.0. Default value: 1.4 (air).

IAUTO Switch for SUBROUTINE AUTO.

IAUTO=1...SUBROUTINE AUTO is turned on; solution parameters (BETA, CON, NDIF, and RGAM) are automatically updated in an attempt to optimize convergence.

IAUTO=0...SUBROUTINE AUTO bypassed; default or user-supplied values remain unchanged.

Acceptable values: 0,1. Default value: 1.

ICHECK Switch for SUBROUTINE CHECK.

ICHECK=1...Input data checked for consistency. Both of the NAMELISTs and the airfoil coordinates (if read in) are checked. If any out-of-range or incorrect value is found then CHECK will either print a warning, correct the value, or cause the solution to be terminated.

ICHECK=0...Input data not checked.

Acceptable values: 0,1. Default value: 1.

IINCR Grid solution output increment. If the final grid coordinates are printed (NOUT=9), the ξ-direction values will be printed with an IINCR increment. Acceptable values: positive integers. Default value: 3.

JINCR Grid solution output increment. If the final grid coordinates are printed (NOUT=9), the η-direction values will be printed with a JINCR increment. Acceptable values: positive integers. Default value: 2.

K Starting element in the ALPHA sequence. K is increased by one before the sequence starts. Acceptable values: positive integers from 0 to M-1. Default value: 0.

M Number of elements in the ALPHA sequence. Acceptable values: integers greater than 1, greater than K, and less than 20. Default value: 8.

MESH Determines which grid generation option is used.

MESH=0...The grid is generated within the program (discussed in chap. 2).

MESH=1...This option reads the grid from unit 48. In addition to being useful for multiple-case runs, this option can be used to read the coordinates of a grid generated elsewhere. The required unformatted inputs are: first record — title of either the airfoil or the mesh used (28 characters); second record — the grid dimensions, NX and NY, and the third record — the grid coordinates, X and Y, read in using (X(I,J),Y(I,J),I=1,NX),J=1,NY)). NX and NY should be the same as NI and NJ — if not, the program will automatically change NI and NJ to NX and NY. It is the user's responsibility to make sure that the program dimensions are not exceeded. See appendix A for directions on how to change the present program dimensions. The GRIDIN NAMELIST data card is not required for MESH=1.

MESH=2...This option reads an initial solution grid from logical unit 48 (same format as above), and adapts it to a new airfoil. This is accomplished by subtracting the difference between the original and new airfoils from each grid point, including the outer boundary grid points. This option is designed for small perturbations between the two airfoils (specifically numerical optimization). If two radically different airfoils are used, the program may generate a flow-field solution with slight inaccuracies. The GRIDIN data card with the airfoil data must be included with this option.

MESH=3...Implementation of this option causes TAIR to read a mesh created by a computer program called GRAPE (ref. 5). The airfoil selection is made within GRAPE, which generates the Poisson grid and writes the information to logical unit 7. TAIR reads this information from logical unit 48, which includes NX and NY, the number of ξ and η coordinates, respectively; TEOPEN, the vertical distance across the trailing edge (important if running an open trailing-edge case); and X and Y, the grid coordinates. The READ statement used for this option in TAIR is compatible with the WRITE statement in GRAPE. This option also performs two tasks necessary to make the GRAPE grid compatible with the TAIR flow solver. First, the ξ lines in GRAPE are numbered from the inner boundary (body surface) to the outer boundary and must be reordered to be consistent with TAIR. The second task concerns the trailing edge of the airfoil. TAIR has its first and NIth points in the

ξ direction located at the trailing edge. This creates a line of double-stored points if the trailing edge is closed, or two parallel lines of points separated by TEOPEN if the trailing edge is open (see fig. 2). When GRAPE is used with TAIR, the GRAPE parameter NTETYP must be set to one, and JMAX, the number of ξ coordinates in GRAPE, must be set to NI-1. This creates the GRAPE mesh shown in figure 2, which is not completely consistent with TAIR. Thus, the second task performed by TAIR is to add the additional line of grid points required by the TAIR flow solver. For good convergence when running GRAPE with TAIR, the ALOW acceleration parameter should be set to 0.08. This is automatically done in SUBROUTINE CHECK. If CHECK is not turned on, that is, if ICHECK=0 (see ICHECK logic discussed above), the user should make the change. Also, NX, NY, NI, and NJ are tested in TAIR, and if the two sets of mesh dimensions differ, NI and NJ will be changed to match with the GRAPE grid. As in the MESH=1 option, the GRIDIN NAMELIST card is not required.

Acceptable values: 0,1,2,3. Default value: 0.

NCASE The number of solutions per job. If several cases using GRAPE-generated grids are run on one job, the mesh parameter must always be set to 3, neither the MESH=1 nor the MESH=2 READ format is compatible with the GRAPE WRITE format. If these GRAPE-generated grid solutions are combined with TAIR-generated grid solutions, the GRAPE cases must be run first, as the MESH=0 option will overwrite unit 48 with the TAIR-generated grid coordinates. INPUT/OUTPUT example 4 shows a multiple-case run that addresses this situation. Acceptable values: any positive integer. Default value: 1.

NDIF Rotated differencing parameter. NDIF must be turned on for cases with strong shocks at the trailing edge to maintain stability. SUBROUTINE AUTO automatically turns the rotated differencing on when it detects the shock moving to the trailing edge.

NDIF=0...No rotated differencing. The spatial differencing scheme is upwind biased along only the ξ direction.

NDIF=1...Rotated differencing. The spatial differencing scheme is upwind biased along both the ξ and η directions.

Acceptable values: 0,1. Default value: 0.

NOUT1 Solution output frequency. An intermediate solution controlled by NOUT (CP's, densities, aerodynamic coefficients, etc.) will be printed every NOUT1 iterations. Note: when the iteration terminates either because the iteration limit (N=NSTEPS) is encountered or because of convergence, a solution is automatically printed. Acceptable values: positive integers. Default value: 201.

NOUT2 Convergence parameter output frequency. The convergence parameters, including RMAX, CMAX, NSP, ALPHA, BETA, and GNP, will be printed every iteration for the first M iterations, and then every NOUT2 iterations. Acceptable values: positive integers. Default value: 8.

NRING Number of inner ξ lines (η = constant lines) for which AFAC logic is applied. Acceptable values: integers between 2 and 10. Default value: 3.

OMEGA Relaxation parameter for the flow-solver algorithm. Linear stability of the AF2 algorithm is maintained for values of OMEGA between 0 and 2. In the present nonlinear case values slightly less than 2 are required for stability with the optimum value being near 1.8. Acceptable values: 0.0 to 2.0. Default value: 1.8.

RGAM Circulation relaxation parameter. If RGAM is too low, the circulation buildup and solution convergence will be slow. If RGAM is too high, the circulation will develop a divergent oscillation. The input value of RGAM is modified or updated as the solution continues by internal logic (MAIN and AUTO). (See chap. 5 for the theory behind this control.) RGAM's effect on convergence is relatively minor except in the case of a shock near the trailing edge. Under this circumstance a lower value of RGAM is automatically implemented when AUTO logic is activated (IAUTO=1). Acceptable values: real numbers between 0.2 and 1.5. Default value: 1.0.

Description of GRIDIN NAMELIST Parameters

AHGRID Largest value in the ALPHA acceleration parameter sequence used for grid generation. Acceptable values: real numbers between 0.01 and 0.05. Default value: 0.02.

ALGRID Smallest value in the ALPHA acceleration parameter sequence used for grid generation. Acceptable values: numbers greater than 0.0 and smaller than 0.01. Default value: 0.00001.

BINN Stretching parameter affecting the grid-point distribution on the inner boundary (airfoil surface).

BINN=0.0...The grid points are distributed evenly. This option is not suitable for airfoils. A warning message will be printed by CHECK if this option is run with any geometry except the circular cylinder geometry (IOPT=3).

BINN=-2.0...The surface grid-point distribution in terms of arc length is read from cards. The first card has the number of points in the array, NS (format I5). The next cards contain the distribution points, starting with 0 at the lower trailing-edge point moving clockwise around the airfoil to 1 at the upper trailing-edge point (format 8F10.6). If NS and NI differ, the

arc-length distribution read from cards will be automatically scaled by cubic spline interpolation to match the NI dimension exactly.

BINN=-1.0...The grid-point distribution is established from a data statement, which was developed by using a circle plane conformal mapping about the NACA 0012 airfoil. If the number of points in the data statement (151) and the number in NI are different, then the arc-length distribution given by the data statement will be automatically scaled in number by cubic spline interpolation to match the NI dimension.

BINN.GT.1.0...(and .LT.10.0) The surface distribution is established from a clustering formula. Values closer to 1 will cluster more at the airfoil leading and trailing edges. Values of BINN much larger than 1 will cause the grid point distribution to approach equal spacing. The suggested airfoil value for this option is 1.05.

Acceptable values: -2.0, -1.0, 0.0, real numbers between 1.0 and 10.0, exclusive. Default value: -1.0.

ERGRID Convergence tolerance for grid generation. Acceptable values: real numbers less than or equal to 0.01. Default value: 0.01.

HTMAX Height of rectangular outer boundary (IOUT=3). Acceptable values: real numbers between 2.0 and 8.0. Default value: 4.0.

IOPEN Open or closed trailing-edge option (IOPT=1 only; IOPEN is ignored for all other values of IOPT).

IOPEN=0...Trailing edge is closed. The standard NACA 00XX airfoil profile is extended to a point at the trailing edge and renormalized.

IOPEN=1...Trailing edge is open. The program will generate a standard NACA 00XX airfoil with the associated opening at the trailing edge.

Acceptable values: 0,1. Default value: 0.

IOPT Determines which airfoil option is used.

IOPT=1...This generates a NACA-00XX-type airfoil with thickness determined by TMAX.

IOPT=2...This IOPT option produces a circular-arc airfoil. The thickness is determined by the TMAX parameter and the leading-edge bluntness by the XC parameter (discussed below). The clustering parameter BINN is automatically changed in CHECK (BINN=1.03) for this option to provide

more grid point clustering at the airfoil leading edge, the smallest element of the ALPHA sequence ALOW is increased to 0.1, and AFAC is increased to 20.

IOPT=3...This option produces a circular cylinder cross-section geometry. BINN is automatically set to zero in SUBROUTINE CHECK, providing equal spacing around the circular perimeter.

IOPT=4...This IOPT permits the user to read in an arbitrary airfoil geometry (see chap. 2).

IOPT=5...The Korn airfoil is used for this option (airfoil 75-06-12 in ref. 6).

Acceptable values: 1,2,3,4,5. Default value: 1.

IOUT Determines which outer boundary is used.

IOUT=1...This generates a circular outer boundary with radius RADMAX centered at XCN and YCN.

IOUT=2...The outer boundary is read from cards. First all X coordinates are read from 1 to NI-1 in the first record, followed by all the Y coordinates in the second record (format 8F10.0).

IOUT=3...This option generates a base rectangular outer boundary with semicircular upstream and downstream ends. The dimensions of the base rectangle are controlled by HTMAX and WDTHMX. When the rectangle becomes too elongated, more grid points in the η-direction will be required to maintain accuracy. In addition, the acceleration parameters may need to be reevaluated for some of these cases.

Acceptable values: 1,2,3. Default value: 1.

KGRID Starting element in the ALPHA sequence used for grid generation. Acceptable values: integers between 0 and MGRID-1. Default value: 0.

MAXIT Maximum number of iterations for grid generation. Acceptable values: integers between 10 and 100. Default value: 50.

MGRID Number of elements in ALPHA sequence used for grid generation. Acceptable values: integers greater than 1 and greater than KGRID. Default value: 8.

OMEG Relaxation factor for grid generation. Acceptable values: real numbers between 1.0 and 2.0. Default value: 2.0.

RADMAX Circular outer boundary radius (IOUT=1). The center of the circle is placed at XCN and YCN, and the radial distance is nondimensionalized

by the chord. RADMAX is related to NJ; if RADMAX is increased dramatically, then NJ should be increased. Acceptable values: real numbers between 3.0 and 18.0. Default value: 6.0.

WDTHMX Width of rectangular outer boundary (IOUT=3). Suggested WDTHMX/HTMAX ratio should not greatly exceed 2. Acceptable values: real numbers between 4.0 and 12.0. Default value: 6.0.

XC Leading-edge bluntness parameter for IOPT=2 case. The leading edge of the circular-arc airfoil will be blunted according to the parameter XC. A parabola will be matched to the airfoil leading edge (both position and slope) at X/C=XC (see fig. 3). Smaller values of XC will produce smaller amounts of blunting. Once blunted, the airfoil is renormalized, causing the maximum thickness to be slightly larger than TMAX. Acceptable values: real numbers between 0.2 and 0.4. Default value: 0.2.

XCN The X coordinate for the center of the circular outer boundary (IOUT=1). XCN is normalized by chord and measured with respect to the airfoil leading edge. Acceptable values: real numbers between -1.0 and 1.0. Default value: 0.5.

YCN The Y coordinate for the center of the circular outer boundary (IOUT=1). YCN is normalized by chord and measured with respect to the airfoil leading edge. Acceptable values: real numbers between -1.0 and 1.0. Default value: 0.0.

INPUT/OUTPUT Examples

This section contains two INPUT/OUTPUT examples. The first (example 4) describes most of the output available beyond the default output (INPUT/OUTPUT example 1 in chap. 2 described all the default output, NOUT $\leq$ 5). The second example (example 5) compares two TAIR solutions, one with an internally generated grid and the other with a GRAPE-generated grid. Discussion is included for each example.

Example 4 is the default case, that is, NACA 0012 airfoil, MINF=0.75, and ALPH=1.0, with the NOUT value changed from the default value of 5 to 8. The input consists of the two NAMELIST data cards, with the NOUT change on the FLOWIN card. The output shown in example 4 is only the additional output generated beyond the default output previously discussed in chapter 2. The last NOUT option, NOUT=9, generates all of the above output plus the grid coordinates. Because of its length, this grid output will not be shown; however, it will be discussed at the end of this section.

The first page of output after the interpolated coordinates contains the convergence history for the ADI grid generation routine. From left to right, the columns are: N, the iteration number; CXMAX, the maximum correction for the X equation; I and J, the position of CXMAX; CYMAX, the maximum correction for the Y equation; I and J, the position of CYMAX; RXMAX, the maximum residual for the X equation; I and J, the position of RXMAX; RYMAX, the maximum

residual for the Y equation; I and J, the position of RYMAX; and ALPHA, the acceleration parameter sequence used for the ADI method. This output will be printed if NOUT≥8. For a description of the internal grid generation algorithm, see chapter 5.

The next three pages of output in example 4 list the transformation metrics (A1, A2, A3, and XJ) for the ξ lines nearest the airfoil. The XJ quantity is the Jacobian of the transformation and is approximately proportional to the negative inverse of the cell area. The A1, A2, and A3 metric arrays used in TAIR are computed from

$$A1 = [\nabla\xi \cdot \nabla\xi]/XJ$$

$$A2 = [\nabla\xi \cdot \nabla\eta]/[4*XJ]$$

$$A3 = [\nabla\eta \cdot \nabla\eta]/XJ$$

and differ slightly from the A_1, A_2, and A_3 metric quantities discussed in the theory (see chap. 5). The A2 quantity indicates the level of cell skewness: if A2 is zero, the cell is orthogonal. A1 is approximately equal to the ratio of the normal side of the cell to the tangential side. A3 is approximately the inverse of A1. A1, A3, and XJ must always be negative due to the left-handed coordinate system used in the code. A change in sign in any of these quantities indicates a bad grid (overlapping coordinate lines) and will cause the solution to diverge. The A2 quantity will show both signs. For symmetric airfoils the sign of A2 above the airfoil will be the opposite of the sign below the airfoil. The A1 values are actually stored at (I+1/2, J), the A2 values at (I,J), the A3 values at (I,J+1/2), and the XJ values at (I+1/2, J+1/2). This output will be printed if NOUT≥8.

The convergence history for the flow solver is printed after the transformation metrics. The first column is the iteration number, N. CMAX and the following I and J are the maximum correction and its position. RMAX and the I and J to its right are the maximum residual and its position. RAVG is the residual averaged over the entire mesh. The BETA parameter used in TAIR varies from iteration to iteration providing IAUTO=1 (see chap. 5 for more information regarding the BETA update logic); therefore, the next column on the convergence history output page shows the value of BETA used for a given iteration. The next column displays the ALPHA sequence used by the flow solver, followed by the buildup of the number of supersonic points (NSP). The circulation and the coefficient of lift calculated from the circulation are shown in the last two columns. This information is automatically printed for the first M iterations, then printed only when N is a multiple of NOUT2. The update messages from SUBROUTINE AUTO, for example, the messages indicating changes in BETA and CON from example 4, are printed in the convergence history output as they occur. One final message is printed after the flow-solver convergence history output indicating that (1) the solution has converged (if the solution has passed the internal convergence test), (2) the solution iteration limit (N=NSTEPS) was encountered before the convergence test was passed, or (3) the solution is diverging. If the convergence history terminates in either of the first two modes, a flow-field solution, controlled by NOUT, is

printed. If the solution diverges no final solution will be printed. The flow-field convergence history output will be printed if NOUT≥6.

The last two pages of output in example 4 show printer contour plots of the density and Mach number arrays plotted in the computational domain. These maps display a one-digit number (0-9) for each grid point in the flow field. For the density map this number (IVAR) is computed by

$$IVAR = IFIX\left[\frac{9.999 * (RHO(I,J) - RHO_{min})}{(RHO_{max} - RHO_{min})}\right]$$

For the Mach number map this number is computed by

$$IVAR = \begin{cases} IFIX\ (9.999\ XM_{i,j}) & \text{if} \quad XM_{i,j} < 1.0 \\ IFIX\ [9.999\ (XM_{i,j} - 1.0)] & \text{if} \quad XM_{i,j} \geq 1.0 \end{cases}$$

where XM is the local Mach number. These maps start on the left side with the value I=ISTART and end on the right side with I=NI (upper vortex sheet boundary). The ISTART parameter is computed as the maximum of 1 and NI-132+1. Therefore, if NI>132, the left-hand portion of the flow field will not be displayed. The J index starts with one at the top of the map (outer boundary) and increases downward until it reaches NJ at the bottom of the map (airfoil boundary). Thus with this type of output the whole flow field can be qualitatively surveyed with only a single page of output.

The NOUT=9 option prints the finite-difference grid. The output printed for each value of I and J (incremented by IINCR and JINCR, respectively) includes the X and Y coordinates, the A1, A2, and A3 transformation metrics, and the Jacobian, XJ. For IINCR=3 and JINCR=2, this option produces eight pages of output.

The last INPUT/OUTPUT example (example 5) is a comparison of a case run with a GRAPE-generated grid and the same case run with the grid generated in TAIR. The airfoil is the NACA 0012, and the conditions are subcritical: MINF=0.63, ALPH=2.0. The input data for this example are shown at the beginning of example 5. As discussed earlier in this chapter, the GRAPE case must be run first. The final airfoil surface solution is all that is desired, so NOUT is set to 3. ALOW is updated for the GRAPE case (see the ALOW parameter discussion in the INPUT section). Note that the GRIDIN card is not used with the MESH=3 option, but must be included for the second case because of the grid generation within TAIR.

The two solutions show very minor differences. Perhaps the biggest difference lies in the wave-drag coefficient, which for this subcritical calculation should be zero. The TAIR-generated grid case predicts a wave-drag coefficient of -0.0007, an obvious error; the GRAPE-generated grid case produces the correct answer (within four digits). The primary speculation for this improved accuracy is associated with the airfoil boundary grid control available from GRAPE (ref. 8). The η mesh lines (ξ = constant lines) are forced to

approach the airfoil orthogonally (or as nearly orthogonally as possible), and as such, the accuracy of the wave-drag coefficient calculation improves.

INPUT/OUTPUT example 4- The following cards form the data deck for the first INPUT/OUTPUT example in chapter 3. This case uses the default parameters, changing only the amount of output. The additional output (over the default amount) is shown on the following pages.

```
$FLOWIN  NOUT=8,    $
$GRIDIN   $
```

****

*** ADI CONVERGENCE HISTORY FOR NUMERICAL GRID GENERATION ***

N	CXMAX	I	J	CYMAX	I	J	RXMAX	I	J	RYMAX	I	J	ALPHA
1	.83438E-01	1	3	.88679E-01	35	5	.21655E-02	1	2	.13484E-02	106	2	.20000E-01
2	.68906E-01	75	5	.15195E+00	36	7	.48887E-03	75	4	.77454E-03	37	5	.67523E-02
3	.60981E-01	124	8	.18846E+00	37	8	.47880E-03	75	2	.61729E-03	36	2	.22797E-02
4	.69160E-01	126	9	.16284E+00	37	10	.17909E-03	128	4	.27473E-03	37	4	.76967E-03
5	.64404E-01	54	10	.10247E+00	112	11	.26652E-03	128	2	.40658E-03	114	2	.25985E-03
6	.44489E-01	54	12	.47780E-01	112	10	.32409E-03	128	2	.43565E-03	113	2	.87731E-04
7	.29526E-01	1	17	.34329E-01	136	22	.36372E-03	129	2	.45956E-03	113	2	.29619E-04
8	.33651E-01	1	19	.15847E-01	132	18	.37344E-03	128	2	.46015E-03	113	2	.10000E-04
9	.14540E-01	128	3	.17591E-01	112	3	.36916E-03	128	2	.45216E-03	113	2	.20000E-01
10	.14062E-01	127	5	.16907E-01	112	5	.10281E-03	128	4	.12177E-03	112	4	.67523E-02
11	.11104E-01	126	7	.13109E-01	111	6	.84514E-04	130	2	.10988E-03	112	2	.22797E-02
12	.66624E-02	1	13	.65583E-02	135	12	.46003E-04	1	2	.51889E-04	138	2	.76967E-03
13	.91053E-02	1	12	.76404E-02	132	13	.46502E-04	1	2	.49412E-04	138	2	.25985E-03
14	.90926E-02	1	13	.77232E-02	129	14	.55806E-04	1	2	.56679E-04	138	2	.87731E-04
15	.61049E-02	1	13	.58185E-02	127	15	.72580E-04	1	2	.64241E-04	137	2	.29619E-04
16	.44253E-02	1	19	.23897E-02	125	13	.78075E-04	1	2	.69537E-04	137	2	.10000E-04
17	.32332E-02	1	3	.25583E-02	135	3	.83876E-04	1	2	.71982E-04	137	2	.20000E-01
18	.36721E-02	1	5	.27769E-02	133	5	.24091E-04	147	4	.18880E-04	134	4	.67523E-02
19	.40659E-02	1	7	.30592E-02	130	7	.18505E-04	1	2	.14094E-04	135	2	.22797E-02
20	.40347E-02	1	8	.31076E-02	126	8	.14347E-04	148	2	.11208E-04	135	2	.76967E-03

*** TRANSFORMATION METRICS NEAR AIRFOIL ***

I	A1(NJ)	A1(NJM)	A2(NJ)	A2(NJM)	A3(NJM)	A3(NJM2)	XJ(NJM)	XJ(NJM2)	XJ(NJ-3)
1	-.2365E+01	-.2617E+01	0.	.1715E-11	-.3964E+00	-.3654E+00	-.9580E+05	-.2387E+05	-.7854E+04
2	-.2395E+01	-.2617E+01	.5018E-01	.1038E-01	-.3963E+00	-.3805E+00	-.6884E+05	-.2051E+05	-.7895E+04
3	-.2424E+01	-.2574E+01	.2799E-01	.9968E-02	-.3961E+00	-.3845E+00	-.4028E+05	-.1715E+05	-.7655E+04
4	-.2437E+01	-.2532E+01	.1296E-01	.6335E-02	-.3991E+00	-.3899E+00	-.2422E+05	-.1364E+05	-.6882E+04
5	-.2442E+01	-.2504E+01	.5081E-02	.2462E-02	-.4026E+00	-.3945E+00	-.1638E+05	-.1060E+05	-.6082E+04
6	-.2445E+01	-.2486E+01	.6384E-03	-.5158E-03	-.4047E+00	-.3981E+00	-.1173E+05	-.8367E+04	-.5303E+04
7	-.2447E+01	-.2474E+01	-.1993E-02	-.2527E-02	-.4061E+00	-.4008E+00	-.8788E+04	-.6725E+04	-.4606E+04
8	-.2448E+01	-.2466E+01	-.3586E-02	-.3786E-02	-.4070E+00	-.4020E+00	-.6836E+04	-.5506E+04	-.4006E+04
9	-.2447E+01	-.2461E+01	-.4538E-02	-.4515E-02	-.4076E+00	-.4043E+00	-.5478E+04	-.4587E+04	-.3501E+04
10	-.2446E+01	-.2457E+01	-.5048E-02	-.4886E-02	-.4081E+00	-.4054E+00	-.4502E+04	-.3882E+04	-.3078E+04
11	-.2444E+01	-.2454E+01	-.5252E-02	-.5015E-02	-.4085E+00	-.4061E+00	-.3779E+04	-.3333E+04	-.2726E+04
12	-.2443E+01	-.2452E+01	-.5255E-02	-.4980E-02	-.4088E+00	-.4067E+00	-.3229E+04	-.2899E+04	-.2430E+04
13	-.2441E+01	-.2450E+01	-.5110E-02	-.4834E-02	-.4090E+00	-.4072E+00	-.2802E+04	-.2551E+04	-.2182E+04
14	-.2440E+01	-.2449E+01	-.4863E-02	-.4614E-02	-.4092E+00	-.4075E+00	-.2465E+04	-.2269E+04	-.1974E+04
15	-.2439E+01	-.2448E+01	-.4547E-02	-.4343E-02	-.4094E+00	-.4077E+00	-.2194E+04	-.2038E+04	-.1797E+04
16	-.2438E+01	-.2447E+01	-.4186E-02	-.4041E-02	-.4096E+00	-.4079E+00	-.1974E+04	-.1847E+04	-.1647E+04
17	-.2438E+01	-.2447E+01	-.3800E-02	-.3720E-02	-.4095E+00	-.4080E+00	-.1793E+04	-.1687E+04	-.1519E+04
18	-.2438E+01	-.2447E+01	-.3403E-02	-.3391E-02	-.4095E+00	-.4080E+00	-.1642E+04	-.1553E+04	-.1410E+04
19	-.2439E+01	-.2447E+01	-.3006E-02	-.3061E-02	-.4094E+00	-.4080E+00	-.1516E+04	-.1439E+04	-.1315E+04
20	-.2439E+01	-.2448E+01	-.2618E-02	-.2738E-02	-.4093E+00	-.4080E+00	-.1410E+04	-.1343E+04	-.1234E+04
21	-.2440E+01	-.2448E+01	-.2245E-02	-.2426E-02	-.4092E+00	-.4079E+00	-.1320E+04	-.1260E+04	-.1164E+04
22	-.2442E+01	-.2449E+01	-.1892E-02	-.2128E-02	-.4090E+00	-.4078E+00	-.1243E+04	-.1190E+04	-.1103E+04
23	-.2443E+01	-.2450E+01	-.1564E-02	-.1847E-02	-.4088E+00	-.4077E+00	-.1178E+04	-.1129E+04	-.1050E+04
24	-.2445E+01	-.2451E+01	-.1262E-02	-.1586E-02	-.4086E+00	-.4076E+00	-.1122E+04	-.1077E+04	-.1005E+04
25	-.2447E+01	-.2453E+01	-.9886E-03	-.1346E-02	-.4083E+00	-.4074E+00	-.1075E+04	-.1033E+04	-.9650E+03
26	-.2449E+01	-.2454E+01	-.7442E-03	-.1127E-02	-.4080E+00	-.4072E+00	-.1034E+04	-.9943E+03	-.9309E+03
27	-.2451E+01	-.2456E+01	-.5292E-03	-.9306E-03	-.4078E+00	-.4070E+00	-.1000E+04	-.9617E+03	-.9017E+03
28	-.2453E+01	-.2457E+01	-.3431E-03	-.7558E-03	-.4075E+00	-.4068E+00	-.9713E+03	-.9342E+03	-.8768E+03
29	-.2455E+01	-.2459E+01	-.1851E-03	-.6026E-03	-.4072E+00	-.4066E+00	-.9474E+03	-.9112E+03	-.8558E+03
30	-.2457E+01	-.2460E+01	-.5396E-04	-.4701E-03	-.4069E+00	-.4063E+00	-.9279E+03	-.8922E+03	-.8384E+03
31	-.2459E+01	-.2462E+01	.5210E-04	-.3574E-03	-.4066E+00	-.4061E+00	-.9125E+03	-.8770E+03	-.8242E+03
32	-.2461E+01	-.2463E+01	.1349E-03	-.2631E-03	-.4063E+00	-.4059E+00	-.9008E+03	-.8653E+03	-.8132E+03
33	-.2463E+01	-.2465E+01	.1967E-03	-.1860E-03	-.4060E+00	-.4057E+00	-.8927E+03	-.8569E+03	-.8050E+03
34	-.2465E+01	-.2466E+01	.2396E-03	-.1244E-03	-.4058E+00	-.4055E+00	-.8880E+03	-.8516E+03	-.7996E+03
35	-.2466E+01	-.2467E+01	.2661E-03	-.7688E-04	-.4056E+00	-.4053E+00	-.8865E+03	-.8493E+03	-.7968E+03
36	-.2468E+01	-.2468E+01	.2785E-03	-.4167E-04	-.4053E+00	-.4051E+00	-.8883E+03	-.8499E+03	-.7966E+03
37	-.2469E+01	-.2470E+01	.2792E-03	-.1718E-04	-.4051E+00	-.4049E+00	-.8931E+03	-.8533E+03	-.7989E+03
38	-.2470E+01	-.2471E+01	.2704E-03	-.1818E-05	-.4049E+00	-.4048E+00	-.9012E+03	-.8597E+03	-.8037E+03
39	-.2472E+01	-.2472E+01	.2543E-03	.5952E-05	-.4047E+00	-.4046E+00	-.9124E+03	-.8690E+03	-.8112E+03
40	-.2473E+01	-.2472E+01	.2329E-03	.7559E-05	-.4046E+00	-.4045E+00	-.9270E+03	-.8813E+03	-.8212E+03
41	-.2473E+01	-.2473E+01	.2079E-03	.4267E-05	-.4044E+00	-.4044E+00	-.9451E+03	-.8967E+03	-.8338E+03
42	-.2474E+01	-.2474E+01	.1809E-03	-.2761E-05	-.4043E+00	-.4042E+00	-.9669E+03	-.9154E+03	-.8493E+03
43	-.2476E+01	-.2476E+01	.1531E-03	-.1258E-04	-.4041E+00	-.4041E+00	-.9927E+03	-.9375E+03	-.8677E+03
44	-.2476E+01	-.2475E+01	.1255E-03	-.2441E-04	-.4040E+00	-.4040E+00	-.1023E+04	-.9634E+03	-.8893E+03
45	-.2476E+01	-.2476E+01	.9860E-04	-.3778E-04	-.4039E+00	-.4039E+00	-.1057E+04	-.9933E+03	-.9142E+03
46	-.2477E+01	-.2476E+01	.7274E-04	-.5210E-04	-.4039E+00	-.4039E+00	-.1097E+04	-.1028E+04	-.9426E+03
47	-.2477E+01	-.2477E+01	.4784E-04	-.6746E-04	-.4038E+00	-.4038E+00	-.1143E+04	-.1067E+04	-.9750E+03
48	-.2477E+01	-.2477E+01	.2346E-04	-.8386E-04	-.4037E+00	-.4037E+00	-.1194E+04	-.1111E+04	-.1012E+04
49	-.2478E+01	-.2477E+01	-.1197E-05	-.1016E-03	-.4037E+00	-.4037E+00	-.1253E+04	-.1162E+04	-.1053E+04
50	-.2478E+01	-.2478E+01	-.2728E-04	-.1210E-03	-.4036E+00	-.4037E+00	-.1321E+04	-.1219E+04	-.1100E+04
51	-.2478E+01	-.2478E+01	-.5625E-04	-.1428E-03	-.4036E+00	-.4036E+00	-.1397E+04	-.1284E+04	-.1152E+04
52	-.2479E+01	-.2478E+01	-.8989E-04	-.1670E-03	-.4035E+00	-.4036E+00	-.1485E+04	-.1357E+04	-.1211E+04
53	-.2479E+01	-.2478E+01	-.1303E-03	-.1967E-03	-.4035E+00	-.4036E+00	-.1585E+04	-.1440E+04	-.1277E+04
54	-.2479E+01	-.2478E+01	-.1797E-03	-.2306E-03	-.4036E+00	-.4036E+00	-.1699E+04	-.1535E+04	-.1351E+04
55	-.2479E+01	-.2478E+01	-.2488E-03	-.2703E-03	-.4035E+00	-.4036E+00	-.1832E+04	-.1643E+04	-.1434E+04
56	-.2479E+01	-.2478E+01	-.3161E-03	-.3168E-03	-.4035E+00	-.4037E+00	-.1985E+04	-.1766E+04	-.1528E+04
57	-.2479E+01	-.2477E+01	-.4084E-03	-.3711E-03	-.4036E+00	-.4037E+00	-.2162E+04	-.1906E+04	-.1633E+04
58	-.2478E+01	-.2476E+01	-.5285E-03	-.4338E-03	-.4037E+00	-.4038E+00	-.2370E+04	-.2068E+04	-.1751E+04
59	-.2477E+01	-.2475E+01	-.6552E-03	-.5058E-03	-.4038E+00	-.4039E+00	-.2614E+04	-.2254E+04	-.1884E+04

60	-.2476E+01	-.2474E+01	-.8149E-03	-.5876E-03	-.4040E+00	-.4041E+00	-.2904E+04	-.2468E+04	-.2033E+04
61	-.2474E+01	-.2472E+01	-.1002E-02	-.6798E-03	-.4043E+00	-.4043E+00	-.3248E+04	-.2717E+04	-.2201E+04
62	-.2471E+01	-.2470E+01	-.1219E-02	-.7825E-03	-.4046E+00	-.4045E+00	-.3662E+04	-.3005E+04	-.2388E+04
63	-.2468E+01	-.2468E+01	-.1465E-02	-.8959E-03	-.4050E+00	-.4048E+00	-.4163E+04	-.3339E+04	-.2598E+04
64	-.2463E+01	-.2465E+01	-.1742E-02	-.1020E-02	-.4056E+00	-.4051E+00	-.4773E+04	-.3727E+04	-.2830E+04
65	-.2458E+01	-.2463E+01	-.2044E-02	-.1152E-02	-.4062E+00	-.4054E+00	-.5521E+04	-.4177E+04	-.3086E+04
66	-.2452E+01	-.2460E+01	-.2364E-02	-.1288E-02	-.4069E+00	-.4056E+00	-.6446E+04	-.4694E+04	-.3364E+04
67	-.2445E+01	-.2459E+01	-.2679E-02	-.1420E-02	-.4075E+00	-.4058E+00	-.7591E+04	-.5282E+04	-.3662E+04
68	-.2439E+01	-.2458E+01	-.2945E-02	-.1530E-02	-.4081E+00	-.4058E+00	-.9000E+04	-.5939E+04	-.3973E+04
69	-.2437E+01	-.2460E+01	-.3078E-02	-.1586E-02	-.4083E+00	-.4055E+00	-.1075E+05	-.6650E+04	-.4288E+04
70	-.2441E+01	-.2465E+01	-.2933E-02	-.1544E-02	-.4079E+00	-.4049E+00	-.1284E+05	-.7381E+04	-.4592E+04
71	-.2456E+01	-.2474E+01	-.2321E-02	-.1360E-02	-.4065E+00	-.4040E+00	-.1524E+05	-.8078E+04	-.4868E+04
72	-.2488E+01	-.2485E+01	-.1138E-02	-.1022E-02	-.4040E+00	-.4030E+00	-.1776E+05	-.8668E+04	-.5098E+04
73	-.2530E+01	-.2497E+01	.3096E-03	-.5996E-03	-.4004E+00	-.4019E+00	-.1997E+05	-.9086E+04	-.5262E+04
74	-.2563E+01	-.2504E+01	.1010E-02	-.2331E-03	-.3970E+00	-.4012E+00	-.2129E+05	-.9300E+04	-.5348E+04
75	-.2563E+01	-.2504E+01	-.2362E-10	-.2620E-10	-.3954E+00	-.4009E+00	-.2129E+05	-.9300E+04	-.5348E+04
76	-.2530E+01	-.2497E+01	-.1010E-02	.2331E-03	-.3970E+00	-.4012E+00	-.1997E+05	-.9086E+04	-.5262E+04
77	-.2488E+01	-.2485E+01	-.3096E-03	.5996E-03	-.4004E+00	-.4019E+00	-.1776E+05	-.8668E+04	-.5098E+04
78	-.2456E+01	-.2474E+01	.1138E-02	.1022E-02	-.4040E+00	-.4030E+00	-.1524E+05	-.8078E+04	-.4868E+04
79	-.2441E+01	-.2465E+01	.2321E-02	.1360E-02	-.4065E+00	-.4040E+00	-.1284E+05	-.7381E+04	-.4592E+04
80	-.2437E+01	-.2460E+01	.2933E-02	.1544E-02	-.4079E+00	-.4049E+00	-.1075E+05	-.6650E+04	-.4288E+04
81	-.2439E+01	-.2458E+01	.3078E-02	.1586E-02	-.4083E+00	-.4055E+00	-.9000E+04	-.5939E+04	-.3973E+04
82	-.2445E+01	-.2459E+01	.2945E-02	.1530E-02	-.4081E+00	-.4058E+00	-.7591E+04	-.5282E+04	-.3662E+04
83	-.2452E+01	-.2460E+01	.2679E-02	.1420E-02	-.4075E+00	-.4058E+00	-.6446E+04	-.4694E+04	-.3364E+04
84	-.2458E+01	-.2463E+01	.2364E-02	.1288E-02	-.4069E+00	-.4056E+00	-.5521E+04	-.4177E+04	-.3086E+04
85	-.2463E+01	-.2465E+01	.2044E-02	.1152E-02	-.4062E+00	-.4054E+00	-.4773E+04	-.3727E+04	-.2830E+04
86	-.2468E+01	-.2468E+01	.1742E-02	.1020E-02	-.4056E+00	-.4051E+00	-.4163E+04	-.3339E+04	-.2598E+04
87	-.2471E+01	-.2470E+01	.1465E-02	.8959E-03	-.4050E+00	-.4048E+00	-.3662E+04	-.3005E+04	-.2388E+04
88	-.2474E+01	-.2472E+01	.1219E-02	.7825E-03	-.4046E+00	-.4045E+00	-.3248E+04	-.2717E+04	-.2201E+04
89	-.2476E+01	-.2474E+01	.1002E-02	.6798E-03	-.4043E+00	-.4043E+00	-.2904E+04	-.2468E+04	-.2033E+04
90	-.2477E+01	-.2475E+01	.8149E-03	.5876E-03	-.4040E+00	-.4041E+00	-.2614E+04	-.2254E+04	-.1884E+04
91	-.2478E+01	-.2476E+01	.6552E-03	.5058E-03	-.4038E+00	-.4039E+00	-.2370E+04	-.2068E+04	-.1751E+04
92	-.2479E+01	-.2477E+01	.5205E-03	.4338E-03	-.4037E+00	-.4038E+00	-.2162E+04	-.1906E+04	-.1633E+04
93	-.2479E+01	-.2478E+01	.4084E-03	.3711E-03	-.4036E+00	-.4037E+00	-.1985E+04	-.1766E+04	-.1528E+04
94	-.2479E+01	-.2478E+01	.3161E-03	.3168E-03	-.4035E+00	-.4037E+00	-.1832E+04	-.1643E+04	-.1434E+04
95	-.2479E+01	-.2478E+01	.2408E-03	.2703E-03	-.4035E+00	-.4036E+00	-.1699E+04	-.1536E+04	-.1351E+04
96	-.2479E+01	-.2478E+01	.1797E-03	.2306E-03	-.4035E+00	-.4036E+00	-.1585E+04	-.1440E+04	-.1277E+04
97	-.2479E+01	-.2478E+01	.1303E-03	.1967E-03	-.4035E+00	-.4036E+00	-.1485E+04	-.1357E+04	-.1211E+04
98	-.2478E+01	-.2478E+01	.8989E-04	.1678E-03	-.4035E+00	-.4036E+00	-.1397E+04	-.1284E+04	-.1152E+04
99	-.2478E+01	-.2478E+01	.5625E-04	.1428E-03	-.4036E+00	-.4036E+00	-.1321E+04	-.1219E+04	-.1100E+04
100	-.2478E+01	-.2477E+01	.2728E-04	.1210E-03	-.4036E+00	-.4037E+00	-.1253E+04	-.1162E+04	-.1053E+04
101	-.2477E+01	-.2477E+01	.1197E-05	.1016E-03	-.4037E+00	-.4037E+00	-.1194E+04	-.1111E+04	-.1012E+04
102	-.2477E+01	-.2477E+01	-.2346E-04	.8386E-04	-.4037E+00	-.4037E+00	-.1143E+04	-.1067E+04	-.9750E+03
103	-.2477E+01	-.2476E+01	-.4784E-04	.6746E-04	-.4038E+00	-.4038E+00	-.1097E+04	-.1028E+04	-.9426E+03
104	-.2476E+01	-.2476E+01	-.7274E-04	.5210E-04	-.4039E+00	-.4039E+00	-.1057E+04	-.9933E+03	-.9142E+03
105	-.2476E+01	-.2475E+01	-.9860E-04	.3770E-04	-.4039E+00	-.4039E+00	-.1023E+04	-.9634E+03	-.8893E+03
106	-.2475E+01	-.2475E+01	-.1255E-03	.2441E-04	-.4040E+00	-.4040E+00	-.9927E+03	-.9375E+03	-.8677E+03
107	-.2474E+01	-.2474E+01	-.1531E-03	.1258E-04	-.4041E+00	-.4041E+00	-.9669E+03	-.9154E+03	-.8493E+03
108	-.2473E+01	-.2473E+01	-.1809E-03	.2761E-05	-.4043E+00	-.4042E+00	-.9451E+03	-.8967E+03	-.8338E+03
109	-.2473E+01	-.2472E+01	-.2079E-03	-.4267E-05	-.4044E+00	-.4044E+00	-.9270E+03	-.8813E+03	-.8212E+03
110	-.2472E+01	-.2472E+01	-.2329E-03	-.7558E-05	-.4045E+00	-.4045E+00	-.9124E+03	-.8698E+03	-.8112E+03
111	-.2470E+01	-.2471E+01	-.2543E-03	-.5952E-05	-.4047E+00	-.4046E+00	-.9012E+03	-.8597E+03	-.8037E+03
112	-.2469E+01	-.2470E+01	-.2704E-03	.1818E-05	-.4049E+00	-.4048E+00	-.8931E+03	-.8533E+03	-.7989E+03
113	-.2468E+01	-.2468E+01	-.2792E-03	.1718E-04	-.4051E+00	-.4049E+00	-.8883E+03	-.8499E+03	-.7966E+03
114	-.2466E+01	-.2467E+01	-.2785E-03	.4167E-04	-.4053E+00	-.4051E+00	-.8865E+03	-.8493E+03	-.7968E+03
115	-.2465E+01	-.2466E+01	-.2661E-03	.7688E-04	-.4055E+00	-.4053E+00	-.8880E+03	-.8516E+03	-.7996E+03
116	-.2463E+01	-.2465E+01	-.2396E-03	.1244E-03	-.4058E+00	-.4055E+00	-.8927E+03	-.8569E+03	-.8050E+03
117	-.2461E+01	-.2463E+01	-.1967E-03	.1860E-03	-.4060E+00	-.4057E+00	-.9000E+03	-.8653E+03	-.8132E+03
118	-.2459E+01	-.2462E+01	-.1349E-03	.2631E-03	-.4063E+00	-.4059E+00	-.9125E+03	-.8770E+03	-.8242E+03
119	-.2457E+01	-.2460E+01	-.5210E-04	.3574E-03	-.4066E+00	-.4061E+00	-.9279E+03	-.8922E+03	-.8384E+03
120	-.2455E+01	-.2459E+01	.5395E-04	.4701E-03	-.4069E+00	-.4063E+00	-.9474E+03	-.9112E+03	-.8558E+03
121	-.2453E+01	-.2457E+01	.1851E-03	.6026E-03	-.4072E+00	-.4066E+00	-.9713E+03	-.9342E+03	-.8768E+03
122	-.2451E+01	-.2456E+01	.3431E-03	.7558E-03	-.4075E+00	-.4068E+00	-.1000E+04	-.9617E+03	-.9017E+03

123	-.2449E+01	-.2454E+01	.5292E-03	.9306E-03	-.4078E+00	-.4070E+00	-.1034E+04	-.9943E+03	-.9309E+03
124	-.2447E+01	-.2453E+01	.7442E-03	.1127E-02	-.4080E+00	-.4072E+00	-.1075E+04	-.1033E+04	-.9650E+03
125	-.2445E+01	-.2451E+01	.9886E-03	.1346E-02	-.4083E+00	-.4074E+00	-.1122E+04	-.1077E+04	-.1005E+04
126	-.2443E+01	-.2450E+01	.1262E-02	.1586E-02	-.4086E+00	-.4076E+00	-.1178E+04	-.1129E+04	-.1050E+04
127	-.2442E+01	-.2449E+01	.1564E-02	.1847E-02	-.4088E+00	-.4077E+00	-.1243E+04	-.1190E+04	-.1103E+04
128	-.2440E+01	-.2448E+01	.1892E-02	.2128E-02	-.4090E+00	-.4078E+00	-.1320E+04	-.1260E+04	-.1164E+04
129	-.2439E+01	-.2448E+01	.2245E-02	.2426E-02	-.4092E+00	-.4079E+00	-.1410E+04	-.1343E+04	-.1234E+04
130	-.2439E+01	-.2447E+01	.2618E-02	.2738E-02	-.4093E+00	-.4080E+00	-.1516E+04	-.1439E+04	-.1315E+04
131	-.2438E+01	-.2447E+01	.3006E-02	.3061E-02	-.4094E+00	-.4080E+00	-.1642E+04	-.1553E+04	-.1410E+04
132	-.2438E+01	-.2447E+01	.3403E-02	.3391E-02	-.4095E+00	-.4080E+00	-.1793E+04	-.1687E+04	-.1519E+04
133	-.2438E+01	-.2447E+01	.3800E-02	.3720E-02	-.4095E+00	-.4080E+00	-.1974E+04	-.1847E+04	-.1647E+04
134	-.2439E+01	-.2448E+01	.4186E-02	.4041E-02	-.4095E+00	-.4079E+00	-.2194E+04	-.2038E+04	-.1797E+04
135	-.2440E+01	-.2449E+01	.4547E-02	.4343E-02	-.4094E+00	-.4077E+00	-.2466E+04	-.2269E+04	-.1974E+04
136	-.2441E+01	-.2450E+01	.4863E-02	.4614E-02	-.4092E+00	-.4075E+00	-.2802E+04	-.2551E+04	-.2182E+04
137	-.2443E+01	-.2452E+01	.5110E-02	.4834E-02	-.4090E+00	-.4072E+00	-.3229E+04	-.2899E+04	-.2430E+04
138	-.2444E+01	-.2454E+01	.5255E-02	.4980E-02	-.4088E+00	-.4067E+00	-.3779E+04	-.3333E+04	-.2725E+04
139	-.2446E+01	-.2457E+01	.5252E-02	.5015E-02	-.4085E+00	-.4061E+00	-.4502E+04	-.3882E+04	-.3078E+04
140	-.2447E+01	-.2461E+01	.5040E-02	.4886E-02	-.4081E+00	-.4054E+00	-.5478E+04	-.4587E+04	-.3501E+04
141	-.2448E+01	-.2466E+01	.4530E-02	.4515E-02	-.4076E+00	-.4043E+00	-.6835E+04	-.5506E+04	-.4006E+04
142	-.2447E+01	-.2474E+01	.3586E-02	.3786E-02	-.4070E+00	-.4028E+00	-.8788E+04	-.6725E+04	-.4606E+04
143	-.2445E+01	-.2486E+01	.1993E-02	.2527E-02	-.4061E+00	-.4008E+00	-.1173E+05	-.8367E+04	-.5303E+04
144	-.2442E+01	-.2504E+01	-.6384E-03	.5158E-03	-.4047E+00	-.3981E+00	-.1638E+05	-.1060E+05	-.6082E+04
145	-.2437E+01	-.2532E+01	-.5081E-02	-.2462E-02	-.4025E+00	-.3945E+00	-.2422E+05	-.1364E+05	-.6882E+04
146	-.2424E+01	-.2574E+01	-.1296E-01	-.6335E-02	-.3991E+00	-.3899E+00	-.4028E+05	-.1715E+05	-.7555E+04
147	-.2395E+01	-.2617E+01	-.2799E-01	-.9968E-02	-.3961E+00	-.3845E+00	-.6804E+05	-.2051E+05	-.7895E+04
148	-.2365E+01	-.2617E+01	-.5018E-01	-.1030E-01	-.3963E+00	-.3805E+00	-.9580E+05	-.2387E+05	-.7854E+04
149	-.2365E+01	-.2617E+01	0.	.1715E-11	-.3964E+00	-.3805E+00	-.9580E+05	-.2387E+05	-.7854E+04

*** AF2 CONVERGENCE HISTORY FOR THE NUMERICAL SOLUTION OF THE CONSERVATIVE, TRANSONIC FULL POTENTIAL EQUATION ***

N	CMAX	I	J	RMAX	I	J	RAVG	BETA	ALPHA	NSP	CIRCULATION	CL(CIR)
1	.68609E-02	74	30	.40929E-02	75	30	.70929E-04	4.5000	.15000E+01	0	.43364E-04	.0166
2	.57898E-02	71	30	.13611E-02	72	30	.40383E-04	4.5000	.96816E+00	0	.61400E-04	.0197
3	.44937E-02	67	29	.14306E-02	74	29	.43173E-04	4.4100	.62490E+00	0	.62942E-04	.0241
4	.66864E-02	73	30	.73517E-03	67	28	.37001E-04	4.3218	.40333E+00	0	.11607E-03	.0444
5	.11027E-01	75	29	.78991E-03	74	28	.35926E-04	4.2354	.26033E+00	0	.14002E-03	.0536
6	.17445E-01	74	29	.59159E-03	73	28	.41358E-04	4.1507	.16003E+00	0	.17443E-03	.0667
7	.21493E-01	74	29	.73741E-03	74	27	.46000E-04	4.0676	.10045E+00	27	.32656E-03	.1246
	*** PARAMETER UPDATE BY SUBROUTINE AUTO... BETA = 3.0 ***											
8	.18659E-01	80	24	.79904E-03	75	27	.43794E-04	3.0000	.70000E-01	65	.36876E-03	.1411
16	.61615E-02	109	30	.37281E-03	103	27	.12971E-04	2.6523	.70000E-01	101	.57732E-03	.2209
24	.33775E-02	108	30	.24220E-03	111	30	.51214E-05	2.1714	.70000E-01	104	.60920E-03	.2331
	*** PARAMETER UPDATE BY SUBROUTINE AUTO... CON =1.20 ***											
32	.12115E-02	108	30	.21134E-03	108	30	.22294E-05	1.8473	.70000E-01	106	.61717E-03	.2361
40	.88083E-03	108	27	.21565E-03	108	30	.18155E-05	1.5716	.70000E-01	106	.62481E-03	.2390
48	.76857E-03	109	27	.43369E-03	109	30	.94047E-06	1.7190	.70000E-01	109	.63248E-03	.2420
56	.53113E-03	109	27	.29545E-03	109	28	.76204E-06	2.6056	.70000E-01	109	.63713E-03	.2438
64	.13180E-03	110	27	.17081E-03	110	30	.48258E-06	2.2168	.70000E-01	110	.63859E-03	.2443
72	.38945E-04	108	27	.48931E-04	110	30	.12924E-06	1.8868	.70000E-01	110	.63889E-03	.2441

*** FINAL CONVERGED SOLUTION ***

*** DENSITY CONTOUR MAP ***

VARMAX = .999712E+00 VARMIN = .512787E+00

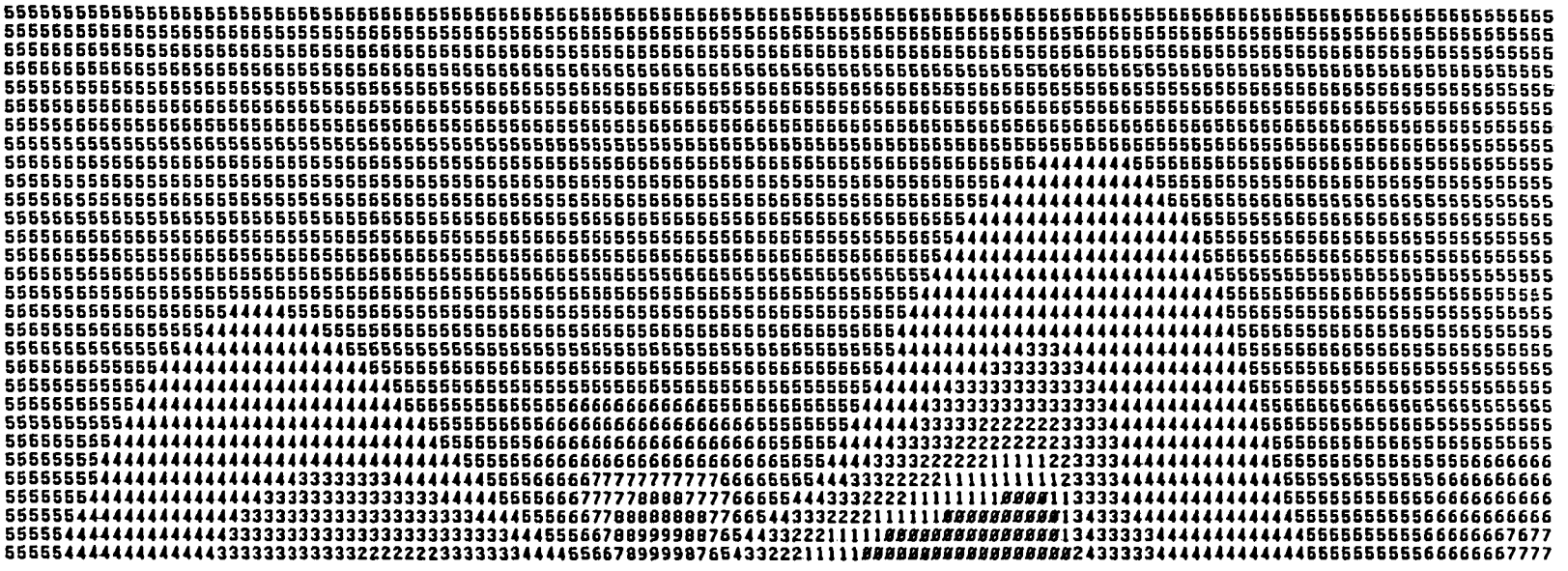

*** MACH NUMBER CONTOUR MAP ***

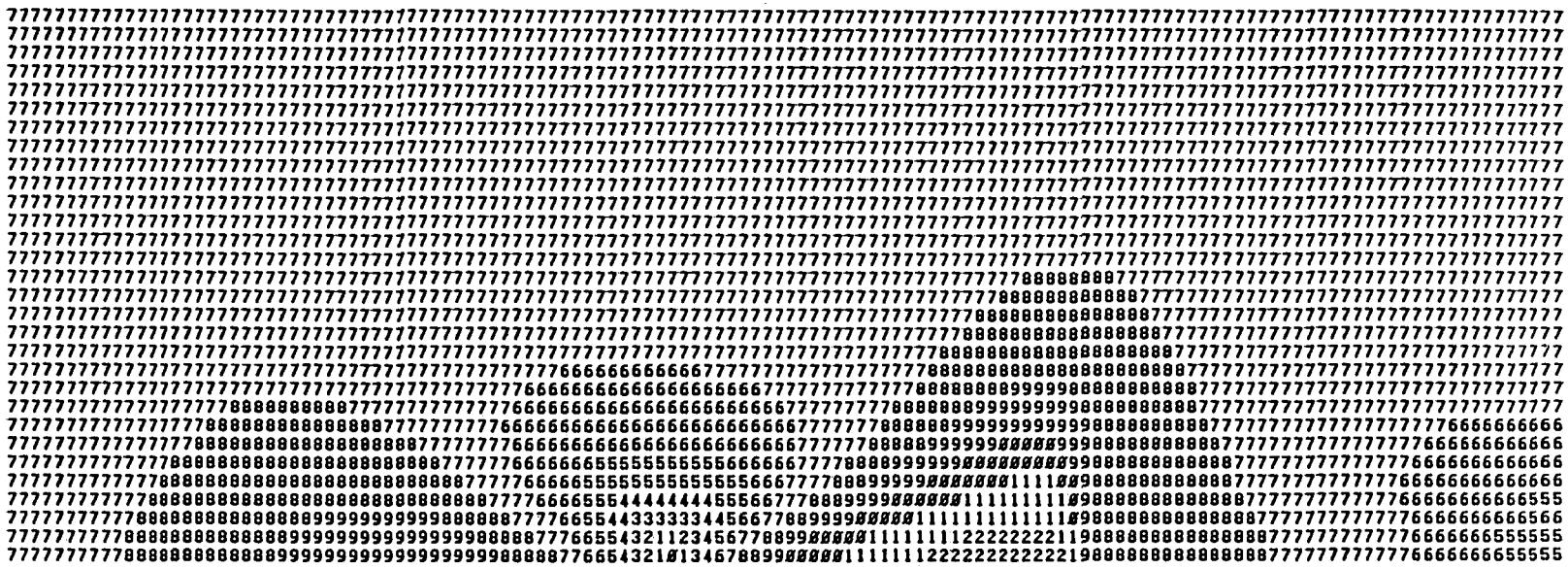

INPUT/OUTPUT example 5- The cards below form the data deck for INPUT/OUTPUT example 5 in chapter 3. This is a multiple-case run comparing a GRAPE generated grid solution to a TAIR generated grid solution. The output for this case is shown on the next two pages.

```
$FLOWIN  MINF=.63,ALPH=2.Ø,NI=141,NJ=31,MESH=3,ALOW=.Ø8,NCASE=2,NOUT=3,  $
$FLOWIN  MINF=.63,ALPH=2.Ø,NI=141,NJ=31,NOUT=3,  $
$GRIDIN   $
```

********** AIRFOIL FROM GRAPE SURFACE SOLUTION.....MINF = .630, ALPH = 2.000 DEG **********

***** SOLUTION AFTER 34 ITERATIONS, RMAX = .3289E-04, NSP = 0, CL(CIR) = .3397 *****

I	X/C	Y/C	CP	RHO	M	I	X/C	Y/C	CP	RHO	M	I	X/C	Y/C	CP	RHO	M
1	.9994	-.0001	.4768	.9029	.4666	48	.2143	-.0582	-.2828	.7793	.7243	95	.2510	.0595	-.7527	.6987	.8781
2	.9979	-.0003	.4322	.8959	.4742	49	.1968	-.0573	-.2788	.7799	.7230	96	.2701	.0598	-.7199	.7044	.8673
3	.9954	-.0007	.3877	.8888	.4914	50	.1798	-.0562	-.2723	.7818	.7208	97	.2897	.0600	-.6875	.7101	.8567
4	.9919	-.0012	.3434	.8817	.5081	51	.1635	-.0549	-.2629	.7826	.7177	98	.3098	.0600	-.6556	.7156	.8462
5	.9873	-.0018	.2992	.8746	.5246	52	.1479	-.0534	-.2501	.7847	.7135	99	.3302	.0598	-.6241	.7211	.8359
6	.9816	-.0026	.2652	.8692	.5370	53	.1329	-.0517	-.2339	.7874	.7082	100	.3511	.0594	-.5933	.7264	.8258
7	.9749	-.0035	.2355	.8644	.5478	54	.1186	-.0498	-.2137	.7908	.7015	101	.3723	.0588	-.5632	.7316	.8159
8	.9671	-.0046	.2006	.8601	.5574	55	.1051	-.0478	-.1883	.7950	.6931	102	.3937	.0581	-.5337	.7367	.8063
9	.9582	-.0058	.1838	.8561	.5662	56	.0923	-.0456	-.1581	.8001	.6831	103	.4154	.0573	-.5049	.7416	.7969
10	.9484	-.0072	.1689	.8524	.5743	57	.0802	-.0433	-.1219	.8061	.6711	104	.4374	.0562	-.4769	.7464	.7878
11	.9376	-.0086	.1398	.8489	.5818	58	.0690	-.0408	-.0790	.8132	.6567	105	.4595	.0551	-.4496	.7511	.7789
12	.9258	-.0102	.1199	.8457	.5887	59	.0585	-.0381	-.0284	.8215	.6396	106	.4818	.0538	-.4230	.7556	.7702
13	.9130	-.0118	.1011	.8427	.5953	60	.0489	-.0353	.0323	.8314	.6198	107	.5041	.0524	-.3972	.7600	.7617
14	.8994	-.0135	.0833	.8398	.6015	61	.0400	-.0324	.1047	.8432	.5948	108	.5265	.0509	-.3721	.7642	.7535
15	.8849	-.0154	.0663	.8370	.6073	62	.0321	-.0294	.1900	.8571	.5641	109	.5489	.0492	-.3477	.7683	.7455
16	.8696	-.0173	.0501	.8344	.6129	63	.0249	-.0262	.2922	.8735	.5271	110	.5713	.0475	-.3239	.7723	.7377
17	.8535	-.0192	.0346	.8318	.6182	64	.0187	-.0230	.4139	.8930	.4813	111	.5936	.0457	-.3007	.7762	.7302
18	.8367	-.0212	.0196	.8294	.6233	65	.0133	-.0196	.5572	.9156	.4236	112	.6157	.0439	-.2781	.7800	.7227
19	.8192	-.0232	.0052	.8270	.6282	66	.0089	-.0161	.7198	.9411	.3507	113	.6376	.0419	-.2561	.7837	.7155
20	.8010	-.0253	-.0088	.8247	.6330	67	.0053	-.0126	.8899	.9674	.2584	114	.6594	.0399	-.2345	.7873	.7084
21	.7822	-.0274	-.0224	.8225	.6376	68	.0027	-.0090	1.0359	.9898	.1436	115	.6808	.0379	-.2133	.7909	.7014
22	.7629	-.0295	-.0357	.8203	.6421	69	.0009	-.0054	1.1831	1.0000	.0066	116	.7019	.0358	-.1925	.7944	.6945
23	.7430	-.0316	-.0487	.8182	.6465	70	.0001	-.0018	1.0329	.9893	.1469	117	.7227	.0337	-.1719	.7978	.6877
24	.7227	-.0337	-.0615	.8161	.6508	71	.0001	.0018	.8046	.9542	.3076	118	.7430	.0316	-.1516	.8012	.6809
25	.7019	-.0358	-.0741	.8140	.6550	72	.0009	.0054	.4567	.8997	.4645	119	.7629	.0295	-.1314	.8046	.6742
26	.6808	-.0379	-.0866	.8119	.6592	73	.0027	.0098	.0700	.8376	.6061	120	.7822	.0274	-.1112	.8078	.6675
27	.6594	-.0399	-.0990	.8099	.6634	74	.0053	.0126	-.2759	.7804	.7220	121	.8010	.0253	-.0910	.8112	.6607
28	.6376	-.0419	-.1113	.8078	.6675	75	.0089	.0161	-.5452	.7347	.8101	122	.8192	.0232	-.0708	.8145	.6539
29	.6157	-.0439	-.1235	.8058	.6716	76	.0133	.0196	-.7387	.7011	.8735	123	.8367	.0212	-.0503	.8179	.6470
30	.5935	-.0457	-.1357	.8038	.6756	77	.0187	.0230	-.8742	.6773	.9184	124	.8535	.0192	-.0296	.8213	.6400
31	.5713	-.0475	-.1479	.8018	.6797	78	.0249	.0262	-.9662	.6608	.9493	125	.8696	.0173	-.0085	.8248	.6329
32	.5489	-.0492	-.1599	.7998	.6837	79	.0321	.0294	-1.0273	.6498	.9699	126	.8849	.0154	.0130	.8283	.6256
33	.5265	-.0509	-.1719	.7978	.6877	80	.0400	.0324	-1.0628	.6434	.9820	127	.8994	.0135	.0350	.8319	.6181
34	.5041	-.0524	-.1838	.7958	.6916	81	.0489	.0353	-1.0881	.6388	.9907	128	.9130	.0118	.0576	.8356	.6103
35	.4818	-.0538	-.1954	.7939	.6955	82	.0585	.0381	-1.0975	.6371	.9940	129	.9258	.0102	.0811	.8394	.6022
36	.4595	-.0551	-.2069	.7920	.6993	83	.0690	.0408	-1.0914	.6382	.9918	130	.9376	.0086	.1053	.8434	.5938
37	.4374	-.0562	-.2180	.7901	.7029	84	.0802	.0433	-1.0797	.6404	.9878	131	.9484	.0072	.1306	.8475	.5850
38	.4154	-.0573	-.2287	.7883	.7065	85	.0923	.0456	-1.0614	.6437	.9816	132	.9582	.0058	.1575	.8518	.5756
39	.3937	-.0581	-.2389	.7866	.7098	86	.1051	.0478	-1.0382	.6479	.9736	133	.9671	.0046	.1859	.8564	.5655
40	.3723	-.0588	-.2485	.7850	.7130	87	.1186	.0498	-1.0128	.6525	.9650	134	.9749	.0036	.2163	.8613	.5547
41	.3511	-.0594	-.2573	.7835	.7159	88	.1329	.0517	-.9822	.6580	.9546	135	.9816	.0026	.2491	.8666	.5429
42	.3302	-.0598	-.2652	.7822	.7185	89	.1479	.0534	-.9506	.6636	.9440	136	.9873	.0018	.2858	.8725	.5295
43	.3098	-.0600	-.2720	.7811	.7207	90	.1635	.0549	-.9184	.6694	.9332	137	.9919	.0012	.3325	.8800	.5122
44	.2897	-.0600	-.2775	.7801	.7225	91	.1798	.0562	-.8854	.6753	.9221	138	.9954	.0007	.3792	.8874	.4946
45	.2701	-.0598	-.2816	.7795	.7239	92	.1968	.0573	-.8520	.6812	.9110	139	.9979	.0003	.4262	.8949	.4765
46	.2510	-.0595	-.2840	.7791	.7247	93	.2143	.0582	-.8188	.6871	.9000	140	.9994	.0001	.4733	.9024	.4580
47	.2324	-.0589	-.2844	.7790	.7248	94	.2324	.0589	-.7857	.6929	.8890	141	.9994	-.0001	.4768	.9029	.4566

*** LIFT, WAVE DRAG, AND QUARTER-CHORD MOMENT COEFFICIENTS.....CL = .3376, CD =-.0000, CM =-.0023 ***

********** NACA 0012 AIRFOIL SURFACE SOLUTION.....MINF = .630, ALPH = 2.000 DEG **********

***** SOLUTION AFTER 30 ITERATIONS, RMAX = .1152E-05, NSP = 0, CL(CIR) = .3365 *****

I	X/C	Y/C	CP	RHO	M	I	X/C	Y/C	CP	RHO	M	I	X/C	Y/C	CP	RHO	M
1	.9994	-.0001	.4460	.8981	.4688	48	.2145	-.0577	-.2813	.7795	.7238	95	.2512	.0590	-.7429	.7004	.8749
2	.9979	-.0003	.4060	.8917	.4843	49	.1969	-.0568	-.2777	.7801	.7226	96	.2703	.0593	-.7104	.7061	.8642
3	.9954	-.0006	.3662	.8854	.4996	50	.1800	-.0557	-.2716	.7812	.7205	97	.2899	.0595	-.6783	.7117	.8536
4	.9919	-.0011	.3264	.8790	.5145	51	.1637	-.0544	-.2624	.7827	.7176	98	.3100	.0594	-.6468	.7172	.8433
5	.9873	-.0018	.2868	.8727	.5291	52	.1481	-.0529	-.2501	.7847	.7135	99	.3304	.0592	-.6158	.7226	.8331
6	.9817	-.0026	.2560	.8677	.5403	53	.1331	-.0513	-.2343	.7874	.7083	100	.3512	.0589	-.5853	.7278	.8232
7	.9749	-.0035	.2287	.8633	.5502	54	.1189	-.0494	-.2145	.7907	.7018	101	.3724	.0583	-.5555	.7329	.8134
8	.9671	-.0046	.2034	.8592	.5593	55	.1053	-.0474	-.1903	.7947	.6938	102	.3939	.0576	-.5264	.7379	.8039
9	.9583	-.0058	.1797	.8554	.5677	56	.0926	-.0453	-.1611	.7996	.6841	103	.4156	.0567	-.4980	.7428	.7947
10	.9484	-.0071	.1575	.8518	.5756	57	.0805	-.0429	-.1261	.8054	.6724	104	.4375	.0557	-.4704	.7476	.7856
11	.9376	-.0085	.1367	.8484	.5829	58	.0692	-.0405	-.0845	.8123	.6586	105	.4596	.0546	-.4434	.7521	.7768
12	.9258	-.0101	.1171	.8453	.5897	59	.0587	-.0378	-.0352	.8204	.6419	106	.4819	.0533	-.4172	.7566	.7683
13	.9131	-.0117	.0986	.8423	.5962	60	.0491	-.0351	.0233	.8300	.6221	107	.5042	.0519	-.3917	.7609	.7599
14	.8994	-.0134	.0811	.8394	.6022	61	.0402	-.0322	.0930	.8414	.5981	108	.5266	.0504	-.3669	.7651	.7518
15	.8850	-.0152	.0644	.8367	.6080	62	.0322	-.0292	.1763	.8549	.5689	109	.5490	.0488	-.3428	.7692	.7440
16	.8697	-.0171	.0485	.8341	.6134	63	.0251	-.0261	.2763	.8710	.5330	110	.5714	.0471	-.3194	.7731	.7363
17	.8536	-.0190	.0332	.8316	.6187	64	.0188	-.0228	.3965	.8902	.4880	111	.5936	.0453	-.2965	.7769	.7288
18	.8368	-.0210	.0186	.8292	.6237	65	.0135	-.0195	.5397	.9129	.4309	112	.6158	.0435	-.2743	.7807	.7215
19	.8192	-.0230	.0044	.8269	.6285	66	.0090	-.0161	.7049	.9387	.3578	113	.6377	.0415	-.2526	.7843	.7143
20	.8011	-.0251	-.0093	.8246	.6332	67	.0054	-.0126	.8888	.9659	.2645	114	.6594	.0396	-.2313	.7879	.7073
21	.7823	-.0272	-.0226	.8224	.6377	68	.0027	-.0090	1.0315	.9891	.1483	115	.6809	.0376	-.2104	.7914	.7004
22	.7629	-.0293	-.0357	.8203	.6421	69	.0010	-.0054	1.1020	.9999	.0105	116	.7020	.0355	-.1899	.7948	.6936
23	.7431	-.0314	-.0484	.8182	.6464	70	.0001	-.0018	1.0369	.9899	.1426	117	.7227	.0334	-.1697	.7981	.6869
24	.7227	-.0334	-.0610	.8161	.6506	71	.0001	.0010	.8130	.9555	.3030	118	.7431	.0314	-.1497	.8015	.6803
25	.7020	-.0355	-.0734	.8141	.6548	72	.0010	.0054	.4615	.9005	.4626	119	.7629	.0293	-.1298	.8048	.6737
26	.6809	-.0376	-.0857	.8121	.6589	73	.0027	.0090	.0610	.8361	.6091	120	.7823	.0272	-.1100	.8081	.6671
27	.6594	-.0396	-.0978	.8101	.6630	74	.0054	.0126	-.3036	.7750	.7311	121	.8011	.0251	-.0901	.8113	.6604
28	.6377	-.0415	-.1099	.8081	.6670	75	.0090	.0161	-.5863	.7276	.8235	122	.8192	.0230	-.0702	.8146	.6537
29	.6158	-.0435	-.1220	.8061	.6711	76	.0135	.0195	-.7831	.6933	.8802	123	.8368	.0210	-.0501	.8179	.6469
30	.5936	-.0453	-.1340	.8041	.6751	77	.0188	.0228	-.9114	.6706	.9300	124	.8536	.0190	-.0297	.8213	.6401
31	.5714	-.0471	-.1460	.8021	.6791	78	.0251	.0261	-.9923	.6662	.9581	125	.8697	.0171	-.0090	.8247	.6330
32	.5490	-.0488	-.1580	.8001	.6830	79	.0322	.0292	-1.0426	.6471	.9762	126	.8850	.0152	.0122	.8282	.6258
33	.5266	-.0504	-.1698	.7981	.6870	80	.0402	.0322	-1.0724	.6417	.9853	127	.8994	.0134	.0339	.8317	.6184
34	.5042	-.0519	-.1815	.7962	.6909	81	.0491	.0351	-1.0873	.6390	.9904	128	.9131	.0117	.0563	.8354	.6108
35	.4819	-.0533	-.1931	.7943	.6947	82	.0587	.0378	-1.0903	.6384	.9915	129	.9258	.0101	.0794	.8391	.6028
36	.4596	-.0546	-.2045	.7924	.6985	83	.0692	.0405	-1.0839	.6396	.9893	130	.9376	.0086	.1034	.8430	.5945
37	.4375	-.0557	-.2155	.7905	.7021	84	.0805	.0429	-1.0700	.6421	.9845	131	.9484	.0071	.1284	.8471	.5858
38	.4156	-.0567	-.2262	.7887	.7056	85	.0926	.0453	-1.0504	.6457	.9770	132	.9583	.0058	.1546	.8514	.5766
39	.3939	-.0576	-.2363	.7870	.7090	86	.1053	.0474	-1.0263	.6500	.9696	133	.9671	.0046	.1821	.8558	.5669
40	.3724	-.0583	-.2459	.7854	.7121	87	.1189	.0494	-.9992	.6549	.9604	134	.9749	.0035	.2110	.8605	.5566
41	.3512	-.0589	-.2547	.7840	.7150	88	.1331	.0513	-.9698	.6602	.9505	135	.9817	.0026	.2417	.8654	.5455
42	.3304	-.0592	-.2626	.7826	.7176	89	.1481	.0529	-.9389	.6657	.9401	136	.9873	.0018	.2756	.8709	.5332
43	.3100	-.0594	-.2694	.7815	.7199	90	.1637	.0544	-.9070	.6714	.9293	137	.9919	.0011	.3182	.8777	.5175
44	.2899	-.0595	-.2751	.7806	.7217	91	.1800	.0557	-.8744	.6772	.9185	138	.9954	.0006	.3609	.8845	.5016
45	.2703	-.0593	-.2793	.7798	.7231	92	.1969	.0568	-.8416	.6830	.9075	139	.9979	.0003	.4038	.8913	.4852
46	.2512	-.0590	-.2819	.7794	.7240	93	.2145	.0577	-.8086	.6889	.8966	140	.9994	.0001	.4467	.8982	.4685
47	.2325	-.0584	-.2826	.7793	.7242	94	.2325	.0584	-.7756	.6947	.8857	141	.9994	-.0001	.4460	.8981	.4688

*** LIFT, WAVE DRAG, AND QUARTER-CHORD MOMENT COEFFICIENTS.....CL = .3338, CD =-.0007, CM =-.0018 ***

4. PROGRAM INFORMATION

This chapter contains individual descriptions of most of the program modules including flowcharts for the larger, more complicated routines. This information should provide the reader with deeper insight into the details of the TAIR program logic and, therefore, allow for more efficient code operation. In addition, this chapter (along with chap. 5 on theoretical development) should provide assistance to the user who wishes to modify the TAIR computer program for new applications.

The TAIR computer program consists of 16 program modules: a main program which contains the AF2 flow-solver logic (MAIN); several major subroutines which provide for solution initialization, grid generation, geometry specifications, solution output, etc. (INITL, GRGEN, GEMPAC, INNER, OUTER, ADI, CHECK, AUTO, and OUTPUT); and several minor subroutines which perform a variety of simpler yet very necessary functions (TRIB, TRIP, CSPLIN, FORCE, PRNPLT, and XYOUT). Each of these routines along with a brief description of its function is listed in table 2. A subroutine tree showing the relation of each routine to its called and calling routines is displayed in figure 4.

In addition, the TAIR program utilizes nine COMMON blocks including a blank, or unlabeled COMMON block used to store the velocity potential (PHI) and density (RHO) arrays, and eight labeled COMMON blocks. These blocks contain NAMELIST variables, boundary-condition arrays, and control variables (COM1 and GRGN), indexing arrays and metric arrays (COM2 and COM4), airfoil coordinates and titles (COM3 and COM5), and miscellaneous solution parameters (CONV and SCRACH). Table 3 displays these nine COMMON blocks along with brief descriptions and the names of the routines which reference each block.

Tables 2 and 3, figure 4, and the flowcharts to be discussed shortly provide the user with a quick reference source for most of the information to follow. Also, prominent program variables (cross-referenced with theoretical names) are listed alphabetically with brief descriptions in appendix B. These measures should enable the user to assimilate quickly much of the information contained in this chapter and should be referred to as needed during the following more detailed discussion.

Description of MAIN Program

Program execution is initiated at the beginning of MAIN with a call to SUBROUTINE INITL, as indicated in the flow chart of figure 5. After receiving the initial solution and transformation metrics from INITL, the multiple-solution loop in MAIN (DO 1001 ICASE=1,NC) is entered. The value of NC is established via the first call to INITL from the NCASE parameter (NAMELIST FLOWIN). Inside the multiple-solution loop, for the second and each succeeding solution, SUBROUTINE INITL is called again for reinitialization of solution parameters. Next MAIN starts the main AF2 iteration loop (DO 1000 N=1,NSTEPS). In the first sweep (bidiagonal along the η-direction), the density coefficients RI and RJ are calculated. If the rotated differencing is turned on (NDIF=1), the RJ coefficient is upwinded. Then the residual R and the first sweep

intermediate result F are calculated. Due to the AF2 algorithm construction, this sweep starts at the airfoil boundary (J=NJ) and proceeds backwards in J to the outer boundary (J=1). In the second sweep of the AF2 flow solver (periodic tridiagonal along the ξ direction), the matrix coefficients A, D, B, and C are calculated, and the correction (COR) is obtained from the tridiagonal solver TRIP. This sweep starts at the outer boundary (J=1) and proceeds forward in J to the airfoil boundary (J=NJ). Then the velocity potential (PHI), the circulation (GNP), and the density (RHO) are obtained for the new iteration level. The density values at the trailing edge are averaged to remove any oscillation that might be caused by the trailing-edge mapping singularity. At this point the solution is checked for convergence (see chap. 3, NAMELIST FLOWIN, for a discussion of ERR, the flow-solver convergence parameter). If the solution is diverging, the iteration procedure is stopped. If the solution is converging, but not yet converged, it goes through another iteration after a call to SUBROUTINE AUTO (providing IAUTO=1). If the solution is declared converged, iteration terminates, the solution is printed according to NOUT, and the program either begins the next case or ends.

Description of SUBROUTINE INITL

This subroutine reads the option and acceleration parameters (NAMELIST FLOWIN), contains a set of default values for all NAMELIST FLOWIN parameters, and computes the mapping metrics, the initial flow-field solution, and most of the solution control parameters. INITL first defines the default values, then reads the NAMELIST FLOWIN data cards and updates the default parameters with user-supplied values. If NOUT$\geq$4, this updated list is printed. If ICHECK=1, SUBROUTINE CHECK is called to ensure that all input parameters are within range. The different MESH functions then follow. If MESH=1 or 2, the number of ξ and η points (NX, NY) and the coordinates of the grid (X, Y) are read from logical unit 48. Then the two body-surface arrays (XB, YB) are defined, TEOPEN is calculated (if MESH=1), and a check is made to ensure that NI and NJ match NX and NY. If the NX and NY values do not match NI and NJ, the NI and NJ values will be changed to NX and NY. An error message announcing this change will always be printed, regardless of the NOUT value. If MESH=3, the program reads the mesh dimensions NX and NY, TEOPEN, and the grid coordinates from unit 48. This information must have been generated by the GRAPE grid generation program (ref. 5). In order to make the GRAPE mesh compatible with TAIR, NI must be one greater than the number of ξ points in the GRAPE grid (called JMAX in GRAPE). A check on grid dimension compatability similar to the MESH=1 or 2 option check is performed for this option. For TAIR, the η coordinates must be renumbered to read from the outer boundary (J=1) to the airfoil surface (J=NJ), instead of the airfoil outward numbering system employed by GRAPE. Since TAIR uses a double-stored row of points along the vortex sheet, and the GRAPE code does not, a second set of points at I=NI must be added to the GRAPE grid. The last task performed in the MESH=3 section is to assign the body-surface arrays, XB and YB.

Next, INITL computes a series of counters, including a periodic indexing array (IA), based on the mesh dimensions. GRGEN is then called to either compute a new mesh (MESH=0) or to add finishing touches to the mesh which was read in from unit 48 (MESH=1,2,3). After INITL has received the grid

coordinates, the metric quantities and the Jacobian are computed. Some smoothing around the trailing edge is done to these quantities to reduce the effect of the trailing-edge mapping singularity on the flow-field solution. If NOUT≥9, SUBROUTINE XYOUT is called to print the grid coordinates and metric quantities. INITL then calculates the free-stream properties and the initial solutions for the velocity potential PHI and the density RHO. Figure 6 shows a brief logical flowchart for this subroutine.

Description of SUBROUTINE GRGEN

SUBROUTINE GRGEN sets up the finite-difference grid, using the SUBROUTINEs GEMPAC, INNER, OUTER, and ADI. If a mesh has already been read in and does not need to be changed (MESH=1 or 3), the main body of the coding is skipped. If a new mesh is generated (MESH=0) or an old mesh is modified (MESH=2), the following steps occur. After the default variables have been set for the GRIDIN NAMELIST parameters, the NAMELIST is read for user updates. If NOUT≥4, this updated list is printed. If the check option is on, GRGEN calls CHECK to scan the NAMELIST parameters. It then calls GEMPAC to determine the airfoil coordinates. If airfoil coordinates are read in (IOPT=4), and the check option is on, the coordinates will be checked for mispunched values. SUBROUTINE INNER is called next to cluster the points about the airfoil surface. This clustering operation is controlled by the BINN parameter. If MESH=0, GRGEN calls OUTER to determine the outer boundary point distribution, fills in the middle of the mesh using an exponential formula to obtain the mesh initial conditions, and then calls SUBROUTINE ADI (the alternating-direction-implicit solver) to solve for the final finite-difference grid. Finally, SUBROUTINE GRGEN creates the double-stored, NIth row of grid points along the vortex sheet. If MESH=2, GRGEN establishes the final mesh by modifying a previously generated mesh stored on unit 48 to adapt to the new airfoil. This simple operation involves a shearing of the old mesh and therefore should only be attempted for relatively small airfoil changes. The value of the clustering control parameter (BINN) used to generate the new airfoil clustering distribution should be identical with the value used to establish the old mesh stored on unit 48. Use of this option eliminates the CALL to ADI and therefore greatly reduces the mesh-generation execution time. This option was intended for use with a numerical optimization application. Finally, GRGEN places the XB and YB arrays at halfpoints using calls to SUBROUTINE CSPLIN (cubic spline interpolation) for all MESH options (0, 1, 2, and 3). If MESH is greater than zero, the program will return to INITL. For MESH=0, GRGEN writes the grid solution to a logical unit 48 before returning to INITL. This grid solution can then be used for second, third, etc. calculations during the same run using the MESH=1 or 2 options, or it can be made permanent by using the appropriate JCL control statements. See figure 7 for a brief logical flowchart of SUBROUTINE GRGEN.

Description of SUBROUTINE GEMPAC

This subroutine establishes the inner boundary shape (J=NJ, airfoil coordinates). The two arrays, XB and YB, are the nondimensionalized inner boundary coordinates starting at the lower trailing-edge point and moving clockwise around the airfoil to the upper trailing-edge point. SUBROUTINE GEMPAC

contains five basic geometry options controlled by the parameter IOPT. For IOPT=1, a NACA-00XX-type airfoil is generated from the standard analytic expression. This airfoil can have an open or closed trailing edge. IOPT=2 generates a circular-arc airfoil with a blunted nose controlled by the XC parameter. IOPT=3 yields the cross section of a circular cylinder. The read-in option for other airfoils is IOPT=4, and the fifth option, IOPT=5, uses the Korn airfoil coordinates stored in a data statement. (See chap. 3 for a complete description of all these options.) After the XB and YB inner boundary arrays are filled, the appropriate airfoil title is assigned to TITLE, the coordinates are normalized so that the X coordinates of the leading and trailing edges are equal to 0.0 and 1.0, respectively, and the trailing-edge thickness (TEOPEN) is calculated. If NOUT≥4, the coordinates will be printed out before the logic returns to GRGEN.

Descriptions of SUBROUTINEs INNER and OUTER

SUBROUTINE INNER distributes the points about the airfoil surface. First it calculates the existing arc-length distribution (S) from the XB and YB body-surface coordinates. Next, the desired arc-length distribution (S2) is computed according to the BINN parameter. If BINN is greater than one, the new arc-length distribution is computed from a stretching formula. The closer the BINN value is to one, the more the points are clustered at the leading and trailing edges. If BINN=0.0, the desired arc-length distribution is equally spaced (note that this distribution option for S2 is unacceptable for standard airfoil calculations). If BINN=-1.0, the new arc-length distribution is taken from a data statement which was calculated using conformal mapping. If BINN=-2.0, the user-supplied distribution is read from cards. (See chap. 3 for a more complete description of these clustering options.) If the desired inner boundary arc-length distribution (S2) is established via the BINN=-1.0 or -2.0 options, the number of points in the distribution will generally not agree with the desired final number of points (NI) input in INITL from NAMELIST FLOWIN. This discrepancy is removed by interpolating the S2 distribution up or down so as to involve NI points. The distribution of points inherent in the S2 array is not changed by this interpolation, only the number of points is changed. The existing and desired arc-length arrays (S and S2) are then used to interpolate new values of XB and YB. The new values of XB and YB are thereby distributed according to the desired arc-length distribution (S2). The interpolation process used is that of cubic spline interpolation (SUBROUTINE CSPLIN). If NOUT≥5, the final XB and YB coordinates will be printed. After setting the X(I,NJ) and Y(I,NJ) coordinate arrays equal to XB and YB, control returns to GRGEN.

SUBROUTINE OUTER sets up the point distribution on the outer boundary of the finite-difference grid. OUTER is divided into three sections; the IOUT parameter determines which section is used. IOUT=1 computes a circular outer boundary with radius RADMAX centered at XCN and YCN, then returns to GRGEN. If IOUT=2, the outer boundary distribution is read from cards, and the logic returns to GRGEN. If IOUT=3, a rectangular mesh with semicircular ends is calculated. The nondimensionalized height and width of the base rectangle are given by HTMAX and WDTHMX, respectively. This latter option should prove useful for wind-tunnel wall applications. However, options for different

flow-solver boundary conditions that model solid-wall or porous-wall conditions have not been included. (See chap. 3 for more details about implementing the IOUT options.)

Description of SUBROUTINE ADI

SUBROUTINE ADI determines the final grid coordinates (X and Y) by requiring that they be solutions to appropriately formulated elliptic partial differential equations. An alternating-direction-implicit iteration scheme is used to determine the final numerical values of X and Y. Pertinent aspects about this algorithm are discussed in chapter 5. SUBROUTINE ADI starts almost immediately with the main iteration loop, DO 1000 N=1,MAXIT. Just inside this loop the ALPHA acceleration parameter, which effectively behaves like the inverse of a time-step, is computed from user-specified values of ALGRID and AHGRID. Inside the first sweep (tridiagonal inversions along the ξ or wrap-around direction), the metrics, the X and Y equation residuals, and the tridiagonal matrix coefficients are all computed. SUBROUTINE ADI then calls SUBROUTINE TRIP (tridiagonal solver with periodic boundary conditions) for the X-equation inversion and SUBROUTINE TRIB (tridiagonal solver with fixed boundary conditions) for the Y-equation inversion. The two intermediate results are stored in the FX and FY two-dimensional arrays. The second sweep (tridiagonal inversions along the η or normal-like direction) uses these values to obtain the new values of X and Y. SUBROUTINE TRIB is used for inverting the tridiagonal matrix equations for both the X and Y equations of the second sweep. If NOUT$\geq$8, the ADI grid-generation convergence history is printed. Finally, a check for convergence is made. If the grid solution has converged, control returns to GRGEN; if not, it returns to the start of the routine for another iteration.

Descriptions of SUBROUTINEs CHECK and AUTO

SUBROUTINE CHECK scans the user inputs to see that there are no out-of-range or incorrect values. The call to CHECK is suppressed if ICHECK is set to zero. This subroutine is divided into three sections, and the variable ICH (set in INITL and GRGEN) designates which section of the routine to use. The first section (ICH=1) checks the parameters in the FLOWIN NAMELIST. The second section (ICH=2) checks the airfoil coordinates for mispunched or erratic points. The last section (ICH=3) checks the parameters in the GRIDIN NAMELIST. If an out-of-range value is detected, one of the following three things will occur. One, the error is serious and the logical LCHECK flag is set to true. The solution is then terminated when the logic returns to MAIN. In a multiple-solution run, execution of the remaining cases will be unaffected, providing the error detected in the preceeding section does not persist. Two, the parameter in error is reset to some predetermined value and the solution continues. Or three, the subroutine issues a warning that an out-of-range or inaccurate parameter has been found but has not been changed. In all of these responses, a message is generated, regardless of the NOUT value.

SUBROUTINE AUTO scans the convergence history and updates the solution parameters (BETA, CON, RGAM, and NDIF) to speed convergence or to prevent

divergence. The call to SUBROUTINE AUTO is suppressed if the IAUTO parameter of NAMELIST FLOWIN is set equal to zero, and none of the solution parameters are changed from their initial values. The first section of logic in this subroutine increases or decreases BETA, the time-like dissipation parameter, based on changes in the average and maximum residuals. (See chap. 5 for more detailed information about this process.) The next section decreases BETA if the NSP builds up slowly, or increases it if the NSP is building rapidly. This reflects the need for more time-like dissipation when the supersonic region is large and less when the supersonic region is small. The section following this activates the rotated differencing (NDIF=1) and lowers the circulation relaxation factor (RGAM) when the supersonic flow approaches the airfoil trailing edge. Next the artificial viscosity parameter (CON) is lowered if the circulation and NSP are building too slowly. For weak-shock calculations this reduced value of CON is superior because it allows for sharper, less-smeared shock profiles. The second-to-last section of logic lowers BETA to remove an additional amount of temporal damping. This level of BETA produces a stable iteration only for weak-shock cases in which the extent of supersonic flow is small. When flow conditions permit this small level of BETA, very fast convergence is possible. If any of these changes is made, a message describing the change will be printed, providing NOUT≥4. The last section looks at only the airfoil surface flow-field solution and, if NOUT≥4, prints a warning when the Mach number exceeds 1.3. This Mach number value, occurring immediately upstream of a normal shock, is generally accepted as the limit where significant discrepancies exist between the full-potential equation and the more exact Euler equation formulations. Solutions which exceed this limit should be interpreted with caution.

Description of SUBROUTINE OUTPUT

SUBROUTINE OUTPUT contains most of the solution output and is called exclusively by MAIN. OUTPUT is divided into four sections and is controlled by the variable II set in MAIN and passed to OUTPUT through the calling argument list. In addition, all output is controlled by the output control parameter NOUT. The first section (II=1) prints the transformation metric quantities near the airfoil surface (NOUT≥8) and sets up the headings for the solution convergence history (NOUT≥6). The second section of OUTPUT (II=2) prints the AF2 convergence history data, providing all print criteria are satisfied. The parameters NOUT and NOUT2 control this operation. If N is a multiple of the NOUT1 parameter, an intermediate airfoil solution will be printed. (Caution: small values for NOUT1 will cause excessive amounts of output.) Included in the intermediate airfoil solution output is the following: if NOUT≥7, contour maps of the density and Mach number will be printed. If NOUT≥3, the title of the airfoil or mesh and the flow-field conditions (MINF and ALPH) will be printed. If NOUT≥2, the iteration number (N), the maximum residual (RMAX), the number of supersonic points (NSP), and the coefficient of lift calculated from the circulation (CL) will be printed. The airfoil surface solution for the Nth iteration is printed next (if NOUT≥3). Finally, SUBROUTINE OUTPUT calls SUBROUTINE FORCE to calculate and print out the lift, wave-drag, and quarter-chord moment coefficients.

When the main iteration loop has ended, either by converging or reaching the maximum number of iterations (N=NSTEPS), SUBROUTINE OUTPUT is again called. If the iteration limit is reached (II=3), or the solution has converged (II=4), a statement indicating the nature of the iteration termination is printed, providing NOUT≥6. After either of these two statements has been printed, the control logic is sent back to the second section of SUBROUTINE OUTPUT to print the final solution. This final solution depends, as before, on NOUT and includes: the printer contour maps, the title line, the last line of convergence information, the airfoil surface solution, and the force coefficients.

Description of Minor Subroutines

The TAIR program contains several smaller subroutines which are classified as utility routines. These routines include CSPLIN, TRIB, TRIP, PRNPLT, XYOUT, and FORCE.

SUBROUTINE CSPLIN performs a cubic spline interpolation. Inputs via the formal parameter argument list include the independent variable array (XX) which defines the new function interpolates, the independent and dependent arrays (X and Y) which define the function to be interpolated, the index limits N1 and N2 for the XX and YY arrays, and the index limits J1 and J2 for the X and Y arrays. The YY array contains the found interpolates resulting from the interpolation process and is passed back to the original calling routine as a formal parameter in the argument list. The A, B, C, D, F, and H arrays are only dummy arrays defined as formal parameters to save storage. If any element of XX is outside the range of X (with a fudge factor added), or if the independent array X is not monotonic, the X, Y, XX, and YY values are printed along with a message explaining the problem, and the program is stopped.

SUBROUTINE FORCE is called by OUTPUT to calculate and print out the lift, wave-drag, and quarter-chord moment coefficients. SUBROUTINE FORCE numerically integrates the airfoil surface pressure coefficient distribution, using a trapezoid rule integration algorithm. The inputs to SUBROUTINE FORCE are made through the formal argument list and include: the number of points on the airfoil surface (NI), the airfoil surface coordinates (X and Y), the pressure coefficient distribution (CP), the angle of attack (ALPH), and the distance across the trailing edge (TEOPEN). The coefficients are printed when NOUT≥1.

SUBROUTINEs TRIB and TRIP are scalar tridiagonal matrix inversion routines with fixed and periodic boundary conditions, respectively. The formal parameter argument lists consist of A, B, and C, which are the below-diagonal, diagonal, and above-diagonal matrix elements, respectively; F, the RHS column vector; X, Q, and S, dummy arrays of scratch storage; and index limits, NL, NU, and JINC, for TRIB and J1, J2, and JINC for TRIP. Inclusion of the JINC parameter allows the inversion of a tridiagonal matrix using every (JINC)th entry in the A, B, C, and F arrays. For all cases in TAIR JINC is equal to one. Each subroutine passes back the result array in the array originally holding the RHS values (F). Neither subroutine prints any output. An object-code version of both TRIB and TRIP suitable for execution on the CDC 7600 computer is available. The object-code version executes approximately twice

as fast as the original FORTRAN version, which allows a 10% reduction in overall computer time for most TAIR calculations. For all computer times listed in this report the faster object-code versions of TRIB and TRIP have been used.

SUBROUTINE PRNPLT (called by SUBROUTINE OUTPUT) produces a two-dimensional printer contour map for the array VAR. Each element of this array is assigned an integer from 0 to 9 according to its size relative to the maximum and minimum variations in the array. The resulting integers are printed across the page with a 132I1 format to create a single page "snapshot" of the entire flow field. If an attempt is made to print a map with no variation, SUBROUTINE PRNPLT will print a warning message and ignore the request. Arrays exceeding 132 in the first dimension are truncated so that the last 132 entries in the array receive a position in the printed contour map. (See chap. 3 for more discussion and an example.)

SUBROUTINE XYOUT is called by SUBROUTINE INITL to print the finite-difference grid metrics (A1, A2, A3, and XJ) and coordinates (X and Y) providing NOUT≥9. The formal parameter argument list includes the grid dimensions NI and NJ and the printout increments in the I and J directions IINCR and JINCR.

5. FULL-POTENTIAL EQUATION ALGORITHM

Theoretical details of the algorithm used in TAIR are now discussed. Emphasis in this section is on relating details of code operation and organization to different aspects of the numerical algorithm. Many of the variables used in this theoretical chapter are listed, briefly defined, and cross-referenced with the corresponding TAIR names in appendix B. This information along with that of the previous chapter is intended to provide enough detail to allow modification of TAIR for new applications. For more information about the algorithm, references 1-3 are suggested.

Governing Equations

The full-potential equation in strong conservation-law form is given by

$$(\rho\Phi_x)_x + (\rho\Phi_y)_y = 0 \tag{1a}$$

$$\rho = \left[1 - \frac{\gamma - 1}{\gamma + 1}\left(\Phi_x^2 + \Phi_y^2\right)\right]^{1/\gamma-1} \tag{1b}$$

where Φ is the full or exact velocity potential, ρ is the fluid density, x and y are Cartesian coordinates in the streamwise and vertical directions, and γ is the ratio of specific heats. The density (ρ) and velocity components (Φ_x and Φ_y) are nondimensionalized by the stagnation density (ρ_s) and the critical speed of sound (a*), respectively.

Equation (1) is transformed from the physical domain (Cartesian coordinates) into the computational domain by using a general independent variable transformation. This general transformation, indicated by (see fig. 1)

$$\xi = \xi(x,y)$$
$$\eta = \eta(x,y) \tag{2}$$

maintains the strong conservation law form of equation (1). The full-potential equation written in the computational domain ($\xi - \eta$ coordinate system) is given by

$$\left(\frac{\rho U}{J}\right)_\xi + \left(\frac{\rho V}{J}\right)_\eta = 0 \tag{3}$$

$$\rho = \left[1 - \frac{\gamma - 1}{\gamma + 1}\left(A_1\Phi_\xi{}^2 + 2A_2\Phi_\xi\Phi_\eta + A_3\Phi_\eta{}^2\right)\right]^{1/\gamma-1} \tag{4}$$

where

$$U = A_1\Phi_\xi + A_2\Phi_\eta$$
$$V = A_2\Phi_\xi + A_3\Phi_\eta$$
$$A_1 = \xi_x{}^2 + \xi_y{}^2 \tag{5}$$
$$A_2 = \xi_x\eta_x + \xi_y\eta_y$$
$$A_3 = \eta_x{}^2 + \eta_y{}^2$$

and

$$J = \xi_x\eta_y - \xi_y\eta_x$$

The U and V quantities are the contravariant velocity components along the ξ and η directions, respectively; A_1, A_2, and A_3 are metric quantities; and J is the Jacobian of the transformation. To evaluate the expressions of equation (5), the following metric identities are necessary:

$$J = 1/(x_\xi y_\eta - x_\eta y_\xi)$$
$$\xi_x = Jy_\eta\,, \quad \eta_x = -Jy_\xi \tag{6}$$
$$\xi_y = -Jx_\eta, \quad \eta_y = Jx_\xi$$

The transformed full-potential equation (eqs. (3), (4)) is only slightly more complicated than the original Cartesian form (eq. (1)) and offers several

significant advantages. The main advantage is that boundaries associated with the physical domain are transformed to boundaries of the computational domain. This aspect is illustrated in figure 1, in which the physical and computational domains for a typical transformation are shown. The inner airfoil boundary becomes the $\eta = \eta_{max}$ computational boundary and the outer physical boundary becomes the $\eta = \eta_{min}$ computational boundary. Note that no restrictions have been placed on the shape of the outer boundary. Arbitrarily shaped outer boundaries, including wind-tunnel walls, may be used.

Another advantage of this approach is the ability to adjust arbitrarily the mesh spacing on the airfoil surface or in the mesh interior, with the provision that the smoothness of the mesh is not disrupted. This, in theory, could be used to cluster mesh points around any gradients in the flow field (e.g., shock waves or the leading-edge stagnation point). The next section introduces the method of generating the finite-difference meshes used in the TAIR program.

Grid Generation

The automatic grid generation scheme used by Thompson et al. (ref. 9) has been adapted for use in the TAIR computer code. Basically, this grid-generation scheme uses numerically generated solutions of Poisson's equation (or, in the present application, Laplace's equation) to establish regular and smooth finite-difference meshes around arbitrary bodies. These equations are transformed to (and solved in) the computational domain (i.e., ξ and η are the independent variables and x and y are the dependent variables). The transformed equations are given by

$$\begin{aligned} Ax_{\xi\xi} - 2Bx_{\xi\eta} + Cx_{\eta\eta} &= 0 \\ Ay_{\xi\xi} - 2By_{\xi\eta} + Cy_{\eta\eta} &= 0 \end{aligned} \tag{7}$$

where

$$A = x_\eta^2 + y_\eta^2 , \quad B = x_\xi x_\eta + y_\xi y_\eta , \quad C = x_\xi^2 + y_\xi^2 \tag{8}$$

The numerical solution of equation (7) is achieved by first replacing all derivatives in equations (7) and (8) by standard second-order-accurate finite differences. A residual operator can be defined and is given by

$$L(\ )_{i,j} = [A_{i,j}\delta_{\xi\xi} - 2B_{i,j}\delta_{\xi\eta} + C_{i,j}\delta_{\eta\eta}](\ )_{i,j} \tag{9}$$

where the i and j subscripts indicate position in the finite-difference mesh. The operators used in equation (9) are defined by

$$\delta_{\xi\xi}(\ )_{i,j} = (\ )_{i+1,j} - 2(\ )_{i,j} + (\ )_{i-1,j}$$

$$\delta_{\xi\eta}(\ )_{i,j} = \frac{1}{4}\left[(\ )_{i+1,j+1} - (\ )_{i+1,j-1} - (\ )_{i-1,j+1} + (\ )_{i-1,j-1}\right] \qquad (10)$$

$$\delta_{\eta\eta}(\ )_{i,j} = (\ )_{i,j+1} - 2(\ )_{i,j} + (\ )_{i,j-1}$$

The spatial increments ($\Delta\xi$ and $\Delta\eta$) are equal to 1 and therefore have been omitted. Once boundary values and an initial solution for $x_{i,j}$ and $y_{i,j}$ have been established, the final interior values can be computed by relaxation. Usually, either successive overrelaxation (SOR) or successive-line overrelaxation (SLOR) is used for this purpose. However, in the TAIR program a faster alternating-direction-implicit (ADI) relaxation algorithm is applied. This algorithm can be expressed by

Step 1:

$$(\alpha - A^n_{i,j}\delta_{\xi\xi})f^n_{i,j} = \alpha\omega Lx^n_{i,j} \qquad (11a)$$

$$(\alpha - A^n_{i,j}\delta_{\xi\xi})g^n_{i,j} = \alpha\omega Ly^n_{i,j} \qquad (11b)$$

Step 2:

$$(\alpha - C^n_{i,j}\delta_{\eta\eta})(x^{n+1}_{i,j} - x^n_{i,j}) = f^n_{i,j} \qquad (12a)$$

$$(\alpha - C^n_{i,j}\delta_{\eta\eta})(y^{n+1}_{i,j} - y^n_{i,j}) = g^n_{i,j} \qquad (12b)$$

where $f^n_{i,j}$ and $g^n_{i,j}$ are intermediate results stored at each point in the finite-difference mesh. In step 1, the f and g arrays are obtained by solving two tridiagonal matrix equations for each η = constant line. The corrected values of x and y are then obtained in the second step from the f and g arrays, respectively, by solving two tridiagonal matrix equations for each ξ = constant line. Because of the implicit construction of this scheme, each point in the finite-difference mesh influences every other point during each iteration. As a result, evolution of the solution proceeds at a much faster rate.

Spatial Differencing

The finite-difference approximations used to discretize equations (3) to (5) in the TAIR computer program are described in this section. These spatial difference approximations, which are valid for both subsonic and supersonic regions of flow, are given by

$$\overset{+}{\delta}_{\xi}\left(\frac{\tilde{\rho}U}{J}\right)_{i+1/2,j} + \overset{+}{\delta}_{\eta}\left(\frac{\tilde{\rho}V}{J}\right)_{i,j+1/2} = 0 \qquad (13)$$

where the $\overleftarrow{\delta}_\xi$ and $\overleftarrow{\delta}_\eta$ backward-difference operators are defined by

$$\begin{aligned}\overleftarrow{\delta}_\xi(\ )_{i,j} &= (\ )_{i,j} - (\ )_{i-1,j} \\ \overleftarrow{\delta}_\eta(\ )_{i,j} &= (\ )_{i,j} - (\ )_{i,j-1}\end{aligned} \tag{14}$$

The quantities $(U/J)_{i+1/2,j}$ and $(V/J)_{i,j+1/2}$ used in equation (13), are computed using standard, second-order-accurate, finite-difference formulas. An example is given by

$$\left(\frac{U}{J}\right)_{i+1/2,j} = \left(\frac{A_1}{J}\right)_{i+1/2,j}(\Phi_{i+1,j} - \Phi_{i,j}) + \frac{1}{4}\left(\frac{A_2}{J}\right)_{i+1/2,j}(\Phi_{i+1,j+1} - \Phi_{i+1,j-1} + \Phi_{i,j+1} - \Phi_{i,j-1}) \tag{15}$$

The Jacobian, J, and the metric quantities, A_1, A_2, and A_3, used both in equation (15) and in the density calculation (to be discussed shortly) are first computed at integer points (i,j) using standard, fourth-order-accurate, finite-difference formulas. These quantities are regrouped and permanently stored at different locations given by

$$\begin{aligned}A1(I,J) &= \left(\frac{A_1}{J}\right)_{i+1/2,j} \\ A2(I,J) &= \frac{1}{4}\left(\frac{A_2}{J}\right)_{i,j} \\ A3(I,J) &= \left(\frac{A_3}{J}\right)_{i,j+1/2} \\ XJ(I,J) &= J_{i+1/2,j+1/2}\end{aligned} \tag{16}$$

where the coded variable names are on the left and the analytical expressions are on the right. Because the interpolation process by which the metric quantities are moved is fourth-order accurate, the final expressions A1, A2, A3, and XJ are themselves fourth-order accurate. During the iteration process, values of A1, A2, A3, and XJ which are required at points other than where they are stored are obtained by second-order accurate averaging.

The density coefficients of equation (13), $\tilde{\rho}_{i+1/2,j}$ and $\bar{\rho}_{i,j+1/2}$, are defined by

$$\tilde{\rho}_{i+1/2,j} = [(1 - \nu)\rho]_{i+1/2,j} + \nu_{i+1/2,j}\rho_{i+k+1/2,j} \tag{17a}$$

$$\bar{\rho}_{i,j+1/2} = [(1 - \nu)\rho]_{i,j+1/2} + \nu_{i,j+1/2}\rho_{i,j+\ell+1/2} \tag{17b}$$

where

$$k = \mp 1 \quad \text{when} \quad U_{i+1/2,j} \gtrless 0$$
$$\ell = \mp 1 \quad \text{when} \quad V_{i,j+1/2} \gtrless 0 \tag{18}$$

The density values required in equation (17) are computed using a binomial series expansion of equation (4). To improve the computational efficiency, only the first four terms are retained. The final density expression, after some rearranging, is given by

$$\rho = 1 + Q2[C1 + Q2(C2 + Q2 \cdot C3)] \tag{19}$$

where

$$C1 = -\frac{1}{\gamma + 1}, \quad C2 = \frac{2 - \gamma}{2(\gamma + 1)^2}, \quad C3 = \frac{-(2 - \gamma)(3 - 2\gamma)}{6(\gamma + 1)^3} \tag{20}$$

and

$$Q2 = A_1\Phi_\xi{}^2 + 2A_2\Phi_\xi\Phi_\eta + A_3\Phi_\eta{}^2$$

Examination of the error produced by this approximation clearly shows that even under the most adverse conditions (e.g., large local values of Q2), the resulting error in ρ will not exceed a few tenths of a percent. Use of this series expansion to compute ρ eliminates the need for the exponentiation operation, which is computationally very expensive. This single simplification saves about 30% of the CPU time required for a flow-field computation.

Values of the density computed from equation (19) are computed and stored at cell centers, that is, at $i + 1/2$, $j + 1/2$, using values of Φ_ξ and Φ_η computed from

$$\Phi_{\xi_{i+1/2,j+1/2}} = \frac{1}{2}(\Phi_{i+1,j+1} - \Phi_{i,j+1} + \Phi_{i+1,j} - \Phi_{i,j})$$
$$\Phi_{\eta_{i+1/2,j+1/2}} = \frac{1}{2}(\Phi_{i+1,j+1} - \Phi_{i+1,j} + \Phi_{i,j+1} - \Phi_{i,j}) \tag{21}$$

Values of the density required at $i + 1/2,j$ or $i,j + 1/2$ are obtained using simple averages. The switching functions, $\nu_{i+1/2,j}$ and $\nu_{i,j+1/2}$, used in equation (17), control the amount of upwinding in the finite-difference scheme, and are defined by (for example)

$$\nu_{i+1/2,j} = \begin{cases} \max[(M^2_{i,j} - 1)\text{CON},0] & \text{for} \quad U_{i+1/2,j} > 0 \\ \max[(M^2_{i+1,j} - 1)\text{CON},0] & \text{for} \quad U_{i+1/2,j} < 0 \end{cases} \tag{22}$$

where $M_{i,j}$ is the local Mach number and CON is a user-specified constant. In TAIR, equation (22) is actually used to compute a quantity called SIGMA, which equals $1 - \nu$. This SIGMA parameter is used in place of ν as the switching function.

Use of the density coefficients given by equation (17) is equivalent to the addition of an appropriately differenced artificial viscosity term. This effectively maintains an upwind influence in the differencing scheme for supersonic regions anywhere in the finite-difference mesh for any orientation of the velocity vector, thus approximating a rotated-differencing scheme. Other variations of this rotated-differencing scheme achieved by this upwind evaluation of the density are discussed in references 10-12. If rotated differencing is not required, that is, if the supersonic flow region is small, the spatial differencing algorithm can be simplified somewhat by upwinding along only the ξ direction. The switching function in equation (17b), $\nu_{i,j+1/2}$, is effectively set to zero for this option. Thus, no tests for supersonic flow or flow direction must be made for the $\bar{\rho}_{i,j+1/2}$ calculation. This logic is coded into TAIR and controlled by the parameter NDIF. If NDIF=1, upwinding along both the ξ and η directions is used. If NDIF=0 (default), only upwinding along the ξ direction is used. If IAUTO=1 and if the region of supersonic flow moves beyond about 90% of chord on the airfoil surface, the default value of NDIF will automatically be changed to one. This mode of operation has not only proven to be efficient, but is also extremely reliable.

AF2 Iteration Scheme

The AF2 fully implicit approximate factorization scheme is given by

Step 1:

$$(\alpha - \overleftarrow{\delta}_\eta B_j) f^n_{i,j} = \alpha\omega L\Phi^n_{i,j} \tag{23a}$$

Step 2:

$$(\alpha\overleftarrow{\delta}_\eta \mp \alpha\beta\overrightarrow{\delta}_\xi - \overleftarrow{\delta}_\xi B_i \overrightarrow{\delta}_\xi) C^n_{i,j} = f^n_{i,j} \tag{23b}$$

where

$$B_i = \left(\frac{\bar{\rho}^n A_1}{J}\right)_{i+1/2,j}, \quad B_j = \left(\frac{\bar{\rho}^n A_3}{J}\right)_{i,j+1/2} \tag{24}$$

In equation (23), the n superscript is an iteration index; α is an acceleration parameter (to be discussed shortly), ω is a relaxation parameter called OMEGA in TAIR; $L\Phi^n_{i,j}$ is the nth iteration residual (defined by eq. (13)), and $f^n_{i,j}$ is an intermediate result stored at each point in the finite-difference mesh. In step 1, the f array is obtained by solving a simple bidiagonal matrix equation for each ξ = constant line. The correction array is then obtained in the second step from the f array by solving a tridiagonal matrix equation for each η = constant line. Note that with the AF2 scheme,

the η direction difference approximation is split between the two steps. This generates a $\Phi_{\eta t}$-type term, which is useful to the iteration scheme as time-like dissipation. (The iterative process is considered as an iteration in pseudotime. Thus the time derivative is introduced by $(\ )^{n+1} - (\ )^{n} \sim \Delta t(\ )_t$.) The split η term also places a sweep direction restriction on both steps, namely, outward (away from the airfoil) for the first step and inward (toward the airfoil) for the second step. No sweep restrictions are placed on either of the two sweeps due to flow direction.

A $\Phi_{\xi t}$-type term has been added inside the parentheses of step 2 (see eq. (23b)) to provide time-dependent dissipation in the ξ direction. The double arrow notation in equation (23b) on the δ_ξ-difference operator indicates that the difference is always upwind, which on the upper surface is a backward difference and on the lower surface is a forward difference. The sign is chosen in such a way that the addition of $\Phi_{\xi t}$ increases the magnitude of the second sweep diagonal. The parameter β is fixed at a value of 0.3 in subsonic regions. In supersonic regions, β (called BETA in TAIR) is initialized via user specification and then updated using logic similar to that presented in reference 13. The updating procedure exists in SUBROUTINE AUTO and is given by

$$\begin{aligned}
&\text{If} \quad \text{RATIO} < 2.0 \quad \text{then} \quad \beta^n = 0.98\ \beta^{n-1} \\
&\text{If} \quad \text{RATIO} > 2.1 \quad \text{then} \quad \beta^n = 1.1\ \beta^{n-1} \\
&\text{If} \quad \beta^n > \text{BHIGH} \quad \text{then} \quad \beta^n = \text{BHIGH} \\
&\text{If} \quad \beta^n < \text{BLOW} \quad \text{then} \quad \beta^n = \text{BLOW}
\end{aligned} \tag{25}$$

where

$$\text{RATIO} = \frac{\text{RAVG}^n}{\text{RAVG}^{n-m}} + \frac{\text{RMAX}^n}{\text{RMAX}^{n-m}} \tag{26}$$

and

$$\text{BHIGH} = \beta^1 + 1\ , \quad \text{BLOW} = \beta^1 - 1 \tag{27}$$

In equation (26), m is the number of elements in the α sequence (see the sequence definition given by eq. (28)), RAVG^n is the nth iteration average residual and RMAX^n is the nth iteration maximum residual. The logic defined by equations (25) to (27) monitors solution convergence through the parameter RATIO. If convergence is progressing satisfactorily, β is reduced; if not, β is increased. BHIGH and BLOW are upper and lower bounds which limit the amount of β variation. In addition to the above logic, other larger increases or decreases in β are possible. During the iteration process, the base value of β including the values of BHIGH and BLOW can be increased or decreased, if the developing solution requires more or less time-like dissipation. This logic, which has largely been developed empirically, automatically keys on the growth rates of NSP (number of supersonic points) and GNP (the amount of circulation). If these quantities grow rapidly, then

β, BHIGH, and BLOW are all increased; if they grow slowly, then these quantities are decreased.

The quantity α appearing in equation (23) (called ALPHA in TAIR) can be considered as Δt^{-1}. This direct analogy to time provides one strategy for obtaining fast convergence, namely, advance time as fast as possible with large time steps (i.e., small values of α). This is effective for attacking the low-frequency errors but not the high-frequency errors. The best overall approach is to use an α sequence containing several values of α. The small values are particularly effective for reducing the low-frequency errors, and the large values are particularly effective for reducing the high-frequency errors. The α sequence used in the TAIR computer program is given by

$$\alpha_k = \alpha_H \left(\frac{\alpha_L}{\alpha_H}\right)^{k-1/m-1} \qquad k = 1,2, \ldots, m \tag{28}$$

where the sequence endpoints are given by α_L and α_H (called ALOW and AHIGH in TAIR), and m is the number of elements in the sequence.

Circulation Update and Boundary Conditions

The airfoil surface boundary condition is that of flow tangency (i.e., no flow through the airfoil surface); it requires that the η contravariant velocity component at the airfoil surface be zero (i.e., $V = 0$). This boundary condition is implemented by applying

$$\left(\frac{\rho V}{J}\right)_{i,NJ-1/2} = -\left(\frac{\rho V}{J}\right)_{i,NJ+1/2} \tag{29}$$

where $j = NJ$ is the airfoil surface. In other expressions (eqs. (15) and (21)) where Φ_η is required at the airfoil surface, the $V = 0$ boundary condition is used again to obtain

$$\Phi_\eta\Big|_{surface} = -\frac{A_2}{A_3}\,\Phi_\xi\Big|_{surface} \tag{30}$$

At the outer boundary of the computational mesh, the velocity potential is held fixed at the initial free-stream value.

Special boundary conditions inherent in the AF2 iteration algorithm arise at the airfoil surface. During each iteration at the beginning of the first sweep, a boundary condition on f (see eq. (23a)) must be applied at the airfoil surface. Because f is a complicated function with little physical meaning, specification of its value is difficult. As the iteration process drives the solution to a steady state, the value of f approaches zero. Therefore, boundary specification of f should be consistent with this fact. Even if the f boundary condition is consistent with the steady-state solution, a poor choice can slow convergence or even cause instability. For lack

of a better boundary condition, $f_\eta = 0$ is used and seems to produce acceptable results.

To facilitate the circulation calculation process, the velocity potential function is written as the sum of two parts

$$\Phi = \phi + \Gamma\xi \tag{31}$$

where the first part is the nonlinear contribution and the second part essentially consists of a vortex with circulation strength, $2\pi\Gamma$ (Γ is referred to as GNP in TAIR). The idea of breaking the velocity potential into different parts was used in reference 14. The velocity potential function stored in the PHI(I,J) array in TAIR consists of only the nonlinear contribution given by ϕ. The vortex solution contribution is added in explicitly by modifying each Φ_ξ term (in eqs. (15) and (21)) to include

$$\Phi_\xi = \phi_\xi + \Gamma \tag{32}$$

The Φ_η terms are, of course, not affected by this modification. Use of this substitution provides for a significant improvement in the circulation convergence rate because each grid point, through equation (32), feels the influence of the most recent value of the circulation during each iteration. At the end of each iteration, the circulation is recomputed from

$$\Gamma^n = \frac{1}{2}\left(\phi^n_{NI-1,NJ} - \phi^n_{2,NJ}\right) \tag{33}$$

where NI - 1,NJ and 2,NJ are one grid point upstream of the trailing edge on the upper and lower surfaces, respectively. To maintain stability for some situations, the new value of the circulation must be underrelaxed. The nth iteration relaxation factor used for the circulation, RG^n, is computed using

$$RG^n = RGAM \cdot \exp\left[-\left|\frac{8(\Gamma^n - 2\Gamma^{n-1} + \Gamma^{n-2})}{\Gamma^n}\right| - \frac{n}{100}\right]$$

$$\text{if} \quad RG^n < \frac{1}{5}\,RGAM\,, \quad \text{then} \quad RG^n = \frac{1}{5}\,RGAM \tag{34}$$

where RGAM is a user-specified constant. Existence of the second difference on the circulation in the exponential term causes RG^n to automatically be reduced if the circulation growth history begins to oscillate. Use of the n/100 term causes an additional smoothing effect in the circulation growth history curve as the iteration process continues.

When calculations are performed on airfoils with open trailing edges, special logic along the vortex sheet boundary must be considered. The amount of openness or difference in y coordinates at the airfoil trailing edge, defined as TEOPEN in TAIR, is continued downstream of the airfoil with constant thickness all the way to the outer boundary. One purpose of this configuration is to simulate the existence of a wake leaving the airfoil trailing edge. The

velocity potential (ϕ) for this situation has different values along $i = 1$ and $i = NI$, when the angle of attack, ALPH, is nonzero. This difference is given by

$$\phi_{NI,j} - \phi_{1,j} = QYINF \cdot TEOPEN \tag{35}$$

where QYINF is the y component of the free-stream velocity. As a result, all differences of ϕ across the vortex sheet must include the amount of this jump to maintain consistent results. In addition, the circulation computation must also be modified to include this jump. Equation (33) becomes

$$\Gamma^n = \frac{1}{2} \left(\phi^n_{NI-1,NJ} - \phi^n_{2,NJ} - QYINF \cdot TEOPEN\right) \tag{36}$$

6. CASE HISTORY

This chapter describes several different cases run with the TAIR computer code and discusses the results. First, a typical finite-difference grid generated by TAIR is shown in figure 8. This grid was generated for a NACA 0012 airfoil and consists of 4470 points (149 × 30, the default grid). Figure 8(a) shows the entire grid, including the circular outer boundary; figure 8(b) shows a close-up of the grid about the airfoil. The clustering of lines at the leading and trailing edges is shown in more detail in figures 8(c) and 8(d). This grid was generated with the center of the circular outer boundary at the default airfoil midchord position and required 20 iterations of the ADI grid generation routine for convergence and about 1.6 sec of computer time on the CDC 7600 computer.

The first flow-solver solution involves the supercritical Korn airfoil at a free-stream Mach number of 0.74 and an angle of attack of 0°. The pressure coefficient distribution for this slightly off-design calculation is shown in figure 9. The present TAIR version (cycle 8) is compared with a past version (cycle 7, ref. 15) and a result from the GRUMFOIL computer code (ref. 16). All three cases are in excellent agreement. The GRUMFOIL computer code is similar to TAIR in that both codes solve the conservative full-potential equation, but differs in that TAIR uses the AF2 iteration scheme and GRUMFOIL uses a hybrid direct-solver/SLOR iteration scheme (ref. 14). This hybrid iteration scheme is composed of one direct-solver iteration (very effective for reducing low-frequency errors but unstable for supersonic regions) followed by several SLOR iterations. The purpose of the SLOR iterations is to smooth high-frequency errors generated by the direct-solver step in regions of supersonic flow.

The second figure associated with this case (fig. 10) presents the rms error (E_{rms}) convergence-history curves for each of the three iteration schemes. The E_{rms} at iteration n (E^n_{rms}) is defined by

$$E^n_{rms} = \left[\frac{\sum_{i=1}^{NI} \left(C^n_{p_i} - C_{p_i} \right)^2}{\sum_{i=1}^{NI} C^2_{p_i}} \right]^{1/2}$$

where $C^n_{p_i}$ is the surface pressure coefficient at the ith grid point and the nth iteration; C_{p_i} is the surface pressure coefficient at the ith grid point taken from the converged solution, and NI is the total number of surface grid points. Using E_{rms} to compare convergence performance is a much more quantitatively correct procedure than using the standard maximum residual quantity. (More discussion on this point can be found in refs. 1, 17.) The four curves shown in figure 10 correspond to the following iteration schemes: (1) AF2 (cycle 8), (2) AF2 (cycle 7), (3) hybrid, and (4) SLOR. There are two major differences between TAIR cycles 7 and 8. One, the circulation updating algorithm of cycle 8 is considerably improved relative to that of cycle 7. This improvement enhances the convergence speed of the TAIR code for cases with reasonably large amounts of lift. Details of the new circulation algorithm are presented in chapter 5. And two, the automatic updating routine used in cycle 8 (SUBROUTINE AUTO, discussed in chap. 4) is more sophisticated than the one used in cycle 7. This change improves the code reliability and in some cases the computational efficiency. The SLOR iteration scheme is simply the GRUMFOIL hybrid iteration scheme without the benefit of the direct-solver step. Each convergence-history curve is constructed by plotting E_{rms} versus CPU time (Ames CDC 7600 computer). The hybrid case has been computed with default values for all relaxation parameters. Convergence for the SLOR scheme has been approximately optimized by a trial-and-error adjustment of the relaxation parameter. The TAIR runs were computed with default values for all relaxation parameters except for the artificial viscosity parameter CON, which was set to 1.2 for a sharper shock profile. Set-up times, that is, the CPU time required for grid generation, solution initialization, and coarse- and medium-mesh calculations, are included in each convergence-history curve. The cycle 7 and 8 AF2 curves include 6.0 and 1.6 sec, respectively, for grid generation and initialization. The difference in these times is partially due to the coding efficiency changes but primarily due to a reduction in the unnecessarily tight grid convergence tolerance first used with cycle 7. The hybrid and SLOR curves use coarse-medium-fine mesh sequences. Converged results from the coarse mesh are interpolated onto the medium mesh, then from the medium mesh onto the fine mesh, thus providing a good initial guess for the fine-mesh calculation. The set-up times for these cases are 23 sec for the hybrid case and 28 sec for the SLOR case. For this calculation a two-order-of-magnitude reduction in E^n_{rms} produced essentially converged results. At this level of convergence the cycle 8 version of the AF2 scheme is about 2 times faster than the cycle 7 version, about 5 times faster than the hybrid scheme, and about 10 times faster than SLOR.

The second case presents an interesting airfoil shock-wave pattern that develops as the free-stream Mach number approaches 1. This case, a NACA 0012 airfoil with Mach number of 0.95 and angle of attack of 4°, shows with Mach

number contours a "fishtail" shock system (fig. 11). Supersonic-to-supersonic oblique shocks emanate from the trailing edge and merge with a normal shock downstream of the airfoil. The oblique shock emanating from the trailing-edge upper surface has been strengthened by the addition of circulation, while the oblique shock emanating from the trailing-edge lower surface has been weakened and is almost nonexistent. The normal shock above the airfoil plane is much stronger than the normal shock below the plane. This shock-wave pattern is characteristic of solutions with free-stream Mach numbers near unity and has been observed experimentally as well as computationally. This case required only about 100 iterations or about 10 sec of computer time on the CDC 7600 computer for convergence. The rapid convergence of this difficult case demonstrates the reliability and efficiency of the present transonic flow solution procedure. For more information about this case and others like it, see references 3 and 4.

The next two figures compare incompressible theory with two results from TAIR. These two figures plot the surface pressure coefficient distributions versus the X/C coordinate direction. Figure 12 shows that the result of a circular cylinder calculation (Mach number of 0.00001 and angle of attack of 0°) is in excellent agreement with classical incompressible theory (ref. 18). Figure 13 presents the result of the NACA 0012 airfoil at Mach number of 0.00001 and angle of attack of 0°. This, too, is in excellent agreement with theory (ref. 19) everywhere except at the trailing edge. Here the TAIR result differs because the density extrapolation used at the airfoil trailing edge has been designed to more closely approximate experimental results rather than the trailing-edge stagnation predicted in the theoretical results of reference 19. These incompressible calculations generally require about 2 sec of CDC 7600 computer time for convergence (20-40 iterations).

The last case discussed in this chapter shows a comparison of computed and experimental results. The three figures (figs. 14-16) show the surface pressure coefficient versus X/C for three supercritical CAST 7 (ref. 7) airfoil calculations. These calculations were run at a Mach number of 0.7 and three different angles of attack. To account for viscous effects, the TAIR angles of attack were found by approximately matching computed and experimental lifts. Generally speaking, the three plots show good agreement between TAIR and experiment. Slight differences occur at the trailing edges, probably due to trailing-edge separation. The two cases with lower angles of attack, -0.15° and 0.55°, show basically good agreement at the shock, but the largest angle of attack case, 1.35°, produces more disagreement because of the relatively strong shock. This is probably due to the lack of shock/boundary layer viscous modeling.

These cases and the cases in the INPUT/OUTPUT sections of chapters 2 and 3 substantiate the claims made at the beginning of this manual about the transonic airfoil analysis computer program TAIR. They show that the code is reliable over a large range of transonic flows and is simple to operate — all of the cases presented can be run with a few changes of the input parameters. TAIR results agree with incompressible theory and with transonic experimental results, and the present algorithm also shows substantial improvement in computational efficiency when compared with other standard relaxation schemes for the conservative full-potential equation.

APPENDIX A

PROGRAM CHANGES TO INCREASE DIMENSIONS

This appendix lists the changes that must be made in the TAIR program to increase (or decrease) the mesh dimensions. The following statements were changed for a CDC 7600 and, due to the overflow of small core memory (SCM), two LEVEL 2 statements were included to assign certain arrays to large core memory (LCM). For other computer systems these LEVEL 2 statements should be omitted. This example illustrates a dimension change from (151,31) to (209,43).

These changes must be made in the COMMON blocks. The default statement is listed first, followed by the appropriate changes.

```
    COMMON /COM2/ A1(151,31),A2(151,31),A3(151,31),XJ(151,31)

    COMMON /COM2/ A1(209,43),A2(209,43),A3(209,43),XJ(209,43)
    LEVEL 2,A1,A2,A3,XJ
(/COM2/ appears in MAIN, INITL, OUTPUT, and XYOUT)

    COMMON /COM3/ XB(151),YB(151)

    COMMON /COM3/ XB(209),YB(209)
(/COM3/ appears in INITL, OUTPUT, GRGEN, INNER, and CHECK)

    COMMON /COM4/ IA(153),A4(151),BODYBC(151)

    COMMON /COM4/ IA(211),A4(209),BODYBC(209)
(/COM4/ appears in MAIN, INITL, OUTPUT, XYOUT, and ADI)

    COMMON PHI(151,31),RHO(151,31)

    COMMON PHI(209,43),RHO(209,43)
(// appears in MAIN, INITL, OUTPUT, and AUTO)

    COMMON /SCRACH/ X(151,31),Y(151,31),ARDUM(151,12)

    COMMON /SCRACH/ X(209,43),Y(209,43),ARDUM(209,12)
(/SCRACH/ appears in MAIN, INITL, OUTPUT, ADI, XYOUT, GRGEN, INNER, and
OUTER)
```

The following additional changes must be made in the various routines as indicated. First the default statements are listed, followed by the appropriate changes.

```
MAIN

     DIMENSION A(151),B(151),C(151),D(151),
    1          SIGMA(151,31),F(151,31),RI(151,31),COR(151),
    2          RJ(151),FIM1(151),FLUXJM(151),RJA3(151)
     DIMENSION RJPH(151),RJMH(151),PXCJM1(151)
     DIMENSION QTRP(151),STRP(151),GNPCY(20),NSPCY(20)

     DIMENSION A(209),B(209),C(209),D(209),
    1          SIGMA(209,43),F(209,43),RI(209,43),COR(209),
    2          RJ(209),FIM1(209),FLUXJM(209),RJA3(209)
     DIMENSION RJPH(209),RJMH(209),PXCJM1(209)
     DIMENSION QTRP(209),STRP(209),GNPCY(20),NSPCY(20)

SUBROUTINE INITL

     DIMENSION XJDUM(151),A1DUM(151),A3DUM(151),XJ1(151),XJNJM(151),
    1          A31(151),A3NJM(151)

     DIMENSION XJDUM(209),A1DUM(209),A3DUM(209),XJ1(209),XJNJM(209),
    1          A31(209),A3NJM(209)

SUBROUTINE OUTPUT

     DIMENSION RA1(151,31)
     DIMENSION IVAR(151),CP(151)
     IMAX=151

     DIMENSION RA1(209,43)
     DIMENSION IVAR(209),CP(209)
     IMAX=209

SUBROUTINE GRGEN

     DIMENSION S(151),S1(151),S2(151),DUM(151),XDUM(151),YDUM(151),
    1          A(151),B(151),C(151),D(151),F(151),H(151)

     DIMENSION S(209),S1(209),S2(209),DUM(209),XDUM(209),YDUM(209),
    1          A(209),B(209),C(209),D(209),F(209),H(209)

SUBROUTINE INNER

     DIMENSION S(151),S2(151),DUM(151),XDUM(151),YDUM(151),
    1          A(151),B(151),C(151),D(151),F(151),H(151)
     DIMENSION SS(151),S3(151),S4(151)

     DIMENSION S(209),S2(209),DUM(209),XDUM(209),YDUM(209),
    1          A(209),B(209),C(209),D(209),F(209),H(209)
     DIMENSION SS(209),S3(209),S4(209)
```

```
SUBROUTINE ADI

    COMMON /COM2/ FX(151,31),FY(151,31),A2(151,31)
    DIMENSION A(151),B(151),C(151),D(151),F(151),G(151),WORK(151)
    DIMENSION QTRP(151),STRP(151)

    COMMON /COM2/ FX(209,43),FY(209,43),A2(209,43)
    LEVEL 2,FX,FY,A2
    DIMENSION A(209),B(209),C(209),D(209),F(209),G(209),WORK(209)
    DIMENSION QTRP(209),STRP(209)

SUBROUTINE CHECK

    IF (NI.LE.151) GO TO 37
    NI=151
    IF (NJ.LE.31) GO TO 41
    NJ=31

    IF (NI.LE.209) GO TO 37
    NI=209
    IF (NJ.LE.43) GO TO 41
    NJ=43
```

APPENDIX B

PROGRAM VARIABLES

This appendix describes the prominent variables in TAIR and, as appropriate, cross-references them with the theoretical variables they represent. The TAIR variable is listed on the left, the theoretical variable (if there is one) is listed beside it in parentheses, and the description is on the right. If the parameter is included in a COMMON block or NAMELIST, a special note is included. More complete descriptions of all NAMELIST parameters can be found in chapters 2 and 3.

AFAC		ALPHA multiplier for small ALPHAs and inner rings. NAMELIST: FLOWIN. COMMON: /COM1/.
AHGRID	(α_H)	Largest value in the grid generation ALPHA acceleration parameter sequence. NAMELIST: GRIDIN. COMMON: /GRGN/.
AHIGH	(α_H)	Largest value in the AF2 ALPHA acceleration parameter sequence. NAMELIST: FLOWIN. COMMON: /COM1/.
ALGRID	(α_L)	Smallest value in the grid generation ALPHA acceleration parameter sequence. NAMELIST: GRIDIN. COMMON: /GRGN/.
ALOW	(α_L)	Smallest value in the AF2 ALPHA acceleration parameter sequence. NAMELIST: FLOWIN. COMMON: /COM1/.
ALPH		Angle of attack (deg). NAMELIST: FLOWIN. COMMON: /COM1/.
ALPHA	(α)	AF2 acceleration parameter used in MAIN. This parameter is effectively the inverse of a pseudotime step and sequentially takes on M values ranging from AHIGH to ALOW. (See chap. 5 for more discussion.) This parameter is also used in SUBROUTINE ADI as an ADI acceleration parameter which sequentially takes on MGRID values ranging from AHGRID to ALGRID. COMMON: /CONV/.
ARDUM		Array used for scratch storage. COMMON: /SCRACH/.
A1	(A_1)	Metric quantity, A1 is approximately the ratio of the normal side of a grid cell to the tangential side. (For more information about this and other metric quantities, see chaps. 3 and 5.) A1 is computed in INITL. COMMON: /COM2/.
A2	(A_2)	Metric quantity. A2 is proportional to the skewness of the grid cell and is computed in INITL. COMMON: /COM2/.
A3	(A_3)	Metric quantity. A3 is approximately the inverse of A1 and is computed in INITL. COMMON: /COM2/.

A4		Special metric grouping computed in INITL and used to implement the airfoil tangency boundary conditions during the residual calculation. COMMON: /COM4/.
BETA	(β)	$\Phi_{\xi t}$ coefficient (acceleration parameter). (See chap. 5 for more information.) NAMELIST: FLOWIN. COMMON: /COM1/.
BHIGH		The upper bound on the BETA parameter discussed in chapter 5 (SUBROUTINE AUTO).
BINN		Stretching parameter for inner boundary grid point distribution. NAMELIST: GRIDIN. COMMON: /GRGN/.
BLOW		The lower bound on the BETA parameter discussed in chapter 5 (SUBROUTINE AUTO).
BODYBC		Special metric grouping computed in INITL and used to implement the airfoil tangency boundary conditions during the density calculation. COMMON: /COM4/.
CMAX		Maximum correction for each iteration. COMMON: /CONV/.
CON		Parameter control for upwind bias on density. NAMELIST: FLOWIN. COMMON: /COM1/.
COR		Correction array (MAIN module).
CPSTAR	(C_p*)	Pressure coefficient at the sonic condition defined in SUBROUTINE INITL. COMMON: /COM1/.
CXMAX		Maximum correction for the X equation calculated in the second sweep of the ADI grid generation routine (SUBROUTINE ADI).
CYMAX		Maximum correction for the Y equation calculated in the second sweep of the ADI grid generation routine (SUBROUTINE ADI).
DYPRES		Nondimensionalized dynamic pressure defined in INITL. COMMON: /COM1/.
ERGRID		Convergence tolerance for ADI grid generation. NAMELIST: GRIDIN. COMMON: /GRGN/.
ERR		Convergence tolerance for AF2 flow solver. NAMELIST: FLOWIN. COMMON: /COM1/.
ETAX	(η_x)	First difference of η with respect to x (SUBROUTINE INITL).
ETAY	(η_y)	First difference of η with respect to y (SUBROUTINE INITL).

F	(f)	First sweep intermediate result. In MAIN, F is equivalenced to X and SIGMA to save storage. (See chap. 5 for more discussion about this quantity.)
FX	(f)	Intermediate X result at end of first sweep of the ADI grid generation routine (SUBROUTINE ADI).
FY	(g)	Intermediate Y result at end of first sweep of the ADI grid generation routine (SUBROUTINE ADI).
G	(γ)	Ratio of specific heats. NAMELIST: FLOWIN. COMMON: /COM1/.
GM	($\gamma - 1$)	G - 1.0. GM is defined in INITL. COMMON: /COM1/.
GN	(Γ^n)	Nth iteration value of circulation; initialized in INITL and used to relax the (N + 1)st value of circulation at the end of the main iteration loop. COMMON: /COM1/.
GNM	(Γ^{n-1})	(N - 1)st iteration value of circulation.
GNP	(Γ^{n+1})	(N + 1)st value of circulation. GNP is initialized in INITL and updated to the (N + 1)st value at the end of each iteration. COMMON: /COM1/.
GNPD		GNP*2.0. GNPD is initialized in INITL and updated in MAIN. COMMON: /COM1/.
GNTE		Circulation quantity involving the velocity potential jump across the airfoil trailing edge. GNTE is initialized in INITL and updated in MAIN. COMMON: /COM1/.
GP	($\gamma + 1$)	G + 1.0. GP is defined in INITL. COMMON: /COM1/.
HTMAX		Height of rectangular outer boundary (IOUT=3). NAMELIST: GRIDIN. COMMON: /GRGN/.
I		ξ coordinate index.
IA		Periodic counter used for differencing around the trailing edge. IA is set up in INITL. COMMON: /COM4/.
IAUTO		Switch for SUBROUTINE AUTO. NAMELIST: FLOWIN. COMMON: /COM1/.
ICASE		DO control variable for multicase loop. ICASE runs from one to NC (MAIN module).
ICHECK		Switch for SUBROUTINE CHECK. NAMELIST: FLOWIN. COMMON: /COM1/.

ICMAX		ξ coordinate position of maximum correction (CMAX). COMMON: /CONV/.
IHALF		Midpoint of ξ-direction coordinates [(NI/2) + 1]. IHALF is defined in INITL. COMMON: /COM1/.
IHM		IHALF - 1. COMMON: /COM1/.
IHP		IHALF + 1. COMMON: /COM1/.
IINCR		Grid solution output increment. NAMELIST: FLOWIN. COMMON: /COM1/.
IOPEN		Open trailing-edge option for IOPT=1. NAMELIST: GRIDIN. COMMON: /GRGN/.
IOPT		Airfoil option parameter. NAMELIST: GRIDIN. COMMON: /GRGN/.
IOUT		Outer boundary option parameter. NAMELIST: GRIDIN. COMMON: /GRGN/.
IRMAX		ξ coordinate position of maximum residual (RMAX). COMMON: /CONV/.
J		η coordinate index.
JCMAX		η coordinate position of maximum correction (CMAX). COMMON: /CONV/.
JINCR		Grid solution output increment. NAMELIST: FLOWIN. COMMON: /COM1/.
JRMAX		η coordinate position of maximum residual (RMAX). COMMON: /CONV/.
K		Starting element in the AF2 ALPHA sequence. NAMELIST: FLOWIN. COMMON: /COM1/.
KGRID		Starting element in the ALPHA sequence used for grid generation. NAMELIST: GRIDIN. COMMON: /GRGN/.
KK	(k)	Counter for the M elements in the AF2 ALPHA sequence. COMMON: /CONV/.
KKGRID	(k)	Counter for the MGRID elements in the grid generation ALPHA sequence (SUBROUTINE ADI).
LCHECK		Logical variable. If an input error in a major variable is detected in CHECK, LCHECK will be set to true and the solution will be stopped. COMMON: /COM1/.

M	(m)	Number of elements in the AF2 ALPHA sequence. NAMELIST: FLOWIN. COMMON: /COM1/.
MAXIT		Maximum number of iterations for grid generation. NAMELIST: GRIDIN. COMMON: /GRGN/.
MESH		Mesh option parameter. NAMELIST: FLOWIN. COMMON: /COM1/.
MGRID	(m)	Number of elements in the ALPHA sequence for grid generation. NAMELIST: GRIDIN. COMMON: /GRGN/.
MINF	(M_∞)	Free-stream Mach number. NAMELIST: FLOWIN. COMMON: /COM1/.
N	(n)	DO control variable for the main iteration loop.
NC		Number of solutions per job (multicase run). The value of NC is established from NCASE after the first call to INITL.
NCASE		Number of solutions in a job. NAMELIST: FLOWIN. COMMON: /COM1/.
NDIF		Rotated differencing parameter. NAMELIST: FLOWIN. COMMON: /COM1/.
NI		Number of points in the ξ direction (around airfoil). NAMELIST: FLOWIN. COMMON: ./COM1/.
NIM		NI - 1. COMMON: /COM1/.
NIM2		NI - 2. COMMON: /COM1/.
NJ		Number of points in the η direction (J=NJ is airfoil surface, J=1 is outer boundary). NAMELIST: FLOWIN. COMMON: /COM1/.
NJM		NJ - 1. COMMON: /COM1/.
NJM2		NJ - 2. COMMON: /COM1/.
NOUT		Primary output control parameter. NAMELIST: FLOWIN. COMMON: /COM1/.
NOUT1		Solution output frequency. NAMELIST: FLOWIN. COMMON: /COM1/.
NOUT2		Convergence parameter output frequency. NAMELIST: FLOWIN. COMMON: /COM1/.
NRING		Number of inner ξ rings for which AFAC logic is applied. NAMELIST: FLOWIN. COMMON: /COM1/.

NSP		Number of supersonic points in the solution. COMMON: /CONV/.
NSTEPS		Maximum number of iterations in main flow-solver. NAMELIST: FLOWIN. COMMON: /COM1/.
NX		Number of points in the ξ direction of the mesh to be read in. This parameter should be compatible with NI (SUBROUTINE INITL).
NY		Number of points in the η direction of the mesh to be read in. This parameter should be compatible with NJ (SUBROUTINE INITL).
OMEG	(ω)	Relaxation parameter for the ADI grid generation algorithm. NAMELIST: GRIDIN. COMMON: /GRGN/.
OMEGA	(ω)	Relaxation parameter for the AF2 flow solver algorithm. NAMELIST: FLOWIN. COMMON: /COM1/.
PHI	(ϕ)	Velocity potential array. PHI is initialized in INITL, and updated every iteration in MAIN. COMMON: / /.
PINF		Nondimensionalized free-stream pressure. PINF is defined in INITL. COMMON: /COM1/.
PSTAR		Nondimensionalized pressure at the sonic condition. PSTAR is defined in INITL.
QINF		Nondimensionalized free-stream velocity. QINF is defined in INITL. COMMON: /COM1/.
QXINF		The X component of the free-stream velocity, defined in INITL.
QYINF		The Y component of the free-stream velocity, defined in INITL. COMMON: /COM1/.
R		Residual calculated in MAIN.
RADMAX		Circular outer boundary radius (IOUT=1). NAMELIST: GRIDIN. COMMON: /GRGN/.
RATIO		The sum of the ratios of the average and maximum residuals at iteration N to the average and maximum residuals at iteration N-M. (See chap. 5 for more details — (SUBROUTINE AUTO).)
RAVG	(R_{avg})	The average residual calculated in MAIN. COMMON: /CONV/.

RG		Circulation relaxation parameter. RG is the working parameter which is gradually lowered as the circulation builds. (See chap. 5 for the details of this process.) Its initial value is RGAM (MAIN module).
RGAM		Circulation relaxation parameter. NAMELIST: FLOWIN. COMMON: /COM1/.
RGAM1		1.0-RGAM. RGAM1 is initialized in INITL, and then redefined as 1.0-RG in MAIN during the iteration process. COMMON: /COM1/.
RHO	(ρ)	The nondimensionalized density array. RHO is stored at (I + 1/2, J + 1/2). It is initialized in INITL and updated every iteration in MAIN. COMMON: / /.
RHOINF		Nondimensionalized free-stream density (SUBROUTINE INITL).
RHO13		Density value at Mach = 1.3. RHO13 is used as a check to see if the local Mach number exceeds 1.3. It is defined in INITL. COMMON: /COM1/.
RI	($\tilde{\rho}$)	The density coefficient in the ξ direction. (See chap. 5 for more discussion of this parameter.)
RJ	($\tilde{\rho}$)	The density coefficient in the η direction. (See chap. 5 for more discussion of this parameter.)
RMAX	($\|R\|_{max}$)	The maximum residual calculated in MAIN. COMMON: /CONV/.
RSTAR		Density at the sonic condition. RSTAR is defined in INITL. COMMON: /COM1/.
RX		The X grid generation equation residual (SUBROUTINE ADI).
RXMAX		The maximum X grid generation equation residual (SUBROUTINE ADI).
RY		The Y grid generation equation residual (SUBROUTINE ADI).
RYMAX		The maximum Y grid generation equation residual (SUBROUTINE ADI).
S		Airfoil arc-length distribution calculated from the initial airfoil coordinates (XB and YB) (SUBROUTINE INNER).
SIGMA	($1 - \nu$)	Switching function for upwinding of the density. (See chap. 5 for details of the ν calculation). SIGMA is equivalenced to F and X to save storage.

S2		The desired airfoil arc-length distribution, dependent on the clustering parameter BINN (SUBROUTINE INNER).
TEOPEN		Distance across an open trailing edge. TEOPEN is calculated in GEMPAC, if MESH=0, or in INITL, if MESH > 0. COMMON: /COM1/.
TITLE		The title of the airfoil or mesh used in a given solution (28-character string). COMMON: /COM5/.
TMAX		Airfoil thickness parameter. NAMELIST: GRIDIN. COMMON: /GRGN/.
WDTHMX		Width of rectangular outer boundary (IOUT=3). NAMELIST: GRIDIN. COMMON: /GRGN/.
X	(x)	The x coordinate of the finite-difference grid. In MAIN, X is equivalenced to SIGMA and F. COMMON: /SCRACH/.
XB		Airfoil surface x coordinates stored at (I + 1/2, NJ). COMMON: /COM3/.
XC		Leading-edge bluntness parameter for IOPT=2 option. NAMELIST: GRIDIN. COMMON: /GRGN/.
XCN		The X coordinate for the center of the circular outer boundary (IOUT=1). NAMELIST: GRIDIN. COMMON: /GRGN/.
XETA	(x_η)	First difference of x with respect to η (SUBROUTINE INITL).
XIX	(ξ_x)	First difference of ξ with respect to x (SUBROUTINE INITL).
XIY	(ξ_y)	First difference of ξ with respect to y (SUBROUTINE INITL).
XJ	(J)	The Jacobian of the numerical mapping transformation. XJ is computed in INITL. (See chaps. 3 and 5 for more information.) COMMON: /COM2/.
XXI	(x_ξ)	First difference of x with respect to ξ (SUBROUTINE INITL).
Y	(y)	The y coordinate of the finite-difference grid. In MAIN, Y is equivalenced to RI. COMMON: /SCRACH/.
YB		Airfoil surface y coordinates stored at (I + 1/2, NJ). COMMON: /COM3/.
YCN		The Y coordinate for the center of the circular outer boundary (IOUT=1). NAMELIST: GRIDIN. COMMON: /GRGN/.
YETA	(y_η)	First difference of y with respect to η (SUBROUTINE INITL).
YXI	(y_ξ)	First difference of y with respect to ξ (SUBROUTINE INITL).

REFERENCES

1. Holst, T. L.; and Ballhaus, W. F.: Fast Conservative Schemes for the Full Potential Equation Applied to Transonic Flows. NASA TM-78469, 1978. (Also AIAA J., vol. 17, no. 2, Feb. 1979, pp. 145-152.)

2. Holst, T. L.: An Implicit Algorithm for the Conservative, Transonic Full Potential Equation Using an Arbitrary Mesh. AIAA Paper 78-1113, July 1978. (Also AIAA J., vol. 17, Oct. 1979, pp. 1038-1956.)

3. Holst, T. L.: A Fast, Conservative Algorithm for Solving the Transonic Full Potential Equation. AIAA Paper 79-1456, July 1979. (Also AIAA J., vol. 18, no. 12, Dec. 1980, pp. 1431-1439.)

4. Holst, T. L.; and Albert, J.: An Implicit Algorithm for the Conservative, Transonic Full Potential Equation with Effective Rotated Differencing. NASA TM-78570, 1979.

5. Sorenson, R. L.: A Computer Program to Generate Two-Dimensional Grids About Airfoils and Other Shapes by the Use of Poisson's Equation. NASA TM-81198, 1980.

6. Bauer, F.; Garabedian, P.; Korn, D.; and Jameson, A.: Supercritical Wing Sections. II. Lecture Notes in Economical and Mathematical Systems, Springer-Verlag, New York, 1975.

7. Stanewsky, E.; Puffert, W.; and Müller, R.: Supercritical Airfoil CAST 7 — Surface Pressure, Wake and Boundary Layer Measurements. AGARD-AR-138, May 1979, pp. A3-1 to A3-35.

8. Steger, J. L.; and Sorenson, R. L.: Automatic Mesh-Point Clustering Near a Boundary in Grid Generation with Elliptic Partial Differential Equations. J. Comp. Phys., vol. 33, no. 3, Dec. 1979, pp. 405-410.

9. Thompson, J. F.; Thames, F. C.; and Mastin, C. W.: Automatic Numerical Generation of Body-Fitted Curvilinear Coordinate System for Field Containing Any Number of Arbitrary Two-Dimensional Bodies. J. Comp. Phys., vol. 15, no. 3, July 1974, pp. 299-319.

10. Hafez, M. M.; Murman, E. M.; and South, J. C.: Artificial Compressibility Methods for Numerical Solution of Transonic Full Potential Equation. AIAA Paper 78-1148, July 1978. (Also AIAA J., vol. 17, Aug. 1979, pp. 838-844.)

11. Eberle, A.: A Finite Volume Method for Calculating Transonic Potential Flow Around Wings from the Pressure Minimum Integral. NASA TM-75,324, 1978.

12. Eberle, A.: Transonic Potential Flow Computations by Finite Elements: Airfoil and Wing Analysis, Airfoil Optimization. Lecture held at the DGLR/GARTEUR 6 Symposium, Transonic Configurations, Bad Harzburg, Germany, June 1978.

13. South, J. C.; and Keller, J. D.: Vector Processor Algorithms for Transonic Flow Calculations. AIAA Paper 79-1457, July 1979. (Also AIAA J., vol. 18, no. 7, July 1980, pp. 786-792.)

14. Jameson, A.: Transonic Potential Flow Calculations Using Conservative Form. AIAA Second Computational Fluid Dynamics Conference Proceedings, June 1975, pp. 148-155.

15. Holst, T. L.: An Implicit Algorithm for the Transonic Full-Potential Equation in Conservative Form. Presented at the Fourth IRIA International Symposium on Computing Methods in Applied Sciences and Engineering, Versailles, France, Dec. 10-14, 1979. North-Holland Publishing Co., 1980.

16. Melnik, R. E.: Wake Curvature and Trailing Edge Interaction Effects in Viscous Flow Over Airfoils. Advanced Technology Airfoil Research, NASA CP-2045, Mar. 1978, pp. 255-270.

17. Ballhaus, W. F.: A Fast Implicit Solution Procedure for Transonic Flows. Lecture Notes in Physics, Computing Methods in Applied Sciences and Engineering, Springer-Verlag, 1977, pp. 90-102.

18. Karamcheti, K.: Principles of Ideal-Fluid Aerodynamics. John Wiley & Sons, Inc., New York, 1966.

19. Abbott, I. H.; and Von Doenhoff, A. E.: Theory of Wing Sections. Dover Publications, Inc., New York, 1959.

TABLE 1.- TAIR OUTPUT OPTIONS CONTROLLED BY NOUT

NOUT									Output information	Total number of pages
1	2	3	4	5	6	7	8	9		
x	x	x	x	x	x	x	x	x	Aerodynamic coefficients	2 lines
	x	x	x	x	x	x	x	x	Last line of convergence history	5 lines
		x	x	x	x	x	x	x	Airfoil surface solution	1
			x	x	x	x	x	x	Input data (NAMELISTs, airfoil coordinates)	5
				x	x	x	x	x	Interpolated airfoil coordinates	6
					x	x	x	x	Complete convergence history	7
						x	x	x	Mach and RHO contour maps	9
							x	x	Grid convergence history and transformation metrics near airfoil	13
								x	Final grid coordinates	21

TABLE 2.- SUBROUTINE REFERENCE CHART

Routine name	Calling routine	Routines called	Description
ADI	GRGEN	TRIB, TRIP	Grid-generation algorithm
AUTO	MAIN		Solution parameter updating
CHECK	INITL, GRGEN		Checks input data
CSPLIN	INNER, GRGEN	TRIB	Cubic spline interpolation
FORCE	OUTPUT		Aerodynamic coefficient calculation
GEMPAC	GRGEN		Aerodynamic geometry input
GRGEN	INITL	CHECK, GEMPAC, INNER, OUTER ADI, CSPLIN	Grid generation input (NAMELIST GRIDIN) and grid initialization
INITL	MAIN	CHECK, GRGEN, XYOUT	Solution input (NAMELIST FLOWIN) and flow-field initialization
INNER	GRGEN	CSPLIN	Distributes grid points on inner (airfoil) boundary
MAIN		INITL, OUTPUT, AUTO, TRIP	Main flow-solver algorithm
OUTER	GRGEN		Outer boundary shape and point distribution
OUTPUT	MAIN	FORCE, PRNPLT	Main flow-solver output
PRNPLT	OUTPUT		Printer contour plot
TRIB	CSPLIN, ADI		Tridiagonal inversion algorithm
TRIP	ADI, MAIN		Tridiagonal periodic inversion algorithm
XYOUT	INITL		Grid-generation output

TABLE 3.- COMMON BLOCK REFERENCE CHART

COMMON block	Calling routine	Description
/ /	MAIN, INITL, GRGEN, AUTO	Blank COMMON...Velocity potential and density arrays
/COM1/	MAIN, INITL, OUTPUT, GRGEN, CHECK, AUTO	General solution parameters and NAMELIST FLOWIN parameters
/COM2/	MAIN, INITL, OUTPUT, XYOUT, ADI	Metric quantities
/COM3/	INITL, OUTPUT, GRGEN, INNER, CHECK	Airfoil coordinates
/COM4/	MAIN, INITL, OUTPUT, XYOUT, ADI	Periodic indexing array and airfoil boundary condition arrays
/COM5/	INITL, OUTPUT, GRGEN, GEMPAC	Airfoil titles
/CONV/	MAIN, OUTPUT, AUTO	Solution convergence parameters
/GRGN/	GRGEN, ADI, CHECK, MAIN	Grid-generation parameters and NAMELIST GRIDIN parameters
/SCRACH/	MAIN, INITL, OUTPUT, ADI, XYOUT, GRGEN, INNER, OUTER	Scratch storage

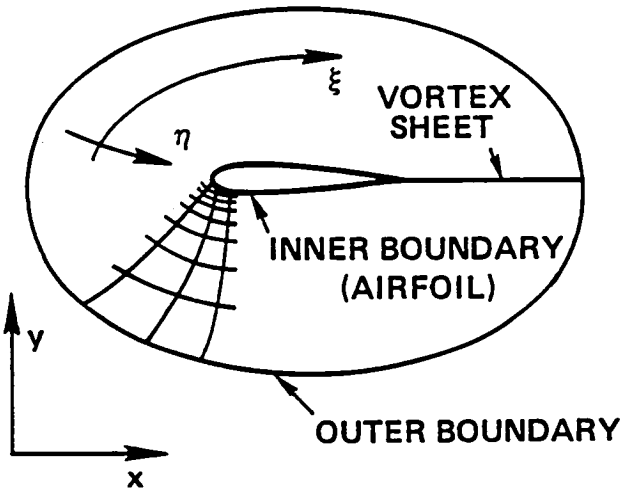

(a) Physical domain.

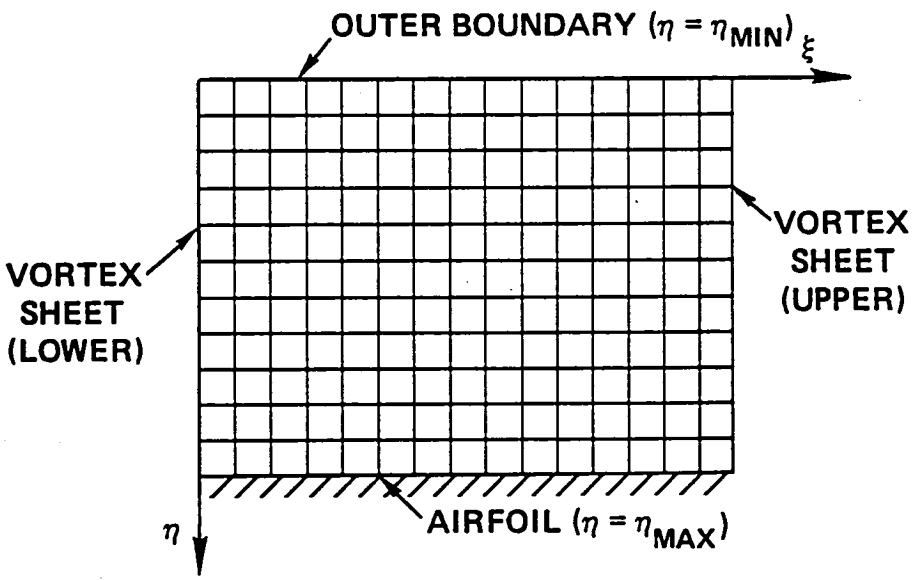

(b) Computational domain.

Figure 1.- Numerically generated finite-difference mesh.

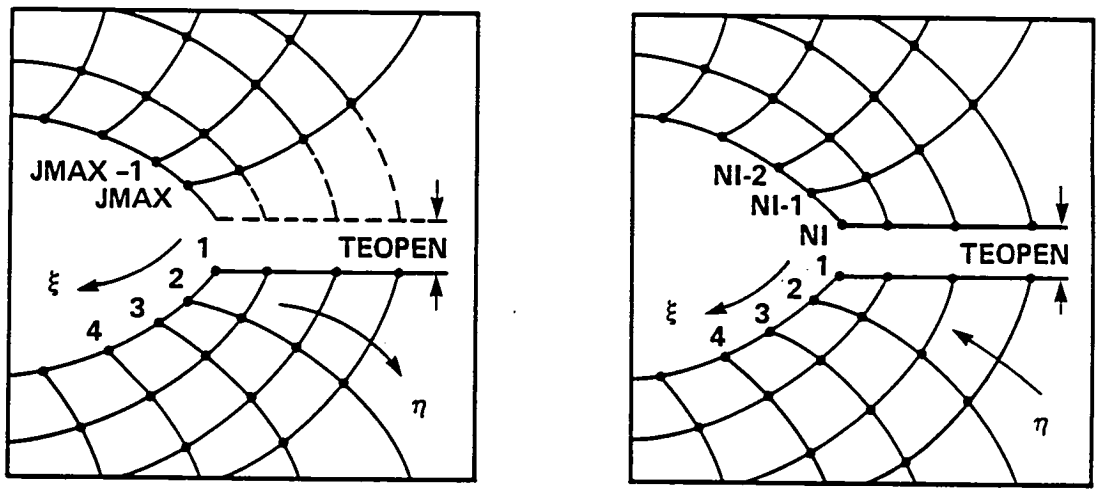

(a) GRAPE trailing edge.

(b) TAIR trailing edge.

Figure 2.- Comparison of GRAPE and TAIR trailing edges.

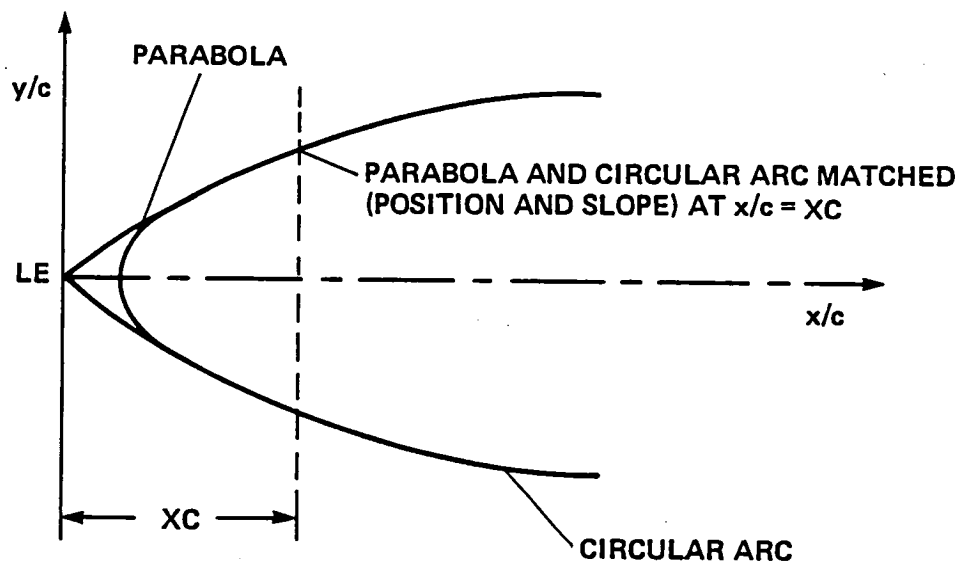

Figure 3.- Bluntness of circular-arc airfoil.

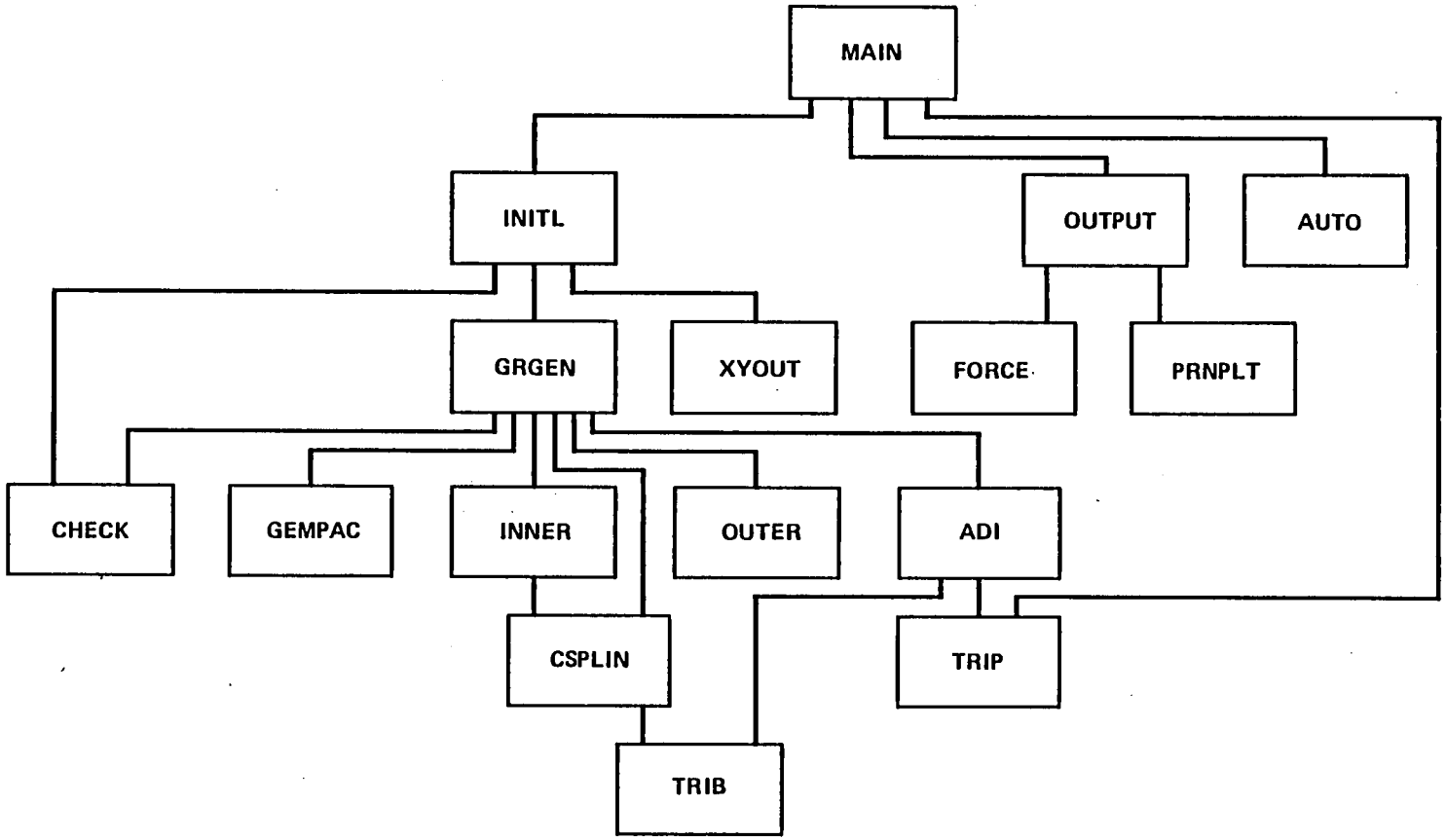

Figure 4.- TAIR SUBROUTINE tree.

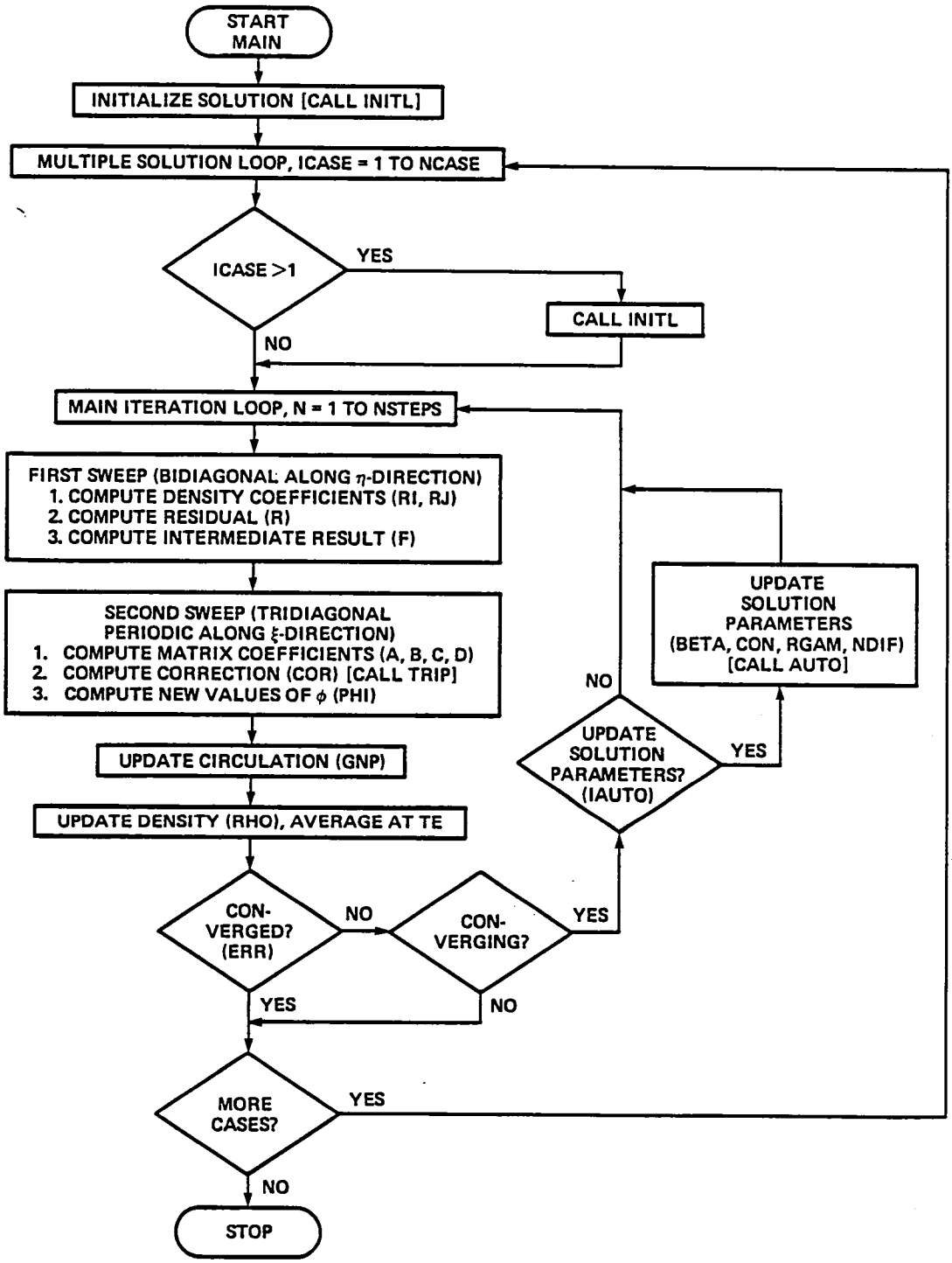

Figure 5.- Flowchart for MAIN module.

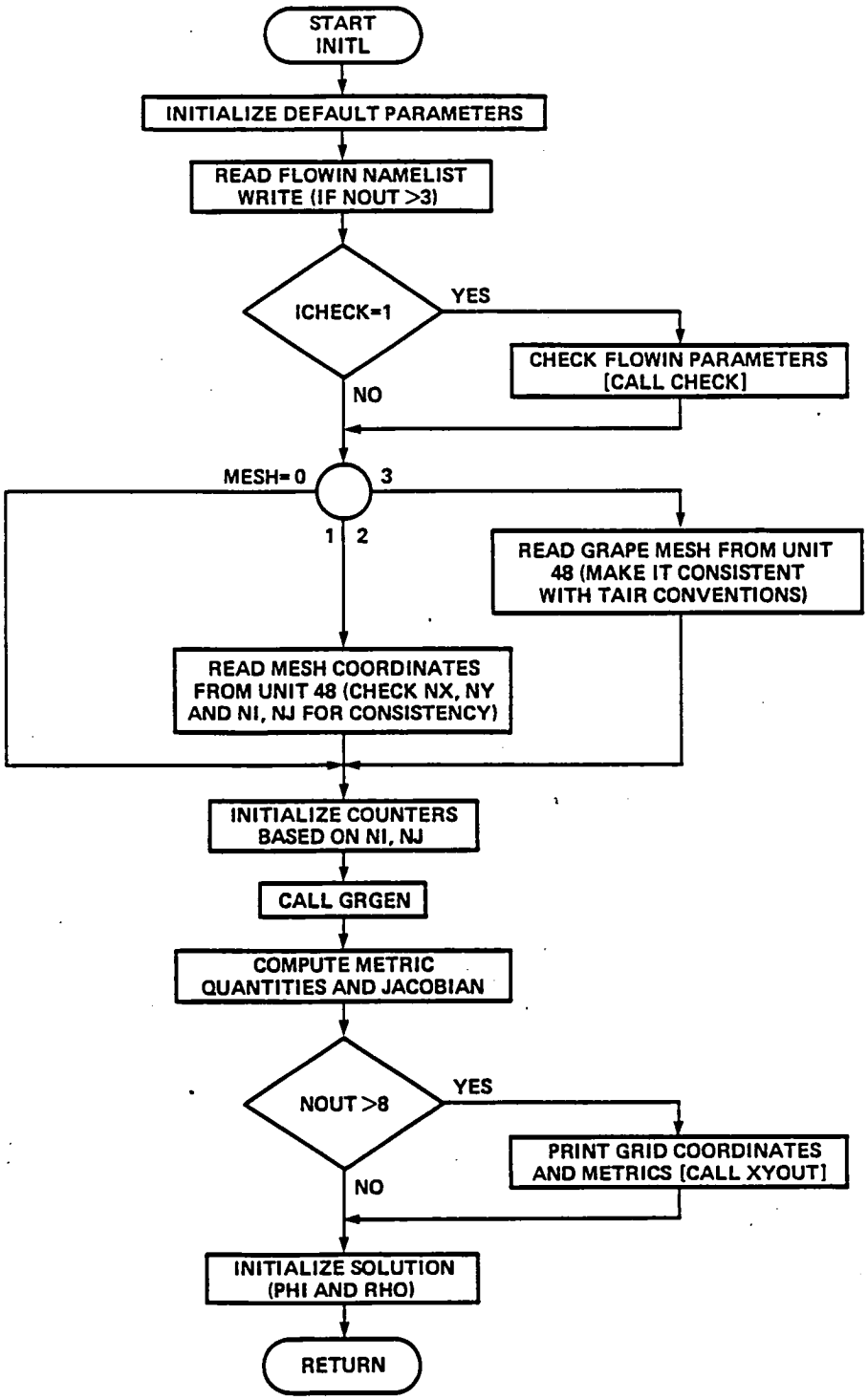

Figure 6.- Logic flow for SUBROUTINE INITL.

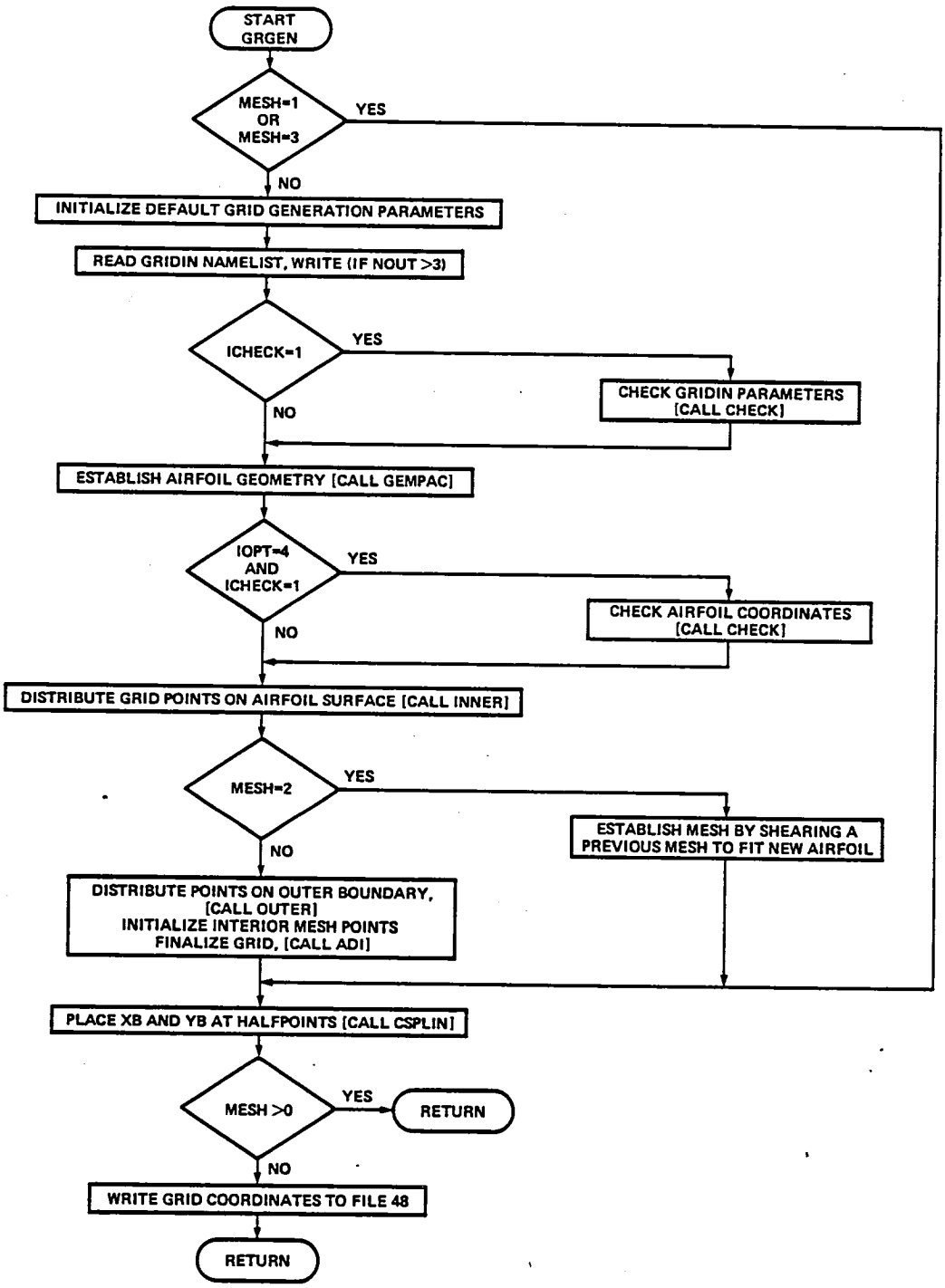

Figure 7.- Logic flowchart for SUBROUTINE GRGEN.

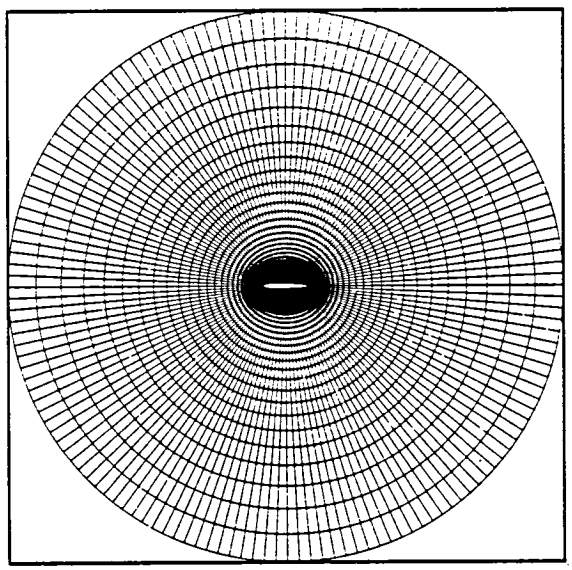

(a) Entire grid.

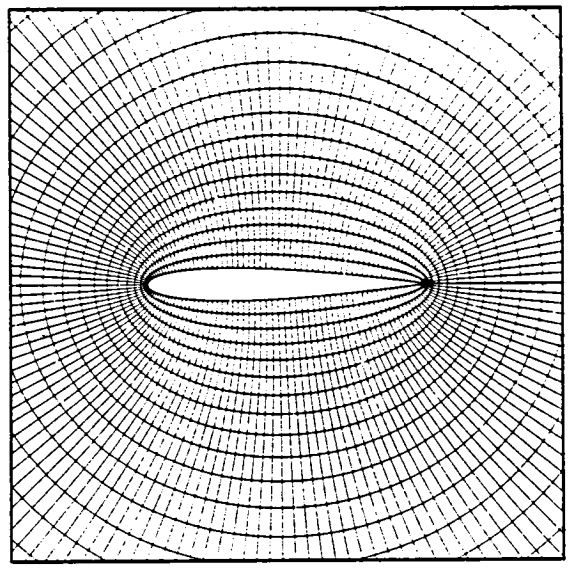

(b) Close-up of grid about airfoil.

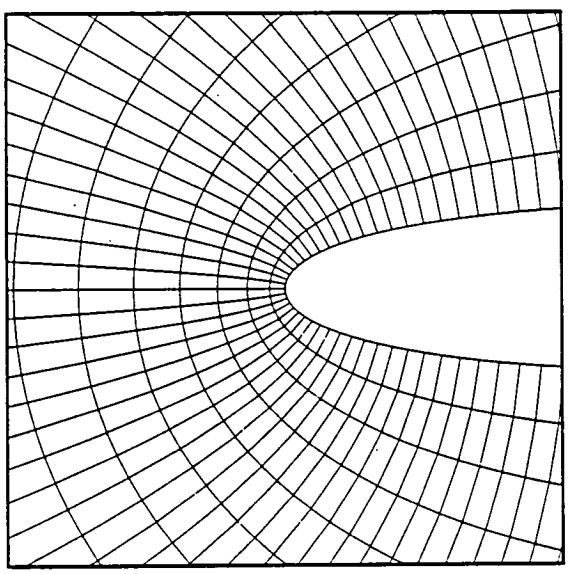

(c) Close-up of grid at airfoil leading edge.

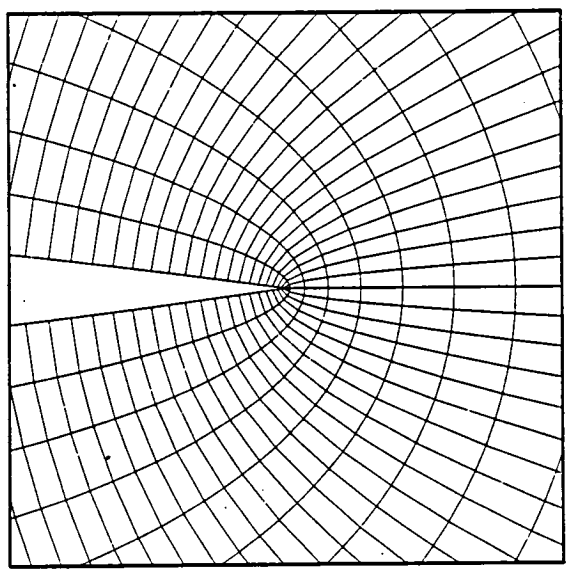

(d) Close-up of grid at airfoil trailing edge.

Figure 8.- TAIR-generated finite-difference grid (the default case).

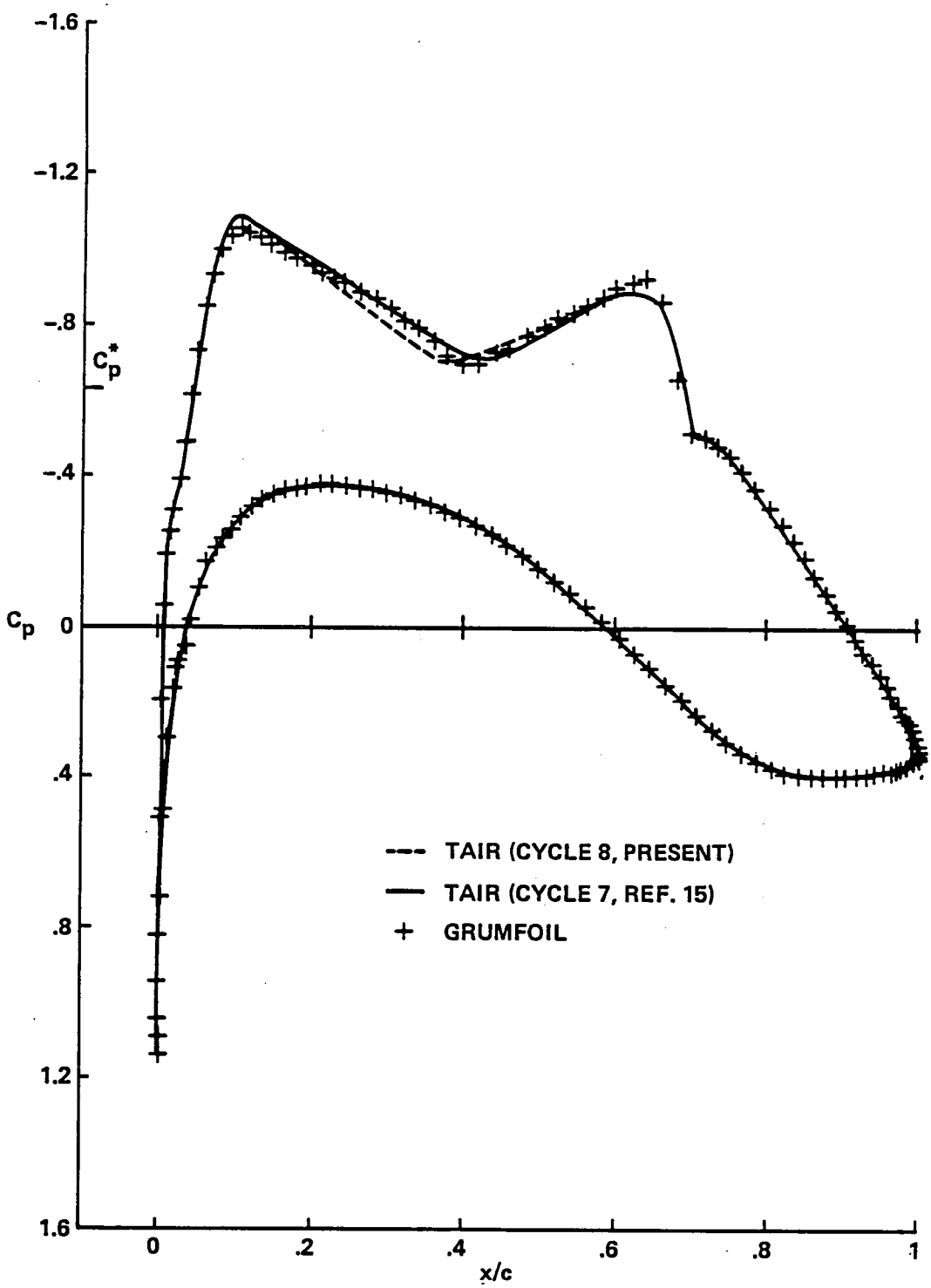

Figure 9.- Pressure coefficient comparison (Korn airfoil, $M_\infty = 0.74$, $\alpha = 0°$).

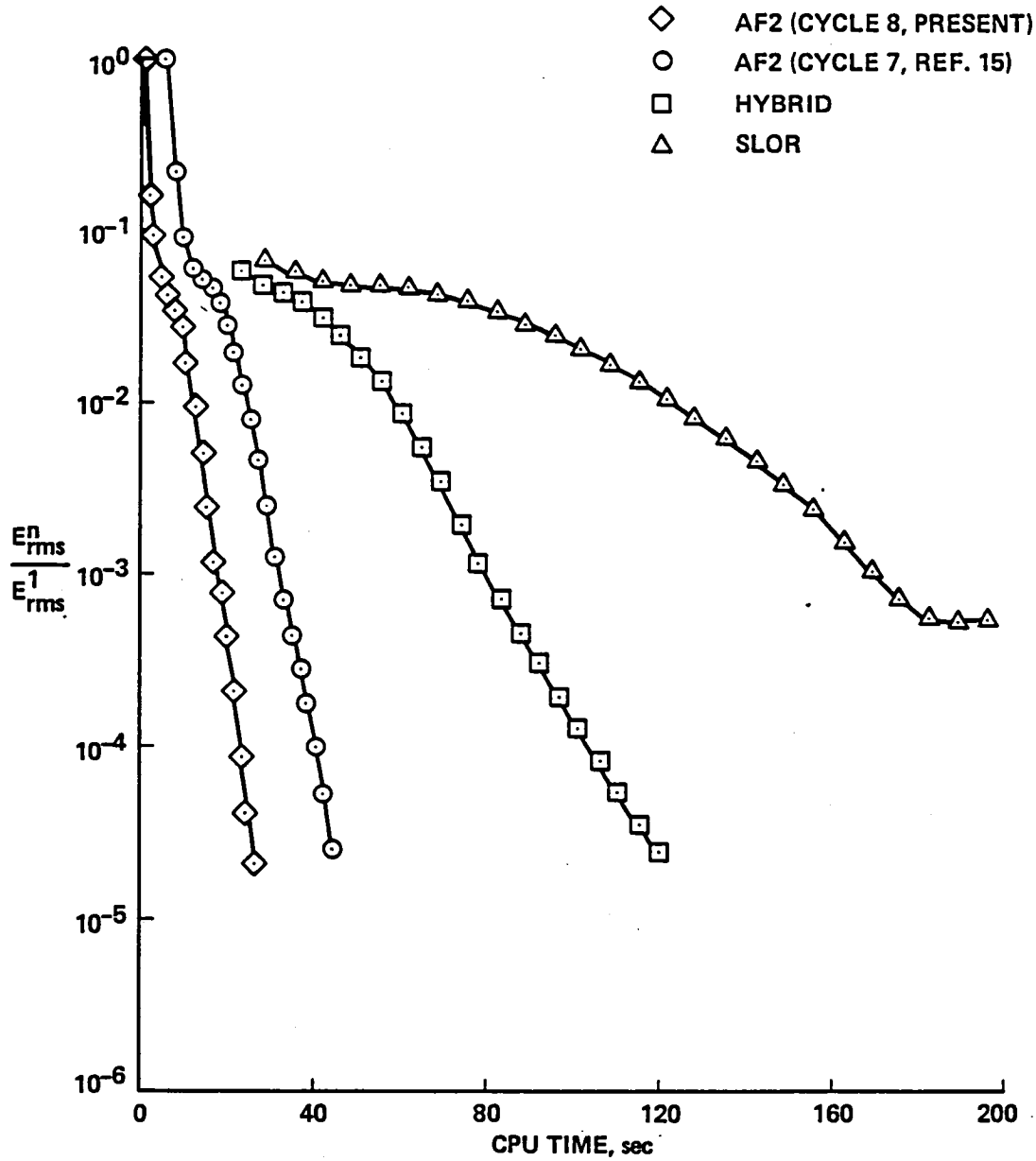

Figure 10.- Convergence-history comparisons (Korn airfoil, $M_\infty = 0.74$, $\alpha = 0°$).

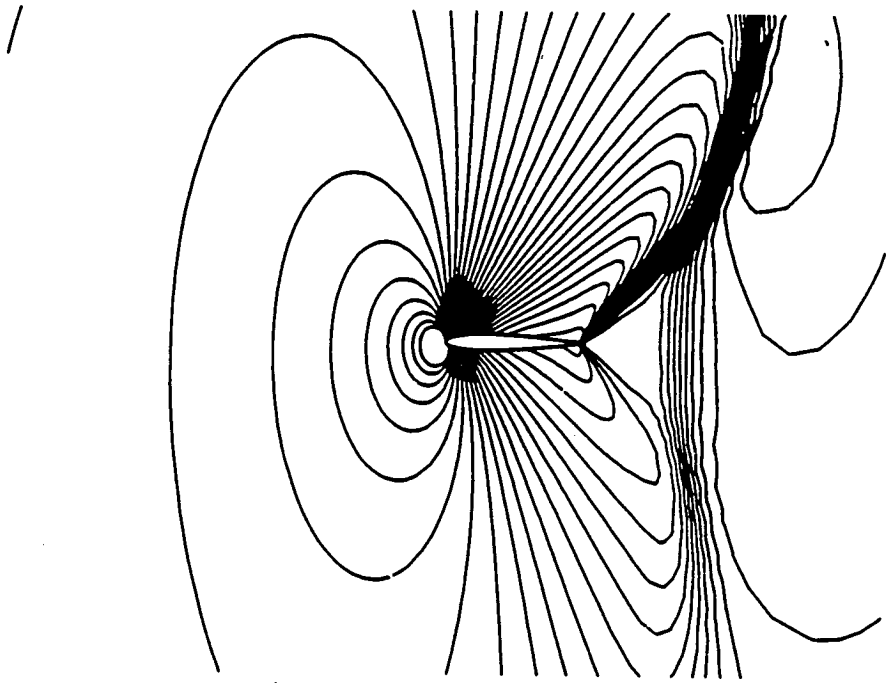

Figure 11.- Mach number contours (NACA 0012 airfoil, $M_\infty = 0.95$, $\alpha = 4°$).

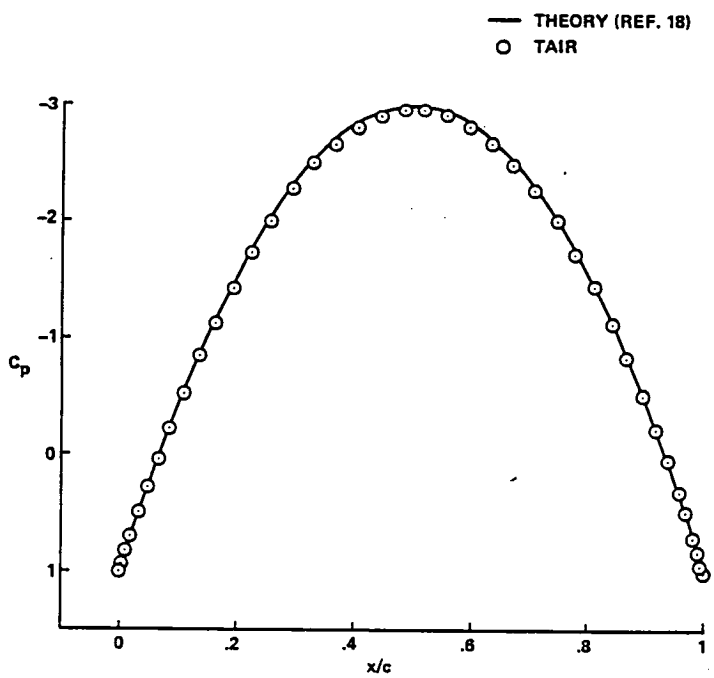

Figure 12.- Pressure coefficient comparison (circular cylinder cross section, $M_\infty = 0.00001$, $\alpha = 0°$).

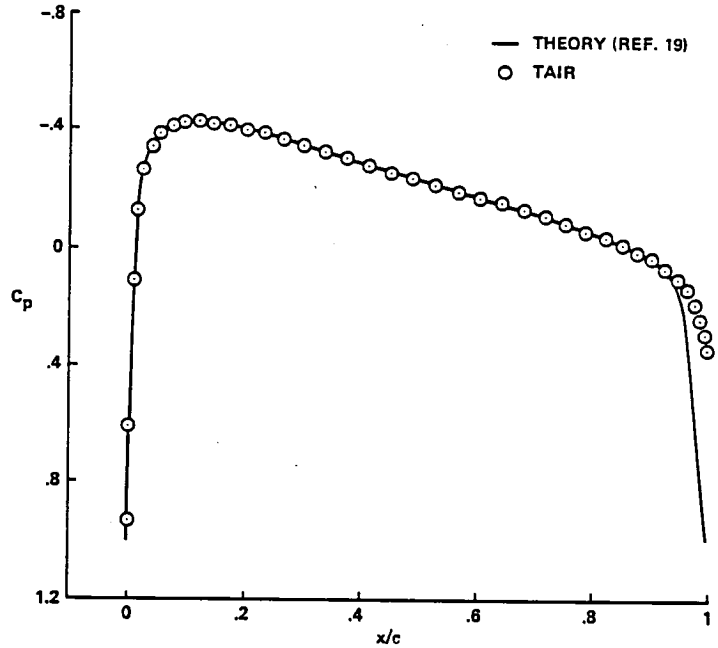

Figure 13.- Pressure coefficient comparison (NACA 0012 airfoil, $M_\infty = 0.00001$, $\alpha = 0°$).

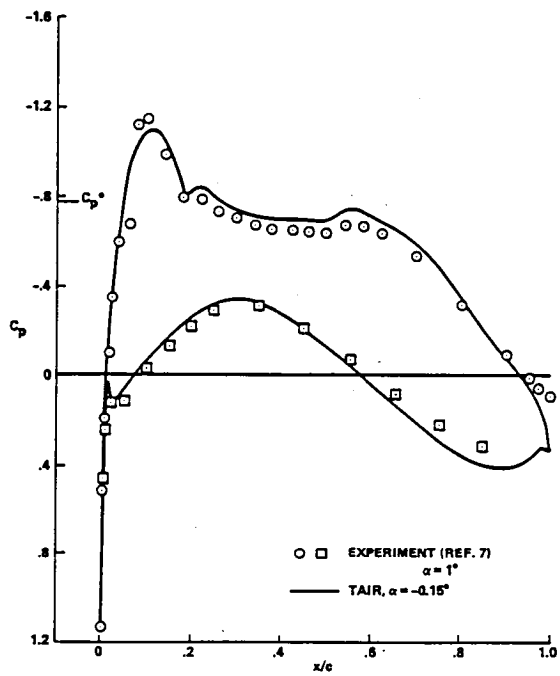

Figure 14.- Pressure coefficient comparison (CAST 7 airfoil, $M_\infty = 0.7$).

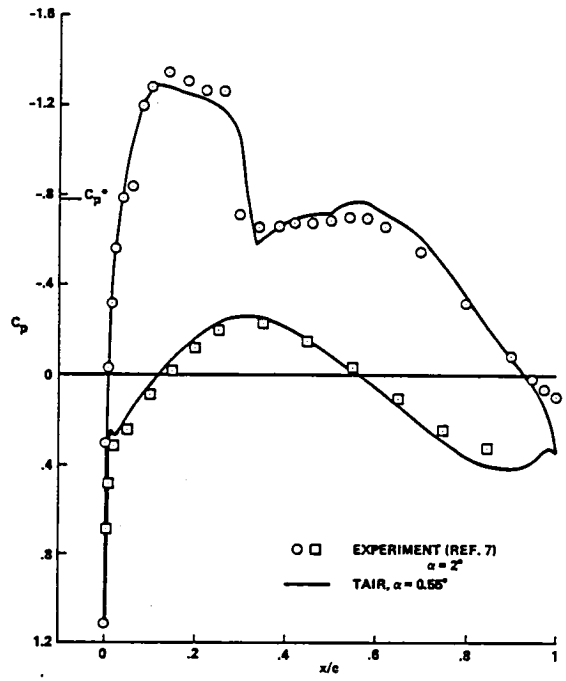

Figure 15.- Pressure coefficient comparison (CAST 7 airfoil, $M_\infty = 0.7$).

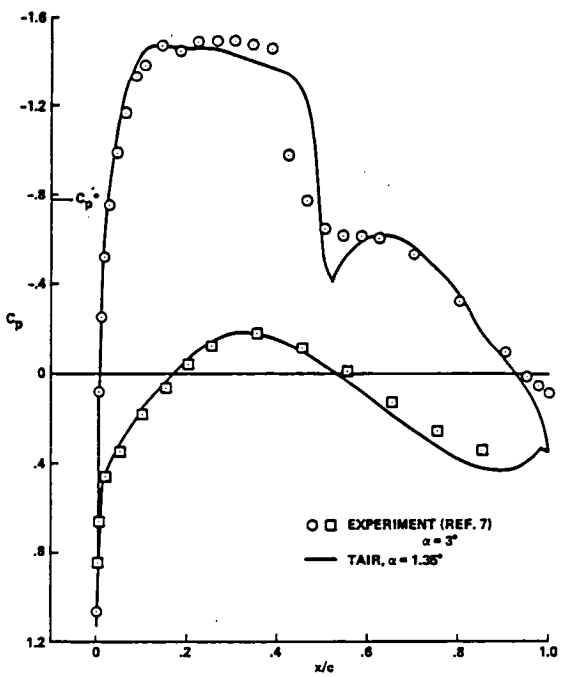

Figure 16.- Pressure coefficient comparison (CAST 7 airfoil, $M_\infty = 0.7$).

1. Report No.	2. Government Accession No.	3. Recipient's Catalog No.
NASA TM-81296		

4. Title and Subtitle	5. Report Date
TAIR — A TRANSONIC AIRFOIL ANALYSIS COMPUTER CODE	May 1981
	6. Performing Organization Code

7. Author(s)	8. Performing Organization Report No.
F. Carroll Dougherty, Terry L. Holst, Karen L. Grundy,* and Scott D. Thomas*	A-8594
	10. Work Unit No. 505-31-11
9. Performing Organization Name and Address	11. Contract or Grant No.
Ames Research Center, NASA Moffett Field, California 94035	
	13. Type of Report and Period Covered
12. Sponsoring Agency Name and Address	Technical Memorandum
National Aeronautics and Space Administration Washington, D.C. 20546	14. Sponsoring Agency Code

15. Supplementary Notes

*With Informatics Inc., Palo Alto, California

16. Abstract

The operation of the TAIR (Transonic AIRfoil) computer code, which uses a fast, fully implicit algorithm to solve the conservative full-potential equation for transonic flow fields about arbitrary airfoils, is described. The code description is given in two levels of sophistication: simplified operation and detailed operation. In addition, detailed descriptions of the program organization and theory are provided to simplify modification of TAIR for new applications. Examples with input and output are given for a wide range of cases, including incompressible, subcritical compressible, and transonic calculations.

17. Key Words (Suggested by Author(s))	18. Distribution Statement
Transonic flow Numerical methods	Unlimited STAR Category - 02

19. Security Classif. (of this report)	20. Security Classif. (of this page)	21. No. of Pages	22. Price*
Unclassified	Unclassified	90	$9.50

*For sale by the National Technical Information Service, Springfield, Virginia 22161

DO NOT REMOVE SLIP FROM MATERIAL

Delete your name from this slip when returning material to the library.

NAME	DATE	MS
M. Muller	6/30/[illegible]	343
John Batina	12/00	499

NASA Langley (Rev. Dec. 1991) RIAD N-75